



UNIVERSIDADE D
COIMBRA

Sofia Pinheiro Lourenço

FROM THE LOCAL DENSITY APPROXIMATION
TO EXACT EXCHANGE IN TIME-DEPENDENT
DENSITY FUNCTIONAL THEORY: THE CASE
OF RARE GAS CATIONIC CLUSTERS

Dissertação no âmbito do Mestrado em Física, ramo de Física da Matéria Condensada,
orientada pelo Professor Doutor Fernando Manuel Silva Nogueira
e apresentada ao Departamento de Física da Faculdade de Ciências e Tecnologia
da Universidade de Coimbra.

Setembro de 2019

From the local density approximation to exact exchange in time-dependent density functional theory

The case of rare-gas cationic clusters

Sofia Pinheiro Lourenço

A thesis submitted for the degree of
Master in Physics



Department of Physics
University of Coimbra
Portugal
September 2019

*Para os meus pais e irmão, por me fazerem sentir tão especial.
Para a minha avó "Voita", que tinha o dom de saber viver.*

Abstract

Upon ionization, the optical absorption of neutral rare-gas clusters shifts from the ultraviolet range to the visible. Within TDDFT, the photoabsorption spectra of the Xe_3^+ cluster, employing traditional DFT functionals, predicts a reasonable position for the two experimental peaks, but their relative intensities appears to be inverted. The improvement on the problem reached within the Hartree-Fock level suggested an explanation based on the unsatisfactory treatment of exchange in common density functionals. The main goal of this thesis project is to continue investigating on how the exact exchange improves peaks' relative height by calculating ground state geometries and absorption spectra with the following functionals: LDA+ADSIC, OEP-SLATER, OEP-KLI, OEP-FULL. In the end, it is concluded that the adequate ground state geometries are necessary for the generation of correct spectra. Also, the bigger the amount of exchange added, the better the spectrum, even though OEP-FULL probably is the level of theory required to invert the peaks.

Resumo

Mediante ionização, o espectro de absorção de clusters neutras de gases raros transita da gama do ultravioleta para a do visível. Em TDDFT e utilizando os tradicionais funcionais para a correlação e troca, é possível fazer boas previsões para o posicionamento dos dois picos experimentais da cluster de Xe_3^+ , mas a intensidade dos mesmos surge trocada. O facto deste problema ter sido resolvido ao nível de Hartree-Fock sugere como possível explicação para esta incapacidade preditiva da DFT a forma insatisfatória como a troca é tratada nos funcionais da densidade típicos. O principal objetivo desta tese é continuar a estudar a forma como a troca exata melhora a intensidade relativa dos picos, calculando-se para tal geometrias de estado fundamental e espectros de absorção com os seguintes funcionais: LDA+ADSIC, OEP-SLATER, OEP-KLI, OEP-FULL. No fim, conclui-se que a aquisição das geometrias de estado fundamental corretas é necessária para a obtenção de espectros comparáveis ao experimental. Também, quanto maior a quantidade de troca incluída no funcional, melhor o espectro, mesmo que a inversão dos picos só venha a acontecer, provavelmente, com a utilização de OEP-FULL.

Contents

Contents	ix
List of Figures	xi
List of Tables	xiii
List of Abbreviations	xiv
1 Introduction	1
2 The Basics of Density Functional Theory	5
2.1 Motivation	5
2.2 The Hohenberg-Kohn Theorem	5
2.3 Kohn-Sham Scheme	8
3 The Exchange-Correlation Functional	11
3.1 Jacob's Ladder	11
3.1.1 Ground Level: Hartree World	12
3.1.2 Level 1: LSDA	12
3.1.3 Level 2: Spin-GGA	13
3.1.4 Level 3: Spin-meta-GGA	15
3.1.5 Levels 4 and 5: Hyper-GGA	15
3.2 Hybrid Functionals	15
3.3 Average Density Self-Interaction Correction	16
3.4 Orbital-Dependent Exchange-Correlation Functionals	16
3.4.1 Motivation	17
3.4.2 Optimized Potential Method (OPM)	17
3.4.3 Krieger-Li-Iafrate (KLI) Approximation	20
3.4.4 Slater Approximation	20
3.4.5 Exact Exchange in DFT	21
4 Time-Dependent Density Functional Theory (TDDFT)	24
4.1 The Basics of TDDFT	24
4.1.1 Hohenberg-Kohn in TDDFT	24

4.1.2	TD Kohn-Sham Scheme	28
4.2	TD Exchange-Correlation Functionals	28
4.2.1	Adiabatic Approximations	28
4.2.2	TD Optimized Potential Method	28
4.2.3	TD Krieger-Li-Iafrate Approximation	32
4.2.4	TD Slater Approximation	33
4.3	Electronic Response to External Fields	34
4.3.1	Full Solution of TD Kohn-Sham Equations	34
4.3.2	Dynamical Polarizability	34
4.3.3	Absorption Cross-Section	35
5	Spin Density Functional Theory (SDFT)	38
5.1	Non-Uniqueness Problem	41
5.1.1	Collinear SDFT	41
5.1.2	Non-collinear SDFT	41
5.2	The Exchange-Correlation Functional	43
5.2.1	Non-collinear LSDA and GGA	43
5.2.2	Optimized Potential Method (OPM)	44
5.2.3	Krieger-Li-Iafrate (KLI) Approximation	46
5.2.4	Slater Potential	49
6	Results and Discussion	51
6.1	Technical Details	51
6.1.1	Pseudopotential	51
6.1.2	Geometry Optimization	51
6.1.3	TDDFT/Absorption Spectrum	51
6.2	Results and Discussion	52
6.2.1	Geometry Optimization	52
6.2.2	TDDFT/Absorption Spectrum	53
7	Conclusions and Future Work	63
	Appendices	64
A	Definition of Density Matrices	64
B	Linearisation of the KLI equations	67
B.1	Simple KLI	67
B.2	Time-dependent KLI	68
B.3	Non-collinear KLI	68
C	Van der Waals Forces	70
	Bibliography	71

List of Figures

1.1	Absorption cross-section of linear Xe_3^+ calculated using the DIM geometry and different exchange-correlation functionals. Experimental results are from reference [11].	2
1.2	Hartree-Fock calculation of the absorption cross-section of linear Xe_3^+ using a contracted quadruple-zeta basis of Ceolin <i>et al.</i> (QZP) and four diffuse-augmented QZP basis sets: s-aug-QZP, d-aug-QZP, t-aug-QZP, q-aug-QZP.	3
1.3	Stages of the project.	4
2.1	Schematic representation of the real system, on the left, and the Kohn-Sham system, on the right. Straight lines in the figure are solely a symbolic way of representing interactions between electrons.	8
3.1	Jacob's ladder of density functional approximations for the xc energy, as proposed by John Perdew [19, 27].	12
6.1	Absorption cross-section of linear Xe_3^+ calculated using the LDA functional for both geometry optimization and time propagation. Comparison to the experimental results, from reference [11].	53
6.2	Absorption cross-section of linear Xe_3^+ calculated using the LDA+ADSIC functional for both geometry optimization and time propagation. Comparison to the experimental results, from reference [11].	54
6.3	Absorption cross-section of linear Xe_3^+ calculated using the LDA functional for geometry optimization and LDA+ADSIC for time propagation. Comparison to the experimental results, from reference [11].	55
6.4	Absorption cross-section of linear Xe_3^+ calculated using OEP-SLATER for both geometry optimization and time propagation. Comparison to the experimental results, from reference [11].	56
6.5	Absorption cross-section of linear Xe_3^+ calculated using LDA for geometry optimization and OEP-SLATER for time propagation. Comparison to the experimental results, from reference [11].	57
6.6	Absorption cross-section of linear Xe_3^+ calculated using OEP-KLI for both geometry optimization and time propagation. Comparison to the experimental results, from reference [11].	58

6.7	Absorption cross-section of linear Xe_3^+ calculated using LDA for geometry optimization and OEP-KLI for time propagation. Comparison to the experimental results, from reference [11].	59
6.8	Comparison between the experimental absorption spectrum of linear Xe_3^+ and theoretical spectra calculated using LDA, OEP-SLATER and OEP-KLI (with the corresponding ground state geometries).	60
6.9	Absorption cross-section of linear Xe_3^+ calculated using OEP-KLI for geometry optimization and OEP-FULL for time propagation. Comparison to the experimental results, from reference [11].	61
6.10	Absorption cross-section of linear Xe_3^+ calculated using LDA for geometry optimization and OEP-FULL for time propagation. Comparison to the experimental results, from reference [11].	62

List of Tables

3.1	Exchange-only ground state energies of closed-subshell atoms: self-consistent OPM results versus HF energies (all energies in mhartree) [6].	23
6.1	Time-propagation step-length, number of steps and exponential method chosen for each exchange-correlation functional.	52
6.2	Xe ₃ ⁺ ground state geometry (linear) and total energy, as predicted by the different exchange-correlation functionals. The quantities b_1 and b_2 are the bond lengths (from the left to the right). DIM values were taken from reference [26].	52

List of Abbreviations

ADSIC Average Density Self-Interaction Correction.

APE Atomic Pseudopotential Engine.

B3LYP Becke, 3-parameter, Lee-Yang-Parr.

DFT Density Functional Theory.

DIM Diatomics In Molecules.

EXX EXact eXchange.

FIRE Fast Inertial Relaxation Engine.

GEA Gradient Expansion Approximation.

GGA Generalized Gradient Approximation.

HF Hartree-Fock.

HK Hohenberg-Kohn.

ID Induced Dipole.

KLI Krieger-Li-Iafrate.

KS Kohn-Sham.

LDA Local Density Approximation.

LSDA Local Spin-Density Approximation.

MGGA Meta-Generalized Gradient Approximation.

occ occupied states.

OEP Optimized Effective Potential.
OPM Optimized Potential Method.
QZP Quadruple-Zeta Polarization.
ROCIS Restricted Open-shell Configuration Interaction Singles.
SDFT Spin Density Functional Theory.
SIC Self-Interaction Correction.
SO Spin-Orbit.
TD Time-Dependent.
TDDFT Time-Dependent Density Functional Theory.
TDKLI Time-Dependent Krieger-Li-Iafrate.
TDOPM Time-Dependent Optimized Potential Method.
UV ultraviolet.
x-only exchange-only.
xc exchange-correlation.

Chapter 1

Introduction

Neutral rare-gas clusters¹ are van der Waals (Appendix C) bound and their first electronic transition is in the UV region. Every atom is bound to its neighbors by the same kind of weak unidirectional force. However, upon ionization one electron is removed from a strongly antibonding orbital. Because of the directional character of the empty p orbital, the bonding becomes much stronger around the charge and differs in character, direction and strength. The optical absorption shifts to the visible.

In 1991, Haberland [11] *et al.* measured the absorption cross-section for Xe_n^+ , $3 \leq n \leq 30$. They found out that all these clusters exhibited three broad peaks in the 1-4 eV region, except Xe_3^+ , for which only two peaks could be observed.

In what concerns theoretical studies, most of the previous works on cationic xenon clusters made use of semiempirical methods, especially the "diatomics in molecules" (DIM) approach, in which a model Hamiltonian is built using high quality *ab initio* diatomic data. Several extensions to the DIM model are required to accurately describe the electronic properties of cationic xenon clusters: inclusion of spin-orbit coupling (DIM+SO extension), consideration of many-body polarization forces (not considered in DIM+SO), account for induced dipole-induced dipole (ID-ID) contributions (DIM+IDID+SO extension).

On the other hand, *ab initio* methods like DFT (Density Functional Theory), implemented with some approximation to the exchange-correlation functional, are in general well capable of describing covalent bonding, but have problems with the long-range correlation present in these systems. Also, these *ab initio* methods must incorporate relativistic effects precisely since those are extremely important in these clusters for correct ground state geometries and proper description of the absorption cross-section: if spin-orbit coupling is neglected, Xe_3^+ absorption cross-section spectrum only exhibits one peak.

¹Clusters and small particles as systems of bound atoms or molecules are an intermediate form of matter between atomic and bulk particles. However, solid clusters differ from small particles since their parameters are not monotonic functions of a number of cluster atoms and have a heightened stability at magic numbers of atoms. In particular, clusters allow to understand additional aspects of the physics of bulk particles.

In [25] the authors have generated, within TDDFT, the photoabsorption spectra of the Xe_3^+ cluster, employing traditional DFT functionals. There they found out that although it was possible to reach a good agreement (close to the expected accuracy of the method) between experimental and simulated results for peak positioning, the relative intensities of the two peaks appeared to be inverted. Three possible sources of error were subsequently identified: geometry, exchange-correlation functional, spin-orbit coupling. In order to test the effect of a precise choice of the exchange-correlation functional, the spectrum was again generated, this time employing an hybrid functional (B3LYP), with a fraction of exact exchange. B3LYP (over DIM ground state geometry) managed to change relative intensities in the correct direction, although they still remained inverted with respect to experiment. In the end, it was concluded that adequate geometries are necessary in order to have a good agreement in peak positioning, while the error in the relative intensities was most likely related to the approximate functional used in the TDDFT calculation.

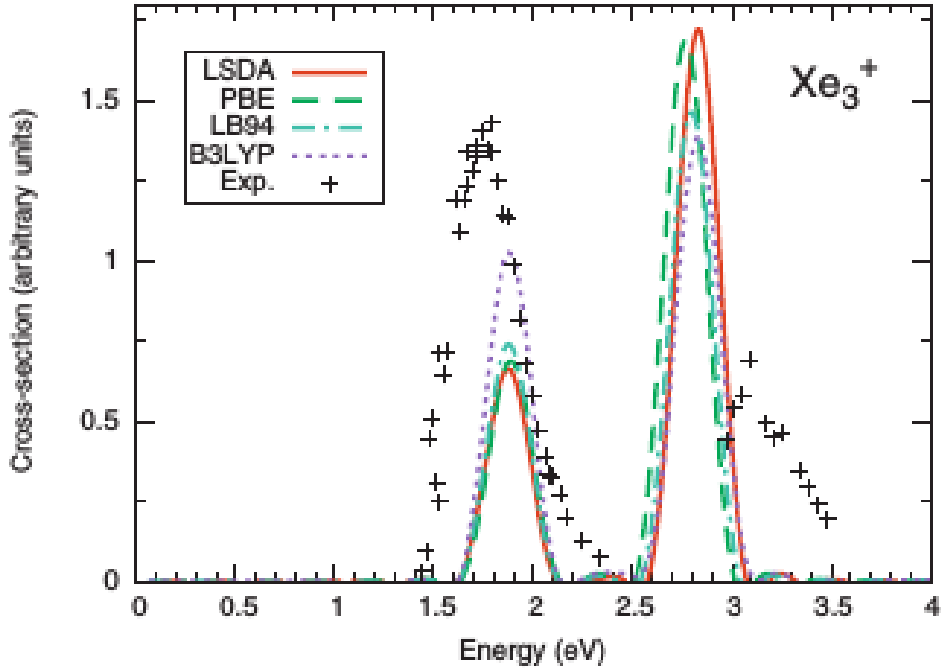


Figure 1.1: Absorption cross-section of linear Xe_3^+ calculated using the DIM geometry and different exchange-correlation functionals. Experimental results are from reference [11].

Bruce Milne² completed the Hartree-Fock study by generating spectra at this level of theory with ORCA v4.1.2 software [23, 22]. The result, as shown in Figure 1.2, supports the thesis that the inversion of the peaks is a consequence, in DFT, of the poor

²Centre for Computational Physics, Department of Physics, University of Coimbra, 3004-516, Coimbra, Portugal

treatment given to the exchange functional, since in this result it is shown that HF is able to invert the peaks. For the generation of the spectra, scalar relativistic effects were included in the simulation, as well as spin-orbit effects, which were considered in ground state calculations through the SOMF1X spin-orbit mean-field approach [12]. Absorption spectra were performed with restricted open-shell configuration interaction singles (ROCIS) method and the effect of spin-orbit coupling on the calculated one-electron excitations was included in the configuration interaction stage yielding the observed splitting of 1.3 eV with the diffuse augmented QZP basis sets.

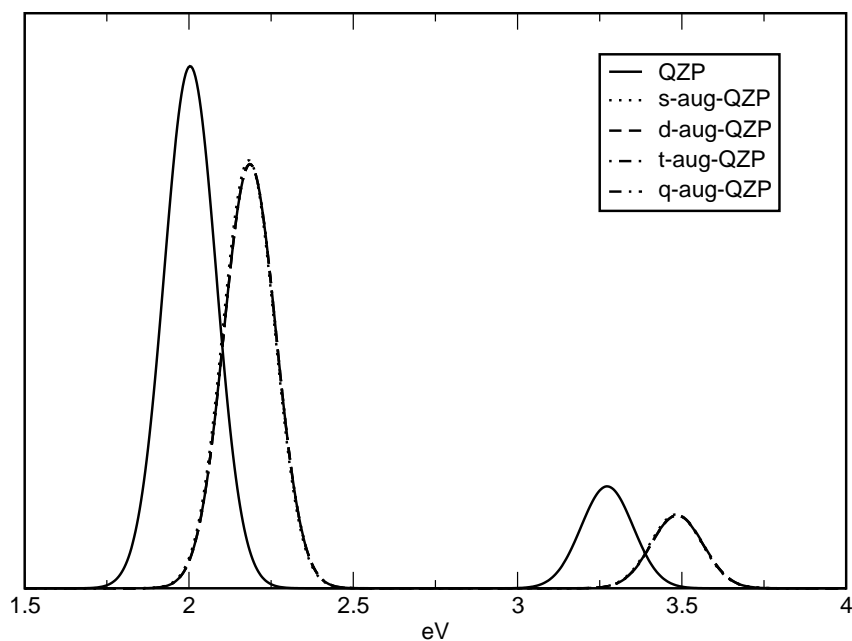


Figure 1.2: Hartree-Fock calculation of the absorption cross-section of linear Xe_3^+ using a contracted quadruple-zeta basis of Ceolin *et al.* (QZP) and four diffuse-augmented QZP basis sets: s-aug-QZP, d-aug-QZP, t-aug-QZP, q-aug-QZP.

In [21], the author concluded the implementation of non-collinear³ KLI equations in the code OCTOPUS and started to study how the spectrum changed with the inclusion of exact exchange, by generating the absorption spectrum of Xe_3^+ using two approximations for DFT exact-exchange potential: OEP-SLATER, OEP-KLI (a DIM geometry was used in both cases). In the end, the Slater approximation was able to invert the intensity of

³Very few numerical implementations have incorporated exact exchange within non-collinear spin DFT, which is needed when one wishes to take into account the effects from spin-orbit coupling.

the peaks, although the position was worse than what was predicted by LSDA. KLI also managed to invert peaks, but the author suggested the repetition of this simulation, due to the large negative peak that appeared in the spectrum.

Given all this background work, the main goal of this thesis project is to continue investigating on how the exact exchange improves peaks' relative height. As so, the project comprises three main steps:

- **Generation of a pseudopotential** A fully-relativistic pseudopotential will be generated for Xe using the APE code;
- **Geometry optimization** The ground state geometry will be obtained with the same functional used in the TD propagation;
- **TDDFT/Absorption spectrum** Time propagation will be performed using the following functionals: OEP-SLATER, OEP-KLI, OEP-FULL (no approximation to the exchange-only potential) and LDA+ADSIC (LDA with Average Density Self-Interaction Correction).

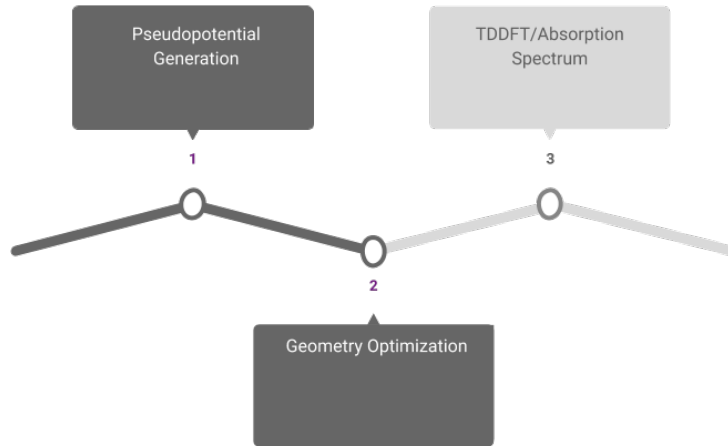


Figure 1.3: Stages of the project.

At last, the novelty in this project relies on the fact that ground state geometries are optimized with the same functional used in the TD propagation and further compared with the same spectrum obtained using a LSDA geometry.

Chapter 2

The Basics of Density Functional Theory

2.1 Motivation

To begin with, let us consider an N -electron system, its N -electron wavefunction being

$$\Psi(\mathbf{x}_1, \mathbf{x}_2, \dots, \mathbf{x}_N), \quad (2.1)$$

with $\mathbf{x}_i = (\mathbf{r}_i, \sigma_i)$, \mathbf{r}_i and σ_i being the space and spin coordinates, respectively. This function depends on $4N$ variables, thus being extremely difficult to store and manipulate.

The Density Functional Theory [6, 24] approach succeeds to restate the problem in terms of a 4 variable-dependent function, the single-particle spin-density^{1 2 3} :

$$\begin{aligned} \rho(\mathbf{x}) &\equiv \gamma(\mathbf{x}_1) = \gamma(\mathbf{x}_1|\mathbf{x}_1) \\ &= N \int |\Psi(123\dots N)|^2(dx'_1). \end{aligned} \quad (2.2)$$

This new function, $\rho(\mathbf{x})$, is interpreted as a representation of the number of particles \times the probability of finding a particle in \mathbf{r} having spin σ when all the other particles have arbitrary space and spin coordinates.

2.2 The Hohenberg-Kohn Theorem

It is not obvious that the problem of calculating the electronic structure of atoms, molecules and solids can be reformulated on the basis of the single-particle density.

¹For more information on the definition of density matrices please consult Appendix A.

²The integral already contains a summation over all spin states.

³In (2.2), $\gamma(\mathbf{x}_1|\mathbf{x}_1)$ is the diagonal of the first-order density matrix, $\Psi(123\dots N) \equiv \Psi(\mathbf{x}_1, \mathbf{x}_2, \dots, \mathbf{x}_N)$ and $\mathbf{x}_1 \rightarrow \mathbf{x}$ in $\rho(\mathbf{x})$ for a matter of convenience. See Appendix A for more information on the definition of density matrices.

Actually, Hohenberg and Kohn [13], in 1964, showed that all properties of a quantum many-body system are functionals of its ground state density. Their theorem - the HK (Hohenberg-Kohn) theorem - was originally formulated for spin-unpolarized systems, so it is enough to consider, for the moment, the electronic density $n(\mathbf{r})$ instead of the whole spin-density $\rho(\mathbf{x})$:

$$n(\mathbf{r}) = \langle \Psi | \hat{n}(\mathbf{r}) | \Psi \rangle. \quad (2.3)$$

HK Theorem

The HK theorem applies to systems of N interacting electrons moving in an external local potential with a non-degenerate ground state and with all electronic densities being v -representable^{4 5}. Such a system is represented by the Hamiltonian

$$\hat{H} = \hat{F} + \hat{V}_{ext}, \quad (2.4)$$

where \hat{V}_{ext} is the external potential operator and \hat{F} is an operator that groups all terms that do not depend on the external field. Provided these conditions:

Statement 1 The ground state particle density $n(\mathbf{r})$ uniquely determines the external potential $V_{ext}(\mathbf{r})$ to within an additive constant.

Proof of Statement 1

Let us consider a set of external potentials $\{\hat{V}_{ext}\}$, the space of ground state wavefunctions $\{\Psi\}$ and the ensemble of all-electron densities $\{n\}$.

$$\{\hat{V}_{ext}\} \xrightarrow{A} \{\Psi\} \xrightarrow{B} \{n\} \quad (2.5)$$

Statement 1 is equivalent to say that mapping $C = A \circ B$ is injective or to say that A and B are both injective. Its proof follows *reductio ad absurdum*.

Therefore, so as to demonstrate that A is injective, let us suppose there are two external potentials $\hat{V}_{ext}^{(1)}$ and $\hat{V}_{ext}^{(2)}$ which differ by more than a constant and which lead to the same ground state wavefunction Ψ . For each of the cases (\hat{F} stays the same since none of its terms depends on the external field):

$$(\hat{F} + \hat{V}_{ext}^{(1)}) |\Psi\rangle = E^{(1)} |\Psi\rangle, \quad (2.6)$$

$$(\hat{F} + \hat{V}_{ext}^{(2)}) |\Psi\rangle = E^{(2)} |\Psi\rangle. \quad (2.7)$$

By taking the difference between (2.6) and (2.7),

$$(\hat{V}_{ext}^{(1)} - \hat{V}_{ext}^{(2)}) |\Psi\rangle = (E^{(1)} - E^{(2)}) |\Psi\rangle, \quad (2.8)$$

⁴Some literature contains extensions of the theorem to degenerate ground states [10] and to N -representable densities [17, 18], i.e. densities coming from an antisymmetric N -electron ground state wavefunction.

⁵This theorem makes use of the variational principle, which requires that for all non-negative, normalized and well-behaved functions $n(\mathbf{r})$, it is possible to find an external potential $\hat{V}_{ext}(\mathbf{r})$ for which $n(\mathbf{r})$ is the ground state density. The density $n(\mathbf{r})$ is then said to be v -representable.

one is able to conclude that $\hat{V}_{ext}^{(1)}$ and $\hat{V}_{ext}^{(2)}$ only differ by a constant, thus contradicting the first assumption. Consequently, A must be injective.

Now, to begin with the proof that B is injective as well, let us suppose there are two different ground state wavefunctions $\Psi^{(1)}$ and $\Psi^{(2)}$ with the same ground state density. From Ritz's variational principle, the expectation value of an Hamiltonian evaluated in a quantum state which is not an eigenvector of that operator is always bigger than the same expectation value evaluated in an eigenstate, i.e.⁶

$$E^{(1)} = \langle \Psi^{(1)} | \hat{H}^{(1)} | \Psi^{(1)} \rangle < \langle \Psi^{(2)} | \hat{H}^{(1)} | \Psi^{(2)} \rangle. \quad (2.9)$$

Additionally,

$$\begin{aligned} \langle \Psi^{(2)} | \hat{H}^{(1)} | \Psi^{(2)} \rangle &= \langle \Psi^{(2)} | \hat{H}^{(2)} | \Psi^{(2)} \rangle + \langle \Psi^{(2)} | \hat{H}^{(1)} - \hat{H}^{(2)} | \Psi^{(2)} \rangle \\ &= E^{(2)} + \langle \Psi^{(2)} | \hat{V}_{ext}^{(1)} - \hat{V}_{ext}^{(2)} | \Psi^{(2)} \rangle \end{aligned} \quad (2.10)$$

and so

$$E^{(1)} < E^{(2)} + \langle \Psi^{(2)} | \hat{V}_{ext}^{(1)} - \hat{V}_{ext}^{(2)} | \Psi^{(2)} \rangle. \quad (2.11)$$

By analogy,

$$E^{(2)} < E^{(1)} + \langle \Psi^{(1)} | \hat{V}_{ext}^{(2)} - \hat{V}_{ext}^{(1)} | \Psi^{(1)} \rangle. \quad (2.12)$$

However, we hypothesized that the ground state density was the same for both wavefunctions, which would imply that

$$\langle \Psi^{(2)} | \hat{V}_{ext}^{(1)} - \hat{V}_{ext}^{(2)} | \Psi^{(2)} \rangle = \int d\mathbf{r} (\hat{V}_{ext}^{(1)} - \hat{V}_{ext}^{(2)}) n(\mathbf{r}) = - \langle \Psi^{(1)} | \hat{V}_{ext}^{(2)} - \hat{V}_{ext}^{(1)} | \Psi^{(1)} \rangle \quad (2.13)$$

and that, after adding (2.11) and (2.12),

$$E^{(1)} + E^{(2)} < E^{(2)} + E^{(1)}. \quad (2.14)$$

This inequality is absurd and leads to the conclusion that B must be injective.

As a final remark, if A and B are both injective, then C is also injective and according to Statement 1, it is possible to obtain the external potential and the many-electron wave function from the density. Since the wavefunction determines every observable of the system, **the ground state expectation value of any physical observable is a unique functional of the ground state density.** \square

Statement 2 The exact ground state energy can be obtained variationally and corresponds to the exact ground state density.

Proof of Statement 2

⁶An equality does not hold in (2.9) because the theorem does not apply to degenerate ground states.

At this point, it is possible to write the total energy of the system as a functional of the density and apply Ritz's variational principle to such a functional, thus obtaining

$$E[n^{(1)}] = \langle \Psi^{(1)} | \hat{H}^{(1)} | \Psi^{(1)} \rangle < \langle \Psi^{(2)} | \hat{H}^{(1)} | \Psi^{(2)} \rangle = E[n^{(2)}], \quad (2.15)$$

meaning that the **exact** ground state density is the one (from the set V of all v -representable densities) that minimizes $E[n]$, the minimum being the **exact** ground state energy:

$$E = \min_{n \in V} E[n]. \quad (2.16)$$

□

As so, it follows that the exact ground state is obtained through minimization of $E[n]$, under the constraint that the total number of particles remains constant ($\int n(\mathbf{r}) d\mathbf{r} - N = 0$):

$$\begin{aligned} \frac{\delta}{\delta n} \left(E[n] - \mu \int n(\mathbf{r}) d\mathbf{r} \right) = 0 &\Leftrightarrow \\ \frac{\delta}{\delta n} F[n] + \frac{\delta}{\delta n} \int n(\mathbf{r}) v_{ext}(\mathbf{r}) d\mathbf{r} - \mu \frac{\delta}{\delta n} \int n(\mathbf{r}) d\mathbf{r} = 0 &\Leftrightarrow \\ \frac{\delta}{\delta n} F[n] + v_{ext}(\mathbf{r}) - \mu = 0 \end{aligned} \quad (2.17)$$

2.3 Kohn-Sham Scheme

It still remains to find an expression for $F[n]$, if the intention is to continue on solving equation (2.17). In order to puzzle out this problem, Kohn and Sham devised a method, in 1965 [14], that requires the usage of an auxiliary system described by the same electronic density $n(\mathbf{r})$ as the real system.

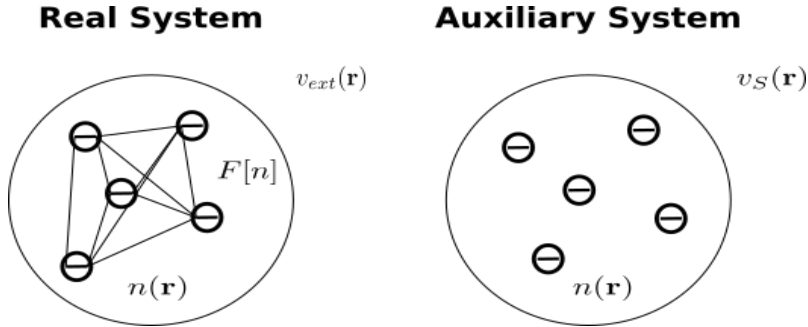


Figure 2.1: Schematic representation of the real system, on the left, and the Kohn-Sham system, on the right. Straight lines in the figure are solely a symbolic way of representing interactions between electrons.

Real System

- The total energy of the system is

$$E[n] = F[n] + \int n(\mathbf{r})v_{ext}(\mathbf{r})d\mathbf{r}; \quad (2.18)$$

- Electrons interact with each other;
- The system is under the influence of an external potential $v_{ext}(\mathbf{r})$;
- The ground state density is $n(\mathbf{r})$.

Auxiliary system

- The total energy of the system is

$$E_S[n] = T_S[n] + \int n(\mathbf{r})v_S(\mathbf{r})d\mathbf{r}, \quad (2.19)$$

with $T_S[n]$ being the kinetic energy of the non-interacting system;

- Electrons only interact through the Pauli exclusion principle. The ground state wavefunction is a Slater determinant of the orbitals $\phi_i(\mathbf{r})$ satisfying⁷

$$\left[-\frac{1}{2}\nabla^2 + v_s(\mathbf{r}) \right] \phi_i(\mathbf{r}) = \epsilon_i \phi_i(\mathbf{r}); \quad (2.20)$$

- The system is under the influence of an external potential $v_s(\mathbf{r})$;
- The ground state density is

$$n(\mathbf{r}) = \sum_{i=1}^{occ} |\phi_i(\mathbf{r})|^2. \quad (2.21)$$

Firstly, in the auxiliary system,

$$\begin{aligned} \frac{\delta}{\delta n} \left(E_S[n] - \mu_S \int n(\mathbf{r})d\mathbf{r} \right) &= 0 \Leftrightarrow \\ \frac{\delta T_S[n]}{\delta n} + v_S(\mathbf{r}) - \mu_S &= 0. \end{aligned} \quad (2.22)$$

Secondly, in the real system

$$F[n] = T_S[n] + J[n] + E_{xc}[n], \quad (2.23)$$

with $J[n]$ being the classical Coulomb energy term

$$J[n] = \frac{1}{2} \int \frac{n(\mathbf{r})n(\mathbf{r}')}{|\mathbf{r} - \mathbf{r}'|} d\mathbf{r}d\mathbf{r}', \quad (2.24)$$

E_{xc} being the exchange and correlation energy

⁷Once more, the ground state is non-degenerate and the external potential is local.

$$E_{xc}[n] = E_{ee}[n] - J[n] + T[n] - T_S[n], \quad (2.25)$$

$T[n]$ being the kinetic energy of the real system and $E_{ee}[n]$ being the total electron-electron interaction energy.

The result of inserting (2.23) in (2.18) and minimizing is

$$\frac{\delta}{\delta n} T_S[n] + v_H[n](\mathbf{r}) + v_{xc}[n](\mathbf{r}) + v_{ext}(\mathbf{r}) - \mu = 0, \quad (2.26)$$

$$v_{xc}[n](\mathbf{r}) = \frac{\delta E_{xc}[n]}{\delta n}, \quad (2.27)$$

$$v_H[n](\mathbf{r}) = \int \frac{n(\mathbf{r}')}{|\mathbf{r} - \mathbf{r}'|} d\mathbf{r}'.^8 \quad (2.28)$$

At last, if we substitute $\frac{\delta}{\delta n} T_S[n]$ in (2.22) by (2.26), we get⁹

$$v_S(\mathbf{r}) = v_{ext}(\mathbf{r}) + v_H[n](\mathbf{r}) + v_{xc}[n](\mathbf{r}) - (\mu - \mu_S). \quad (2.29)$$

The quantity $\mu - \mu_S$ does not depend on \mathbf{r} , so it can be absorbed by the external potential which, according to the HK theorem, is uniquely determined by the density within an additive constant. Finally, equation (2.20) may be rewritten, with $v_S(\mathbf{r})$ given by (2.29):

$$\left[-\frac{1}{2} \nabla^2 + v_s[n](\mathbf{r}) \right] \phi_i(\mathbf{r}) = \epsilon_i \phi_i(\mathbf{r}), \quad (2.30)$$

$$v_s[n](\mathbf{r}) = v_{ext}(\mathbf{r}) + v_H[n](\mathbf{r}) + v_{xc}[n](\mathbf{r}). \quad (2.31)$$

Equations (2.30) and (2.21) are the so-called Kohn-Sham equations¹⁰. They can be transformed into a generalized eigenvalue problem through expansion of the KS orbitals in a basis and then solved self-consistently. This KS approach is, in principle, exact if the exact form of the exchange-correlation functional is used. However, implementation of the exact form is unfeasible and one has to resort to approximations.

⁸This term is the Hartree potential.

⁹The potential v_S is sometimes called Kohn-Sham effective potential and is local.

¹⁰KS orbitals and energies have no physical meaning.

Chapter 3

The Exchange-Correlation Functional

In order to surpass the complexity of the intricate motion of particles in an interacting system, a simplified picture emerged in which systems of interacting real particles are described in terms of approximately non-interacting fictitious bodies called "quasi particles". In particular, the "quasi electron" is composed by a bare particle plus the surrounding exchange-correlation cloud, which screens real particles [20]. The exchange-correlation cloud is created by three effects: (a) self-interaction correction, a classical effect which guarantees that an electron cannot interact with itself, (b) the (quantum) Pauli exclusion principle, which tends to keep two electrons with parallel spins apart in space, and (c) the Coulomb repulsion, which tends to keep any two electrons apart in space. Effects (a) and (b) are responsible for the exchange energy, which gives a "static" picture of this cloud, while effect (c) is responsible for the correlation energy, the "moving part", i.e. the energy component resulting from correlations between the real particle and the movement of other particles.

Due to the infeasibility of implementing the exact expression for E_c and thus for E_{xc} , one usually resorts to approximations. This chapter will focus on the construction of such approximations, following the hierarchical structure named Jacob's ladder. The three simplest approximations (LDA, GGA and meta-GGA) will be presented in their spin-polarized versions (LSDA, spin-GGA and spin-meta-GGA) since they are natural extensions of their spin-unpolarized counterparts. In the end, exact exchange (EXX) will be defined in the context of DFT and the OPM will be introduced as a method to construct the multiplicative EXX potential. Two further simplifications of the OPM will be analysed: the KLI approximation and the even simpler Slater approximation.

3.1 Jacob's Ladder

The main line of development of density functionals for the exchange-correlation energy suggests a Jacob's ladder in which the level of accuracy of the approximation for E_{xc} increases as one climbs from the Hartree world up to the heaven of "chemical

accuracy¹.

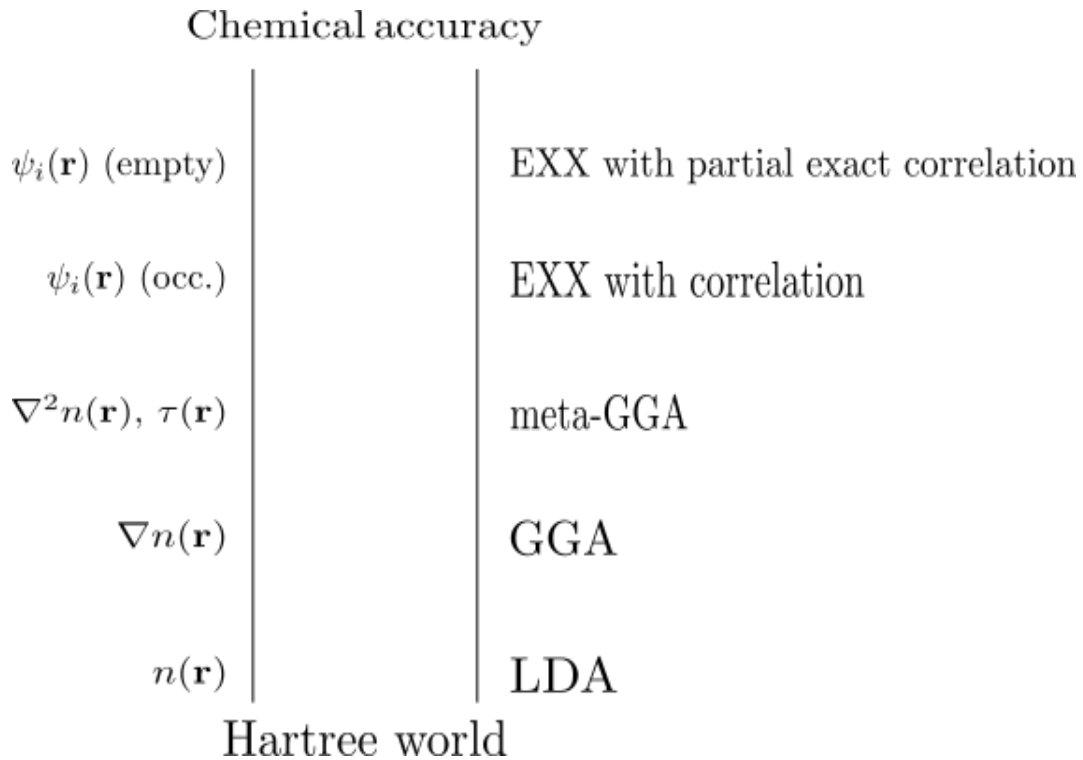


Figure 3.1: Jacob’s ladder of density functional approximations for the xc energy, as proposed by John Perdew [19, 27].

3.1.1 Ground Level: Hartree World

The removal of v_{xc} from the KS equations leads to the Hartree equations without self-interaction correction and thus to a full neglecting of exchange and correlation effects.

3.1.2 Level 1: LSDA

The local spin-density approximation LSDA (LDA when applied to spin-unpolarized systems) is a functional of only the spin-up and spin-down electronic densities: $n_\uparrow(\mathbf{r})$ and $n_\downarrow(\mathbf{r})$, respectively. In this approximation, the expression for an arbitrary energy component G is given by

$$G^{LSDA}[n_\uparrow, n_\downarrow] = \int d\mathbf{r} n(\mathbf{r}) g^{LSDA}(n_\uparrow(\mathbf{r}), n_\downarrow(\mathbf{r})), \quad (3.1)$$

where $g^{LSDA}(n_\uparrow(\mathbf{r}), n_\downarrow(\mathbf{r}))$ is that energy component per particle in an electron gas with uniform spin densities n_\uparrow and n_\downarrow , and is the sum of the exchange energy density e_x

¹“Chemical accuracy” is the accuracy needed to predict the rates of chemical reactions (energy errors of the order of 1 kcal/mol = 0.0434 eV).

with the correlation energy density e_c .

The exchange energy per particle in a spin-channel is given by the LDA expression, with $n_{\downarrow,\uparrow} \rightarrow n$ and $n_{\uparrow,\downarrow} \rightarrow 0$

$$e_x^{LDA}(n) = -\frac{3}{4\pi}(3\pi^2n)^{1/3} = -\frac{3}{4\pi} \frac{(9\pi/4)^{1/3}}{r_s}, \quad (3.2)$$

r_s being the average distance between two electrons in the gas.

By contrast, analytic expressions for $e_c^{LDA}(n)$ are known only on extreme limits. The high-density limit is obtained from many-body perturbation theory:

$$e_c^{LDA}(n) = c_0 \ln r_s - c_1 + c_2 r_s \ln r_s - c_3 r_s + \dots \quad (r_s \rightarrow 0). \quad (3.3)$$

The low-density limit is the limit in which the uniform fluid phase is unstable against the formation of a close-packed Wigner lattice of localized electrons [6]:

$$e_c^{LDA}(n) = -\frac{d_0}{r_s} + \frac{d_1}{r_s^{3/2}} + \dots \quad (r_s \rightarrow \infty). \quad (3.4)$$

Some of the constants in (3.3) and (3.4) are found by fitting to accurate Quantum Monte Carlo energies.

By construction, LSDA is exact for a uniform density or, more generally, for a density that varies slowly over space. More precisely, LSDA should be valid when the length scale of the density variation is large in comparison with length scales set by the local density, such as the Fermi wavelength $2\pi/k_F$ or the screening length $1/k_s$. Although this condition is rarely satisfied in real electronic systems, LSDA still is successful in those cases where electrons see an almost-complete cancellation between the nonlocalities of exchange and correlation². In the end, LSDA always fails in the one-electron limit [6] as a consequence of the non-cancellation of self-interaction.

On the whole, LSDA has been a standard approximation in solid state physics but it was never popular in the world of quantum chemistry because although it provides reasonable molecular geometries and vibration frequencies, it can strongly overestimate atomization energies. Atomization energy errors were greatly reduced by the spin generalized gradient approximation (spin-GGA).

3.1.3 Level 2: Spin-GGA

The spin generalized gradient approximation spin-GGA is a functional of both the electronic densities and their gradients $\nabla n_{\uparrow}(\mathbf{r})$ and $\nabla n_{\downarrow}(\mathbf{r})$:

$$E_{xc}^{spin-GGA}[n_{\uparrow}(\mathbf{r}), n_{\downarrow}(\mathbf{r})] = \int d\mathbf{r} n(\mathbf{r}) e_{xc}^{spin-GGA}(n_{\uparrow}(\mathbf{r}), n_{\downarrow}(\mathbf{r}), \nabla n_{\uparrow}(\mathbf{r}), \nabla n_{\downarrow}(\mathbf{r})). \quad (3.5)$$

²This is the reason why LSDA is almost always a better approximation for E_{xc} than it is for E_x and E_c separately.

This functional is the natural step beyond LSDA, thus preserving all the good features of the latter and even improving over others, mainly over those related to atomic and molecular systems. Unfortunately, spin-GGA cannot contribute to solving some of LSDA problems, like the self-interaction error. As an alternative, one could be tempted to think that, instead of spin-GGA, LSDA successor would be more like a gradient expansion which would systematically correct it. Such a functional is obtained through the gradient expansion method (GEA).

In order to infer to what extent a GEA would be advantageous, we begin with the (without the inclusion of spin, for the sake of simplicity) definition of two measures of inhomogeneity. The first one

$$s = \frac{|\nabla n|}{2k_F n} \quad (3.6)$$

is a reduced density gradient that measures how fast and how much the density varies on the scale of the local Fermi wavelength $2\pi/k_F$. The second one

$$t = \frac{|\nabla n|}{2k_s n} \quad (3.7)$$

measures density variation on the scale of the screening length $1/k_s$. Therefore, the quantity (3.6) is relevant for the expansion of the exchange energy functional ³:

$$E_x[n(\mathbf{r})] = A_x \int d\mathbf{r} n(\mathbf{r})^{4/3} [1 + \mu s^2 + \dots]. \quad (3.8)$$

For the correlation part, it matters to expand in (3.7) and so

$$E_c[n(\mathbf{r})] = \int d\mathbf{r} n(\mathbf{r}) [e_c(n) + \beta(n)t^2 + \dots]. \quad (3.9)$$

Finally, the GEA approximation (which is a special case of a GGA) is obtained by neglecting the dotted terms in (3.8) and (3.9). For this functional type, while the form of the density is easy to guess, the coefficients can only be calculated by hard work, summarily described on p.37 of [6]. Numerical tests of these gradient expansions for atoms show that the second-order gradient term provides a modestly useful correction to the local spin density approximation for E_x , but seriously worsens LSDA's results for E_c and E_{xc} , predicting positive correlation energies.

To conclude, both LSDA and spin-GGA are exact only for the electron gas of uniform density and represent controlled extrapolations away from the slowly-varying limit (since they preserve many features of the exact E_{xc}), while (spin-)GEA is an uncontrolled extrapolation.

³In order to perform this expansion it is necessary to know some desired scaling properties of the exchange energy functional (equation (1.106) of [6])

3.1.4 Level 3: Spin-meta-GGA

The meta-GGA approximation results from adding the ingredients $\nabla^2 n_\uparrow(\mathbf{r})$, $\nabla^2 n_\downarrow(\mathbf{r})$, τ_\uparrow and τ_\downarrow (or at least one of them) to the functional dependence:

$$E_{xc}^{spin-MGGA}[n_\uparrow(\mathbf{r}), n_\downarrow(\mathbf{r})] = \int d\mathbf{r} n(\mathbf{r}) e_{xc}^{spin-MGGA}(n_\uparrow, n_\downarrow, \nabla n_\uparrow, \nabla n_\downarrow, \nabla^2 n_\uparrow, \nabla^2 n_\downarrow, \tau_\uparrow, \tau_\downarrow). \quad (3.10)$$

One of the new ingredients, τ_σ , is the Kohn-Sham orbital kinetic energy density for electrons of spin σ and is an implicit functional of the density, since the density and the Kohn-Sham orbitals are mathematically related:

$$\tau_\sigma(\mathbf{r}) = \frac{1}{2} \sum_i^{occ} |\nabla \phi_{i\sigma}(\mathbf{r})|^2. \quad (3.11)$$

Among the functionals belonging to the hierarchy of Figure 3.1, meta-GGA is the highest stage which avoids full nonlocality: LDA is a local functional of the density; GGA is a semi-local functional of the density since it requires the density in an infinitesimal neighborhood around \mathbf{r} ; meta-GGA is a fully nonlocal functional of the density, but a semi-local functional of the orbitals.

In practice, meta-GGA improves GGA on the calculation of atomization energies, metal surface energies and lattice constants for solids, but not of bond lengths of molecules, especially for hydrogen bonds [27]. Additionally, meta-GGA is self-correlation free, i.e.

$$E_c[n, 0] = 0 \quad (N = 1), \quad (3.12)$$

with $[n, 0]$ denoting the density of both spin-channels.

3.1.5 Levels 4 and 5: Hyper-GGA

Hyper-GGA has exact exchange EXX⁴ and is a functional of the Kohn-Sham orbitals, as well as all the other variables previously mentioned. At its lowest level (level 4), the correlation energy density is approximated while at level 5 a portion of exact correlation already starts to be implemented through the inclusion of non-occupied Kohn-Sham orbitals.

The construction of $E_{xc}[n_\uparrow, n_\downarrow]$ from the Kohn-Sham orbitals in hyper-GGA is what probably is required to solve the self-interaction problem and other problems of LSDA and spin-GGA, which persist even when a self-interaction correction (SIC) is "manually" added to LSDA.

3.2 Hybrid Functionals

Hybrid functionals are perhaps the most accurate density functionals in use for quantum chemical calculations. The idea behind them is the junction of a fraction a of

⁴The exact exchange in DFT is summarily explained in section 3.4.5.

exact (Hartree-Fock) exchange with approximate (DFT) exchange and correlation. The simplest such hybrid functional is

$$E_{xc}^{hyb} = aE_x^{exact} + (1 - a)E_x^{GGA} + E_c^{GGA}, \quad (3.13)$$

where the mixing coefficient a - not equal to or close to 1, because full exact exchange is incompatible with GGA correlation - is adjusted in order to reproduce experimental values. Since Jacob's ladder contains only functionals constructed without empirical input, hybrid functionals are not considered as part of it.

3.3 Average Density Self-Interaction Correction

The Hartree potential acting on single-particle KS wavefunctions

$$v_H[n](\mathbf{r}) = \int \frac{\sum_k^{occ} |\phi_k(\mathbf{r}')|^2}{|\mathbf{r} - \mathbf{r}'|} d\mathbf{r}' \quad (3.14)$$

contains a sum over **all** occupied states, therefore including the eigenvector it is acting on.

This self-interaction term, corresponding (for the j th eigenvector) to

$$v_{SI}(\mathbf{r}) = \int \frac{|\phi_j(\mathbf{r}')|^2}{|\mathbf{r} - \mathbf{r}'|} d\mathbf{r}', \quad (3.15)$$

should be entirely cancelled by the exact exchange potential functional. However, because it is common practice to approximate exchange and correlation, the cancellation is not exact and there remains a non-physical self-interaction error.

A rather crude though efficient way to alleviate the error consists of removing the self-interaction by subtracting a fraction $1/N$ from the total density. The remaining $n(N - 1)/N$ then characterizes the density of all the other electrons seen by the actual spectator electron [16].

In what concerns the exchange-correlation energy term (and using LDA as an example), it is corrected by the average density self-interaction correction in the following way:

$$\begin{aligned} E_{xc}^{LDA+ADSIC}[n] &= E_{xc}^{LDA}[n] - \frac{1}{N} E_{ee}[n] \\ &= \left(1 - \frac{1}{N}\right) E_{xc}^{LDA}[n] - \frac{1}{N} J[n]. \end{aligned} \quad (3.16)$$

3.4 Orbital-Dependent Exchange-Correlation Functionals

Given some orbital-dependent xc-functional, the first question to be addressed is the evaluation of the corresponding multiplicative xc-potential v_{xc} .

3.4.1 Motivation

The motivation for orbital-dependent functionals - namely those implicit functionals appearing on the top of Jacob's ladder (Figure 3.1) - comes from the knowledge of those situations where nowadays extensively used GGA fails:

- **Heavy Elements** There is a tendency of GGA to lose accuracy with increasing nuclear charge. For light molecules, since GGA consistently stretches bond lengths (R_e) and reduces bond energies (D_e) compared with LDA, it corrects LDA's underestimation of R_e and the accompanying overestimation of D_e . However, in the case of heavy constituents LDA results are often rather close to the experimental numbers, so that GGA overcorrects LDA values.
- **Negative Ions** If one electron moves sufficiently far from the nucleus, it must experience the remaining net charge of the system, which consists of $N - 1$ electrons and N protons. However, v_H still contains the Coulomb self-repulsion, which has to be eliminated by v_x . The component of v_x which cancels the self-interaction in the Hartree potential must be as nonlocal as v_H itself. Since neither LDA or GGA are nonlocal, this term stays and as a consequence it is not possible to reproduce the $1/r$ behaviour of v_x and v_S , which is required to obtain a Rydberg series. The system is then unable to bind an additional electron.
- **Dispersion Forces** In this case, LDA and GGA fail to reproduce this kind of van der Waals forces due to the short-range nature of their correlation functional. In order to succeed with this description, the correlation functional would have to be nonlocal.
- **Strongly Correlated Systems** Some results suggest that the inappropriate handling of self-interaction is responsible for the failure of LDA and the standard GGAs in the description of strongly correlated systems.

3.4.2 Optimized Potential Method (OPM)

In order to produce single-particle orbitals we need to use the proper single-particle potential: namely the one which is **optimized** in the sense that its orbitals minimize the total-energy functional. In the case of orbital-dependent functionals, the usual procedure of directly calculating the multiplicative potential v_{xc} by taking the functional derivative of E_{xc} with respect to n , the electronic density, is not possible because the functional dependence of ϕ_k on n is not known. Therefore, the traditional way of obtaining the potential is substituted by what is called the Optimized Potential Method (OPM) [4, 28].

There are three different ways to derive the OPM equation which yield the multiplicative xc-potential [6]. Here we will follow the total energy minimization derivation because it represents the original approach and also shows more clearly the physics behind OPM. The first step in this derivation consists of requiring that the total energy is stationary

with respect to the KS potential. This requirement becomes intuitive if we recall that the Hohenberg-Kohn theorem guarantees (for a system under a local external potential) that there is a unique relation between n and v_S and therefore the standard minimization of E_{tot} with respect to n can be replaced by a minimization with respect to v_S :

$$\frac{\delta E_{tot}[\phi_k, \epsilon_k]}{\delta v_S(\mathbf{r})} = 0. \quad (3.17)$$

The derivative in (3.17) can be transformed into derivatives with respect to ϕ_k and ϵ_k , using the chain rule for functional differentiation:

$$\frac{\delta E_{tot}[\phi_k, \epsilon_k]}{\delta v_S(\mathbf{r})} = \sum_k^{occ} \left\{ \int d\mathbf{r}' \left[\frac{\delta \phi_k^*(\mathbf{r}')}{\delta v_S(\mathbf{r})} \frac{\delta E_{tot}}{\delta \phi_k^*(\mathbf{r}')} + c.c. \right] + \frac{\delta \epsilon_k}{\delta v_S(\mathbf{r})} \frac{\partial E_{tot}}{\partial \epsilon_k} \right\}. \quad (3.18)$$

Now it matters to find expressions for $\delta E_{tot}/\delta \phi_k^*(\mathbf{r})$ and $\partial E_{tot}/\partial \epsilon_k$. Once E_{tot} is related to T_S , E_{xc} , E_{ext} and E_H and the expressions for these energy functionals are known, these functional derivatives can be derived in a straightforward manner:

$$\frac{\delta E_{tot}}{\delta \phi_k^*(\mathbf{r})} = \Theta_k \left[-\frac{\nabla^2}{2m} + v_{ext}(\mathbf{r}) + v_H(\mathbf{r}) \right] \phi_k(\mathbf{r}) + \frac{\delta E_{xc}}{\delta \phi_k^*(\mathbf{r})}, \quad (3.19)$$

$$\frac{\partial E_{tot}}{\partial \epsilon_k} = \frac{\partial E_{xc}}{\partial \epsilon_k}. \quad (3.20)$$

One can then use KS equations to rewrite (3.19)

$$\frac{\delta E_{tot}}{\delta \phi_k^*(\mathbf{r})} = \Theta_k \left[\epsilon_k - v_{xc}(\mathbf{r}) \right] \phi_k(\mathbf{r}) + \frac{\delta E_{xc}}{\delta \phi_k^*(\mathbf{r})}. \quad (3.21)$$

Returning to (3.18), the derivatives $\delta \phi_k^*/\delta v_S$ and $\delta \epsilon_k/\delta v_S$ can be evaluated by varying v_S infinitesimally and looking at how ϕ_k and ϵ_k react, through KS equations:

$$\left\{ -\frac{\nabla^2}{2m} + v_s(\mathbf{r}) + \delta v_s(\mathbf{r}) \right\} \left[\phi_k(\mathbf{r}) + \delta \phi_k(\mathbf{r}) \right] = \left[\epsilon_k + \delta \epsilon_k \right] \left[\phi_k(\mathbf{r}) + \delta \phi_k(\mathbf{r}) \right]. \quad (3.22)$$

To first order one thus finds

$$\left\{ -\frac{\nabla^2}{2m} + v_s(\mathbf{r}) - \epsilon_k \right\} \delta \phi_k(\mathbf{r}) = \left[\delta \epsilon_k - \delta v_s(\mathbf{r}) \right] \phi_k(\mathbf{r}). \quad (3.23)$$

Multiplication by $\phi_k^*(\mathbf{r})$, integration over \mathbf{r} and use of the unperturbed KS equation then yield [3]

$$\delta \epsilon_k = \int d\mathbf{r} \phi_k^*(\mathbf{r}) \delta v_S(\mathbf{r}) \phi_k(\mathbf{r}). \quad (3.24)$$

Moreover, the inhomogeneous differential equation can be solved with the aid of the associated Green's function,

$$\left\{ -\frac{\nabla^2}{2m} + v_S(\mathbf{r}) - \epsilon_k \right\} G_k(\mathbf{r}, \mathbf{r}') = \delta^{(3)}(\mathbf{r} - \mathbf{r}') - \phi_k(\mathbf{r})\phi_k^*(\mathbf{r}'), \quad (3.25)$$

$$G_k(\mathbf{r}, \mathbf{r}') = \sum_{l \neq k}^{all} \frac{\phi_l(\mathbf{r})\phi_l^*(\mathbf{r}')}{\epsilon_l - \epsilon_k}. \quad (3.26)$$

In terms of the Green's function, $\delta\phi_k$ is given by

$$\delta\phi_k(\mathbf{r}) = - \int d\mathbf{r}' G_k(\mathbf{r}, \mathbf{r}') \delta v_S(\mathbf{r}') \phi_k(\mathbf{r}'). \quad (3.27)$$

From (3.27) and (3.24) it follows, respectively

$$\frac{\delta\phi_k^*(\mathbf{r})}{\delta v_S(\mathbf{r}')} = -\phi_k^*(\mathbf{r}') G_k(\mathbf{r}', \mathbf{r}), \quad (3.28)$$

$$\frac{\delta\epsilon_k}{\delta v_S(\mathbf{r})} = \phi_k^*(\mathbf{r})\phi_k^*(\mathbf{r}). \quad (3.29)$$

Insertion of (3.28), (3.29), (3.20) and (3.21) into (3.18) leads to

$$\int d\mathbf{r}' \left[\left(-\sum_k^{occ} \phi_k^*(\mathbf{r}) G_k(\mathbf{r}, \mathbf{r}') \phi_k(\mathbf{r}') + c.c. \right) (\epsilon_k - v_{xc}(\mathbf{r}')) - \sum_k^{occ} \left(\phi_k^*(\mathbf{r}) G_k(\mathbf{r}, \mathbf{r}') \frac{\delta E_{xc}}{\delta\phi_k^*(\mathbf{r}')} + c.c. \right) \right] + \sum_k^{occ} |\phi_k(\mathbf{r})|^2 \frac{\partial E_{xc}}{\partial\epsilon_k} = 0 \quad (3.30)$$

The inverse of $\delta v_s/\delta n$ is the static response function of the KS auxiliary system:

$$\chi_S(\mathbf{r}, \mathbf{r}') = \frac{\delta n(\mathbf{r})}{\delta v_S(\mathbf{r}')} = - \sum_k^{occ} \phi_k^*(\mathbf{r}) G_k(\mathbf{r}, \mathbf{r}') \phi_k(\mathbf{r}') + c.c.. \quad (3.31)$$

The inhomogeneity is defined as

$$\Lambda_{xc}(\mathbf{r}) = \sum_k^{occ} \left\{ - \int d\mathbf{r}' \left[\phi_k^*(\mathbf{r}) G_k(\mathbf{r}, \mathbf{r}') \frac{\delta E_{xc}}{\delta\phi_k^*(\mathbf{r}')} + c.c. \right] + |\phi_k(\mathbf{r})|^2 \frac{\partial E_{xc}}{\partial\epsilon_k} \right\}. \quad (3.32)$$

After identification of $\chi_S(\mathbf{r}, \mathbf{r}')$ and $\Lambda_{xc}(\mathbf{r})$ in (3.30) and usage of the orthogonality relation (which follows from definition (3.26))

$$\int d\mathbf{r} \phi_k^*(\mathbf{r}) G_k(\mathbf{r}, \mathbf{r}') = \int d\mathbf{r}' G_k(\mathbf{r}, \mathbf{r}') \phi_k(\mathbf{r}') = 0, \quad (3.33)$$

one ends up with the OPM integral equation:

$$\int d\mathbf{r}' \chi_S(\mathbf{r}, \mathbf{r}') v_{xc}(\mathbf{r}') = \Lambda_{xc}(\mathbf{r}). \quad (3.34)$$

3.4.3 Krieger-Li-Iafrate (KLI) Approximation

OPM calculations are very inefficient. The main reason for this inefficiency is the presence of the Green's function both in the response function (3.31) and in the inhomogeneity (3.32), as this function depends on the complete spectrum, not just on occupied states.

To solve this problem, Krieger, Li and Iafrate had the idea of approximating the denominator of (3.26) by an average $\Delta\bar{\epsilon}$

$$G_k(\mathbf{r}, \mathbf{r}') \approx \sum_{l \neq k}^{all} \frac{\phi_l(\mathbf{r})\phi_l^*(\mathbf{r}')}{\Delta\bar{\epsilon}} = \frac{\delta^{(3)}(\mathbf{r} - \mathbf{r}') - \phi_k(\mathbf{r})\phi_k^*(\mathbf{r}')}{\Delta\bar{\epsilon}}, \quad (3.35)$$

which, nevertheless, only speeds up the calculation of G_k , but not of the other OPM ingredients.

Insertion into the OPM equation leads to

$$v_{xc}^{KLI}(\mathbf{r}) = \frac{1}{2n(\mathbf{r})} \sum_k^{occ} \left\{ \left[\phi_k^*(\mathbf{r}) \frac{\delta E_{xc}}{\delta \phi_k^*(\mathbf{r})} + c.c. \right] + |\phi_k(\mathbf{r})|^2 \left[\Delta v_k^{KLI} - \Delta\bar{\epsilon} \frac{\partial E_{xc}}{\partial \epsilon_k} \right] \right\}, \quad (3.36)$$

$$\Delta v_k^{KLI} = \int d\mathbf{r}' \left\{ |\phi_k(\mathbf{r}')|^2 v_{xc}^{KLI}(\mathbf{r}') - \phi_k^*(\mathbf{r}') \frac{\delta E_{xc}}{\delta \phi_k^*(\mathbf{r}')} \right\} + c.c.. \quad (3.37)$$

In the exchange-only limit,

$$v_x^{KLI}(\mathbf{r}) = \frac{1}{2n(\mathbf{r})} \sum_k^{occ} \left\{ \left[\phi_k^*(\mathbf{r}) \frac{\delta E_x}{\delta \phi_k^*(\mathbf{r})} + c.c. \right] + |\phi_k(\mathbf{r})|^2 \Delta v_k^{KLI} \right\}, \quad (3.38)$$

$$\Delta v_k^{KLI} = \int d\mathbf{r}' \left\{ |\phi_k(\mathbf{r}')|^2 v_x^{KLI}(\mathbf{r}') - \phi_k^*(\mathbf{r}') \frac{\delta E_x}{\delta \phi_k^*(\mathbf{r}')} \right\} + c.c.. \quad (3.39)$$

and one does not have to bother with the $\partial E_x / \partial \epsilon_k$ term, which is identically 0 since E_x only depends on the eigenvectors, not the eigenvalues.

There are two alternative methods to solve (3.38). One can either linearise the exchange-only version of (3.36) and (3.37), thus determining Δv_k^{KLI} without prior knowledge of v_x^{KLI} or one can solve the problem self-consistently, starting from an approximation to Δv_k^{KLI} . In the OCTOPUS code, the implemented alternative for the evaluation of (3.38) is the one that implies linearisation (Appendix B).

3.4.4 Slater Approximation

The Slater approximation provides a simplification, beyond KLI, to the expression for the multiplicative potential. The main ingredient to construct such a simplification is the Slater potential [32], which arose from the necessity of simplifying the Hartree-Fock equations. These equations can be regarded as ordinary Schrödinger equations for the motion of electrons. Each electron moves in a slightly different potential field, which is

computed by electrostatics from all the charges of the system, corrected by the removal of an exchange charge, equal in magnitude to one electron and surrounding the electron whose motion is being investigated. By forming a weighted average of the exchange charges over the various electronic wavefunctions at a given point of space, we set up a single averaged potential field (the Slater one) in which we can consider all electrons to move, thus leading to a great simplification of the Hartree-Fock method [21]:

$$v_{slater}(\mathbf{r}) = \frac{1}{2n(\mathbf{r})} \sum_k^{occ} \left[\frac{\delta E_x}{\delta \phi_k(\mathbf{r})} \phi_k(\mathbf{r}) + c.c. \right]. \quad (3.40)$$

This allows us to rewrite (3.38) in a more compact way

$$v_x^{KLI}(\mathbf{r}) = v_{slater}(\mathbf{r}) + \frac{1}{2n(\mathbf{r})} \sum_k^{occ} \phi_k^*(\mathbf{r}) \Delta v_k^{KLI} \phi_k(\mathbf{r}). \quad (3.41)$$

The Slater approximation thus consists in discarding the second term in (3.41):

$$v_x^{KLI}(\mathbf{r}) \approx v_{slater}(\mathbf{r}). \quad (3.42)$$

3.4.5 Exact Exchange in DFT

The whole point of developing the OPM equations was to have a way of constructing the multiplicative potential arising from orbital dependent energy functionals, like EXX.

At this point we note that the precise definition of $E_x[n]$ is somewhat arbitrary. It is nevertheless the natural first choice to define the exchange functional in such a way that the total energy E^{HF} and density n_{HF} of the Hartree-Fock (HF) approximation are reproduced in DFT if the correlation functional is completely neglected. The corresponding ground state exchange-only energy functional $\tilde{E}[n]$,

$$\tilde{E}[n] = T_S[n] + E_{ext}[n] + J[n] + \tilde{E}_x[n] \quad (3.43)$$

is hence to be minimized by n_{HF} ,

$$E^{HF} = \tilde{E}[n_{HF}], \quad (3.44)$$

while for any other density one must have

$$E^{HF} < \tilde{E}[n], \quad \forall n \neq n_{HF}. \quad (3.45)$$

One could then set up a KS scheme on the basis of $\tilde{E}_x[n]$. Unfortunately, this definition creates difficulties:

- No explicit expression for the exact functional $\tilde{E}_x[n]$ is available;
- No virial relation can be formulated;
- A gradient expansion does not exist for $\tilde{E}_x[n]$.

For these reasons, an alternative definition of the exchange energy functional has become the standard in DFT,

$$E_x[n] := \langle \Phi_n^{min} | \hat{V}_{ee} | \Phi_n^{min} \rangle - J[n], \quad (3.46)$$

where $|\Phi_n^{min}\rangle$ is the single Slater determinant that yields n and minimizes $\langle \hat{T} \rangle$. By evaluating explicitly (3.46), one obtains the standard Fock expression written, however, in terms of the KS orbitals

$$E_x[n] = -\frac{1}{2} \sum_{kl}^{occ} \int d\mathbf{r} \int d\mathbf{r}' \frac{\phi_k^*(\mathbf{r})\phi_l(\mathbf{r})\phi_l^*(\mathbf{r}')\phi_k(\mathbf{r}')}{|\mathbf{r} - \mathbf{r}'|}. \quad (3.47)$$

In spite of the agreement of functional (3.46) with the Fock expression, the density which minimizes the total x-only energy functional of DFT,

$$E^{x-only}[n] := T_S[n] + E_{ext}[n] + E_H[n] + E_x[n], \quad (3.48)$$

is not identical with n_{HF} . As a matter of fact, the multiplicative nature of the total KS potential v_S represents a subsidiary condition in the minimization procedure. In the HF approach one thus has some additional variational freedom, which, in general, leads to a lower energy minimum,

$$E^{HF} \leq \min_n E^{x-only}[n]. \quad (3.49)$$

In other words, HF orbitals are not included in the variational space available to x-only DFT, which implies that the insertion of the HF ground state density into $E^{x-only}[n]$ does not yield the HF ground state energy,

$$E^{HF} \neq E^{x-only}[n_{HF}] \geq \min_n E^{x-only}[n]. \quad (3.50)$$

The x-only DFT minimization coincides with the HF scheme only in those special situations when the HF potential can be recast as a local potential for the occupied states. The main differences between the two approaches are the following:

- While the HF wavefunction is meant to provide an approximation for the many-body wavefunction (has physical meaning) itself, the Kohn-Sham wavefunction is meant to reproduce the exact particle density;
- While Hartree-Fock orbitals are produced by a non-local effective potential, Kohn-Sham orbitals are produced by a single particle equation with a local effective potential. Nevertheless, and as can be seen in Table 3.1, the additional variational freedom of the HF approach thus appears to be of very limited importance;
- The EXX (Kohn-Sham exact exchange) potential decays asymptotically as $-1/r$ for finite systems and this asymptotic form acts on all orbitals. Therefore, the KS EXX potential supports a whole Rydberg series of unoccupied bound states as well as

negative ions. By contrast, the HF potential decays as $-1/r$ for occupied orbitals, but decays exponentially for virtual orbitals. Therefore, the HF approximation does not support a Rydberg series [8, 1].

Table 3.1: Exchange-only ground state energies of closed-subshell atoms: self-consistent OPM results versus HF energies (all energies in mhartree) [6].

Atom	E_{tot}^{OPM}	$E_{tot}^{HF} - E_{tot}^{OPM}$
He	-2861.7	0.0
Be	-14572.4	-0.6
Ne	-128545.4	-1.7
Mg	-199611.6	-3.1
Ar	-526812.2	-5.3
Ca	-676751.9	-6.3
Zn	-1777834.4	-13.8
Kr	-2752042.9	-12.0
Sr	-3131533.4	-12.2
Pd	-4937906.0	-15.0
Cd	-5465114.4	-18.7
Xe	-7232121.1	-17.3
Ba	-7883526.6	-17.3
Yb	-13391416.3	-39.9
Hg	-18408960.5	-31.0
Rn	-21866745.7	-26.5
Ra	-23094277.9	-25.8
No	-32789472.7	-39.5

Chapter 4

Time-Dependent Density Functional Theory (TDDFT)

There exists a necessity to extend DFT to systems under the influence of time-dependent external potentials $\hat{V}_{ext}(\mathbf{r}, t)$, so as to provide a treatment of excitations and more general time-dependent phenomena.

In this context, two regimes can be observed: if the time-dependent potential is weak, it is sufficient to resort to linear-response theory to study the system; if the time-dependent potential is strong (such as in the case of strong laser fields), a full solution to Kohn-Sham equations is required.

The aim of this chapter is to extend its predecessors to include time-dependence. As so, the first sections will be a reformulation of DFT foundations and exchange-correlation functionals. Following it, there is a whole new section dedicated to characterising electronic response to external fields, based on the evaluation of the absorption cross-section. The latter is intimately related to the concept of dynamical polarizability, which will also be defined.

4.1 The Basics of TDDFT

4.1.1 Hohenberg-Kohn in TDDFT

In time-dependent systems there is no variational principle on the basis of the total energy for it is not a conserved quantity. There exists, however, a quantity analogous to the energy, the quantum mechanical action

$$A[\Psi] = \int_{t_0}^{t_1} dt \langle \Psi(t) | i \frac{\partial}{\partial t} - \hat{H}(t) | \Psi(t) \rangle, \quad (4.1)$$

which provides a stationary point - but no minimum - at the solution of the time-dependent Schrödinger equation. Anyhow, even on the basis of the quantum mechanical action, the HK theorem cannot be trivially generalized to time-dependent systems and

a new theorem - the Runge-Gross theorem [29] - is needed to extend HK to arbitrary time-dependent situations (described by v -representable densities).

Statement 1 (Runge-Gross theorem) For every single-particle potential $v_{ext}(\mathbf{r}, t)$ which can be Taylor expanded around $t = t_0$ and for a given fixed initial state $\Psi(t_0) = \Psi_0$, the map $G : v_{ext}(\mathbf{r}, t) \rightarrow n(\mathbf{r}, t)$ can be inverted up to an additive merely time-dependent function in the potential.

Proof of Statement 1

If a given potential v_{ext} is Taylor expandable around the initial time t_0 , then

$$v_{ext}(\mathbf{r}, t) = \sum_k^{all} c_k(\mathbf{r})(t - t_0)^k, \quad (4.2)$$

$$c_k(\mathbf{r}) = \frac{1}{k!} \frac{\partial^k}{\partial t^k} v_{ext}(\mathbf{r}, t) \Big|_{t=t_0}. \quad (4.3)$$

Moreover, if two potentials are different by more than a purely time-dependent function, at least one of the coefficients in (4.3) will differ by more than a constant, i.e.

$$\exists_{k \geq 0} : u_k(\mathbf{r}) \neq \text{constant}, \quad (4.4)$$

with

$$u_k(\mathbf{r}) = \frac{\partial^k}{\partial t^k} [v_{ext}^{(1)}(\mathbf{r}, t) - v_{ext}^{(2)}(\mathbf{r}, t)] \Big|_{t=t_0}, \quad (4.5)$$

and $v_{ext}^{(1)}, v_{ext}^{(2)}$ being two different external single-particle potentials.

Firstly, it will be demonstrated that if $v_{ext}^{(1)} \neq v_{ext}^{(2)} + c(t)$, then current densities $\mathbf{j}^{(1)}$ and $\mathbf{j}^{(2)}$

$$\mathbf{j}(\mathbf{r}, t) = \langle \Psi(t) | \hat{\mathbf{j}}(\mathbf{r}) | \Psi(t) \rangle, \quad (4.6)$$

are also different, with

$$\hat{\mathbf{j}}(\mathbf{r}) = -\frac{1}{2i} \left\{ \left[\nabla \hat{\psi}^\dagger(\mathbf{r}) \right] \hat{\psi}(\mathbf{r}) - \hat{\psi}^\dagger(\mathbf{r}) \left[\nabla \hat{\psi}(\mathbf{r}) \right] \right\}. \quad (4.7)$$

Therefore, as the quantum-mechanical equation of motion is valid for any operator $\hat{O}(t)$

$$i \frac{d}{dt} \langle \Psi(t) | \hat{O}(t) | \Psi(t) \rangle = \langle \Psi(t) | i \frac{\partial}{\partial t} \hat{O}(t) + \left[\hat{O}(t), \hat{H}(t) \right] | \Psi(t) \rangle, \quad (4.8)$$

it may be applied to the current density, giving

$$i \frac{d}{dt} \mathbf{j}^{(1)}(\mathbf{r}, t) = \left\langle \Psi^{(1)}(t) \left| \left[\hat{\mathbf{j}}(\mathbf{r}), \hat{H}^{(1)}(t) \right] \right| \Psi^{(1)}(t) \right\rangle, \quad (4.9)$$

$$i \frac{d}{dt} \mathbf{j}^{(2)}(\mathbf{r}, t) = \left\langle \Psi^{(2)}(t) \left| \left[\hat{\mathbf{j}}(\mathbf{r}), \hat{H}^{(2)}(t) \right] \right| \Psi^{(2)}(t) \right\rangle. \quad (4.10)$$

Densities and current densities of the two systems must be equal at t_0 since the starting point was a fixed many-body state. Also, at that time the difference between the two equations of motion is given by:

$$\begin{aligned}
i \frac{d}{dt} [\mathbf{j}^{(1)}(\mathbf{r}, t) - \mathbf{j}^{(2)}(\mathbf{r}, t)] \Big|_{t=t_0} &= \langle \Psi_0 | [\hat{\mathbf{j}}(\mathbf{r}), \hat{H}^{(1)}(t_0) - \hat{H}^{(2)}(t_0)] | \Psi_0 \rangle \\
&= \langle \Psi_0 | [\hat{\mathbf{j}}(\mathbf{r}), v_{ext}^{(1)}(\mathbf{r}, t_0) - v_{ext}^{(2)}(\mathbf{r}, t_0)] | \Psi_0 \rangle \\
&= i n_0(\mathbf{r}) \nabla [v_{ext}^{(1)}(\mathbf{r}, t_0) - v_{ext}^{(2)}(\mathbf{r}, t_0)].
\end{aligned} \tag{4.11}$$

1

At this point, if it is assumed that (4.4) is fulfilled already for $k = 0$, then the derivative on the left-hand side of (4.11) differs from zero and the two current densities will consequently deviate for $t > t_0$. Alternatively, if the criterion is verified only for $k > 0$, the equation of motion should be applied $k + 1$ times, in order to obtain

$$\frac{d^{k+1}}{dt^{k+1}} [\mathbf{j}^{(1)}(\mathbf{r}, t) - \mathbf{j}^{(2)}(\mathbf{r}, t)] \Big|_{t=t_0} = n_0(\mathbf{r}) \nabla u_k(\mathbf{r}). \tag{4.15}$$

Again, the right-hand side differs from 0, which implies that the two current densities differ for $t > t_0$.

The second part of the proof consists of showing that a difference in current densities $\mathbf{j}^{(1)} \neq \mathbf{j}^{(2)}$ for all $t > 0$ implies $n^{(1)} \neq n^{(2)}$. To prove that, we first evaluate the continuity equation

1

$$\begin{aligned}
\frac{\partial}{\partial t} \mathbf{j} &= -\frac{iN}{2} \int d\mathbf{r}_2 \dots d\mathbf{r}_N \frac{\partial}{\partial t} (\Psi^\dagger \nabla \Psi - \Psi \nabla \Psi^\dagger) \\
&= -\frac{iN}{2} \int d\mathbf{r}_2 \dots d\mathbf{r}_N \left(\frac{\partial \Psi^\dagger}{\partial t} \nabla \Psi + \Psi^\dagger \nabla \frac{\partial \Psi}{\partial t} - \frac{\partial \Psi}{\partial t} \nabla \Psi^\dagger - \Psi \nabla \frac{\partial \Psi^\dagger}{\partial t} \right) \\
&= \frac{N}{2} \int d\mathbf{r}_2 \dots d\mathbf{r}_N \left((H \Psi^\dagger) \nabla \Psi - \Psi^\dagger \nabla (H \Psi) + (H \Psi) \nabla \Psi^\dagger - \Psi \nabla (H \Psi^\dagger) \right)
\end{aligned} \tag{4.12}$$

$$\Delta v = v_{ext}^{(1)}(\mathbf{r}, t_0) - v_{ext}^{(2)}(\mathbf{r}, t_0) \tag{4.13}$$

$$\begin{aligned}
\frac{\partial}{\partial t} [\mathbf{j}^{(1)}(\mathbf{r}, t) - \mathbf{j}^{(2)}(\mathbf{r}, t)] \Big|_{t=t_0} &= \frac{N}{2} \int d\mathbf{r}_2 \dots d\mathbf{r}_N \left(\Delta v \Psi^\dagger \nabla \Psi - \Psi^\dagger \nabla (\Delta v \Psi) + \Delta v \Psi \nabla \Psi^\dagger - \Psi \nabla (\Delta v \Psi^\dagger) \right) \Big|_{t=t_0} \\
&= -\frac{N}{2} \int d\mathbf{r}_2 \dots d\mathbf{r}_N \left(\Psi^\dagger (\nabla \Delta v) \Psi + \Psi (\nabla \Delta v) \Psi^\dagger \right) \Big|_{t=t_0} \\
&= -N \int d\mathbf{r}_2 \dots d\mathbf{r}_N |\Psi|^2 \nabla \Delta v \Big|_{t=t_0} \\
&= -n_0(\mathbf{r}) \nabla [v_{ext}^{(1)}(\mathbf{r}, t_0) - v_{ext}^{(2)}(\mathbf{r}, t_0)]
\end{aligned} \tag{4.14}$$

$$\frac{\partial}{\partial t} \left[n^{(1)}(\mathbf{r}, t) - n^{(2)}(\mathbf{r}, t) \right] = -\nabla \cdot \left[\mathbf{j}^{(1)}(\mathbf{r}, t) - \mathbf{j}^{(2)}(\mathbf{r}, t) \right]. \quad (4.16)$$

As before, we seek for the k th time derivative of the external potential, so we take the $(k + 1)$ th time-derivative of equation (4.16) to obtain (at $t = t_0$)

$$\begin{aligned} \frac{\partial^{k+2}}{\partial t^{k+2}} \left[n^{(1)}(\mathbf{r}, t) - n^{(2)}(\mathbf{r}, t) \right] \Big|_{t=t_0} &= -\nabla \cdot \frac{\partial^{k+1}}{\partial t^{k+1}} \left[\mathbf{j}^{(1)}(\mathbf{r}, t) - \mathbf{j}^{(2)}(\mathbf{r}, t) \right] \Big|_{t=t_0} \\ &= -\nabla \cdot \left[n_0(\mathbf{r}) \nabla u_k(\mathbf{r}) \right]. \end{aligned} \quad (4.17)$$

While assuming that $\nabla \cdot \left[n_0(\mathbf{r}) \nabla u_k(\mathbf{r}) \right] = 0$ with $u_k(\mathbf{r}) \neq \text{constant}$, we then apply Green's theorem

$$\int d\mathbf{r} n_0(\mathbf{r}) \left[\nabla u_k(\mathbf{r}) \right]^2 = - \int d\mathbf{r} u_k(\mathbf{r}) \nabla \cdot \left[n_0(\mathbf{r}) \nabla u_k(\mathbf{r}) \right] + \int_S n_0(\mathbf{r}) u_k(\mathbf{r}) \nabla u_k(\mathbf{r}) \cdot d\mathbf{S}, \quad (4.18)$$

and we note that the first term on the right-hand side is zero by assumption and the second one vanishes in the limit $r \rightarrow \infty$ (if density decays in a reasonable manner). Consequently, either $n_0(\mathbf{r})$ is 0 or $\nabla u_k(\mathbf{r})$ is 0. As the density cannot be zero for all \mathbf{r} , the second possibility must be verified, but as that would contradict our initial assumption, according to which u_k is not a constant, then $\nabla \cdot \left[n_0(\mathbf{r}) \nabla u_k(\mathbf{r}) \right] \neq 0$ and $n^{(1)} \neq n^{(2)}$ for $t > t_0, \forall k \geq 0$. \square

Statement 2 The action integral (4.1) is a functional of the density ($A[n]$) and has a stationary point at the exact ground state density of the system, i.e.

$$\frac{\delta A}{\delta n(\mathbf{r}, t)} = 0 \quad (4.19)$$

Proof of Statement 2

Although the wavefunction is determined by the density only within a TD phase factor (not uniquely determined), the expectation value

$$\langle \Psi(t) | i \frac{\partial}{\partial t} - \hat{H}(t) | \Psi(t) \rangle = \langle \Psi(t) | i \frac{\partial}{\partial t} - \hat{T} - \hat{W} - \hat{V}(t) | \Psi(t) \rangle \quad (4.20)$$

is uniquely determined since the function $C(t)$ contained in the potential $\hat{V}(t)$ is cancelled by the time derivative of the time-dependent phase in the wavefunction $\dot{\alpha}(t) = C(t)$. Therefore, the action is a unique functional of the density and since it is stationary for the exact solution of the TD Schrödinger equation, the corresponding action density functional must be stationary for the exact TD ground state density of the system.

4.1.2 TD Kohn-Sham Scheme

In TD Kohn-Sham equations

$$i \frac{\partial}{\partial t} \phi_i(\mathbf{r}, t) = \left[-\frac{\nabla^2}{2} + v_s(\mathbf{r}, t) \right] \phi_i(\mathbf{r}, t), \quad (4.21)$$

$$v_s(\mathbf{r}, t) = v_{ext}(\mathbf{r}, t) + v_H(\mathbf{r}, t) + v_{xc}(\mathbf{r}, t), \quad (4.22)$$

all right-hand terms in (4.22) except v_{xc} are the same as in the static case, but with a time-dependence introduced via the density n . The exception, the time-dependent xc potential, is written as the functional derivative of the xc part of \tilde{A}

$$v_{xc}(\mathbf{r}, t) = \left. \frac{\delta \tilde{A}_{xc}}{\delta n(\mathbf{r}, \tau)} \right|_{n(\mathbf{r}, t)}, \quad (4.23)$$

where \tilde{A} is a new action functional defined (according to Keldish formalism [15]) to solve a problem related to causality.

4.2 TD Exchange-Correlation Functionals

4.2.1 Adiabatic Approximations

In the adiabatic approximation of exchange-correlation energy (explicit density) functionals, the same functional form is applied, but its evaluation is performed at each time with a time-dependent density $n(\mathbf{r}, t)$, giving an xc functional that is local in time:

$$v_{xc}^{adiabatic} = v_{xc}[n](\mathbf{r}) \Big|_{n=n(\mathbf{r}, t)}. \quad (4.24)$$

4.2.2 TD Optimized Potential Method

In order to derive a time-dependent generalization of the OPM [33] we consider an N -electron system at some finite time t_0 which for all times up until t_0 has been in the ground state associated with a time-independent potential $v_S(\mathbf{r})$. We assume that the corresponding stationary OPM problem has been solved for that system, i.e. a local effective potential and a set of N single-particle orbitals $\{\phi_j\}$ - with energy eigenvalues ϵ_j - minimizing an energy functional are assumed to be known. From t_0 on, an additional time-dependent potential is switched on and stays so until an arbitrary time t_1 . This way, in order to have a TDOPM, one starts by writing the quantum mechanical action in terms of KS orbitals²:

$$A[\phi_j] = \sum_j^{occ} \int_{-\infty}^{t_1} dt \int d\mathbf{r} \phi_j^*(\mathbf{r}, t) \left[i \frac{\partial}{\partial t} + \frac{\nabla^2}{2} - v_{ext}(\mathbf{r}, t) - v_H(\mathbf{r}, t) \right] \phi_j(\mathbf{r}, t) - A_{xc}[\phi_j]. \quad (4.25)$$

²In order to recover the static limit from the time-dependent formalism one had to extend the time integral in (4.25) to $-\infty$.

We then make use of Schrödinger's equation to further simplify it

$$\begin{aligned} i\frac{\partial}{\partial t}\phi_j(\mathbf{r}, t) &= \left[-\frac{\nabla^2}{2} + v_S(\mathbf{r}, t) \right] \phi_j(\mathbf{r}, t) \Leftrightarrow \\ \left[i\frac{\partial}{\partial t} + \frac{\nabla^2}{2} - v_{ext}(\mathbf{r}, t) - v_H(\mathbf{r}, t) \right] \phi_j(\mathbf{r}, t) &= v_{xc}(\mathbf{r}, t)\phi_j(\mathbf{r}, t), \end{aligned} \quad (4.26)$$

with $\phi_j(\mathbf{r}, t) = \psi_j(\mathbf{r})\exp[-i\epsilon_j(t - t_0)]$ for $-\infty < t \leq t_0$:

$$A[\phi_j] = \sum_j^{occ} \int_{-\infty}^{t_1} dt \int d\mathbf{r} \phi_j^*(\mathbf{r}, t) v_{xc}(\mathbf{r}, t) \phi_j(\mathbf{r}, t) - A_{xc}[\phi_j]. \quad (4.27)$$

Just as in the time-independent version of the OPM we were searching for the potential that minimized the energy, when time-dependence is included, we start looking for the potential that makes the action stationary. In mathematical language, this translates to

$$\frac{\delta A[\phi_j]}{\delta v_S(\mathbf{r}, t)} = \sum_j^{occ} \int_{-\infty}^{\infty} dt' \int d\mathbf{r}' \left(\frac{\delta A[\phi_j]}{\delta \phi_j^*(\mathbf{r}', t')} \frac{\delta \phi_j^*(\mathbf{r}', t')}{\delta v_S(\mathbf{r}, t)} + c.c. \right) = 0. \quad (4.28)$$

The first multiplicative quantity on the right-hand side of (4.28) corresponds to the functional derivative of (4.27) with respect to the complex conjugate of the j th KS orbital

$$\begin{aligned} \frac{\delta A[\phi_j]}{\delta \phi_j^*(\mathbf{r}', t')} &= \Theta(t_1 - t') v_{xc}(\mathbf{r}', t') \phi_j(\mathbf{r}', t') - \Theta(t_1 - t') \frac{\delta A_{xc}}{\delta \phi_j^*(\mathbf{r}', t')} \\ &= \left[v_{xc}(\mathbf{r}', t') - \frac{1}{\phi_j(\mathbf{r}', t')} \frac{\delta A_{xc}[\phi_j]}{\delta \phi_j^*(\mathbf{r}', t')} \right] \phi_j(\mathbf{r}', t') \Theta(t_1 - t'), \end{aligned} \quad (4.29)$$

or

$$\frac{\delta A[\phi_j]}{\delta \phi_j^*(\mathbf{r}', t')} = \left[v_{xc}(\mathbf{r}', t') - u_{xcj}^*(\mathbf{r}', t') \right] \phi_j(\mathbf{r}', t') \Theta(t_1 - t'), \quad (4.30)$$

with u_{xcj}^* being a new defined potential:

$$u_{xcj}^*(\mathbf{r}', t') = \frac{1}{\phi_j(\mathbf{r}', t')} \frac{\delta A_{xc}[\phi_j]}{\delta \phi_j^*(\mathbf{r}', t')}. \quad (4.31)$$

In order to evaluate the second multiplicative factor $\delta \phi_j^*(\mathbf{r}', t')/\delta v_S(\mathbf{r}, t)$, we consider two sets of orbitals: $\{\phi_j(\mathbf{r}, t)\}$, representing unperturbed states with null variations with respect to variations in the potential at $t = t_1$; $\{\phi'_j(\mathbf{r}, t)\}$ which solve the backward Schrödinger equation

$$i\frac{\partial}{\partial t}\phi'_j(\mathbf{r}, t) = \left(-\frac{\nabla^2}{2} + v_S(\mathbf{r}, t) + \delta v_S(\mathbf{r}, t) \right) \phi'_j(\mathbf{r}, t), \quad j = 1, \dots, N, \quad (4.32)$$

subject to the initial condition $\phi'_j(\mathbf{r}, t_1) = \phi_j(\mathbf{r}, t_1)$. Equation (4.32) cannot be treated with time-dependent perturbation theory as the unperturbed Hamiltonian already has a time-dependence. Alternatively, one uses Dirac's method of variation of constants [9]. Following the method, we first expand the perturbed wavefunction in terms of the unperturbed set

$$\phi'_j(\mathbf{r}, t) = \sum_k^{all} c_{jk}(t) \phi_k(\mathbf{r}, t) \quad (4.33)$$

and insert this expansion in (4.32). The resulting equation

$$i \sum_k^{all} \dot{c}_{jk}(t) \phi_k(\mathbf{r}, t) = \sum_k^{all} c_{jk}(t) \delta v_S(\mathbf{r}, t) \phi_k(\mathbf{r}, t) \quad (4.34)$$

is then multiplied by $\phi_l^*(\mathbf{r}, t)$ and integrated over all space, yielding

$$\dot{c}_{jl}(t) = \frac{1}{i} \sum_k^{all} c_{jk}(t) \int d\mathbf{r} \phi_l^*(\mathbf{r}, t) \delta v_S(\mathbf{r}, t) \phi_k(\mathbf{r}, t). \quad (4.35)$$

We now insert the ansatz

$$c_{jk}(t) = c_{jk}^{(0)}(t) + c_{jk}^{(1)}(t) + \dots \quad (4.36)$$

on (4.35), further collecting terms according to their order

$$\begin{aligned} \dot{c}_{jl}^{(0)}(t) &= 0 \\ \dot{c}_{jl}^{(1)}(t) &= \frac{1}{i} \sum_k^{all} c_{jk}^{(0)}(t) \int d\mathbf{r} \phi_l^*(\mathbf{r}, t) \delta v_S(\mathbf{r}, t) \phi_k(\mathbf{r}, t) \\ &\dots \end{aligned} \quad (4.37)$$

Since $c_{jk}^{(0)}(t) = \delta_{jk}$ and $c_{jk}^{(1)}(t_1) = 0$, then

$$c_{jl}^{(1)}(t) = \frac{1}{i} \int_{t_1}^t dt' \int d\mathbf{r} \phi_l^*(\mathbf{r}, t') \delta v_S(\mathbf{r}, t') \phi_j(\mathbf{r}, t'). \quad (4.38)$$

Finally, to first-order

$$\delta \phi_j(\mathbf{r}, t) = \sum_k^{all} c_{jk}^{(1)}(t) \phi_k(\mathbf{r}, t) = i \sum_k^{all} \int_t^{t_1} dt' d\mathbf{r}' \phi_k^*(\mathbf{r}', t') \delta v_S(\mathbf{r}', t') \phi_j(\mathbf{r}', t') \phi_k(\mathbf{r}, t) \quad (4.39)$$

and so

$$\frac{\delta\phi_j(\mathbf{r}', t')}{\delta v_S(\mathbf{r}, t)} = i \sum_k^{all} \phi_k^*(\mathbf{r}, t) \phi_j(\mathbf{r}, t) \phi_k(\mathbf{r}', t') \Theta(t_1 - t) \Theta(t - t'), \quad (4.40)$$

$$\frac{\delta\phi_j^*(\mathbf{r}', t')}{\delta v_S(\mathbf{r}, t)} = -i \sum_k^{all} \phi_k(\mathbf{r}, t) \phi_j^*(\mathbf{r}, t) \phi_k^*(\mathbf{r}', t') \Theta(t_1 - t) \Theta(t - t'). \quad (4.41)$$

In closing, we insert (4.30) and (4.41) in (4.28)

$$\begin{aligned} & \sum_j^{occ} \int_{-\infty}^{+\infty} dt' \int d\mathbf{r}' \left[v_{xc}(\mathbf{r}', t') - u_{xcj}^*(\mathbf{r}', t') \right] \phi_j(\mathbf{r}', t') \Theta(t_1 - t') \times \\ & \left[-i \sum_k^{all} \phi_k(\mathbf{r}, t) \phi_j^*(\mathbf{r}, t) \phi_k^*(\mathbf{r}', t') \Theta(t_1 - t) \Theta(t - t') \right] + c.c. = 0 \Leftrightarrow \\ & -i \sum_j^{occ} \int_{-\infty}^{t_1} dt' \int d\mathbf{r}' \left[v_{xc}(\mathbf{r}', t') - u_{xcj}^*(\mathbf{r}', t') \right] \phi_j(\mathbf{r}', t') \phi_j^*(\mathbf{r}, t) \times \\ & \left[\sum_k^{all} \phi_k(\mathbf{r}, t) \phi_k^*(\mathbf{r}', t') \Theta(t - t') \right] + c.c. = 0, \end{aligned} \quad (4.42)$$

we define the retarded Green's function of the system

$$-iG_R^*(\mathbf{r}t, \mathbf{r}'t') = \sum_k^{all} \phi_k(\mathbf{r}, t) \phi_k^*(\mathbf{r}', t') \Theta(t - t'), \quad (4.43)$$

and use it to write the final form of TDOPM equation

$$\sum_j^{occ} \int_{-\infty}^{t_1} dt' \int d\mathbf{r}' \left[v_{xc}(\mathbf{r}', t') - u_{xcj}^*(\mathbf{r}', t') \right] \phi_j(\mathbf{r}', t') \phi_j^*(\mathbf{r}, t) G_R^*(\mathbf{r}t, \mathbf{r}'t') + c.c. = 0. \quad (4.44)$$

Furthermore, in the exchange-only limit

$$A_x[\phi_j] = -\frac{1}{2} \sum_{j,k}^{occ} \int_{t_0}^{t_1} dt \int d\mathbf{r} \int d\mathbf{r}' \frac{\phi_j^*(\mathbf{r}', t) \phi_k(\mathbf{r}', t) \phi_j(\mathbf{r}, t) \phi_k^*(\mathbf{r}, t)}{|\mathbf{r} - \mathbf{r}'|}, \quad (4.45)$$

$$u_{xj}^*(\mathbf{r}', t') = \frac{1}{\phi_j(\mathbf{r}', t')} \frac{\delta A_x[\phi_j]}{\delta \phi_j^*(\mathbf{r}', t')} \quad (4.46)$$

and

$$\sum_j^{occ} \int_{-\infty}^{t_1} dt' \int d\mathbf{r}' \left[v_x(\mathbf{r}', t') - u_{xj}^*(\mathbf{r}', t') \right] \phi_j(\mathbf{r}', t') \phi_j^*(\mathbf{r}, t) G_R^*(\mathbf{r}t, \mathbf{r}'t') + c.c. = 0. \quad (4.47)$$

4.2.3 TD Krieger-Li-Iafate Approximation

At this point, just as in the time-independent version of the theory, we seek for a simplified, easier to implement scheme for OPM. Therefore, one starts by rewriting TDOPM, giving it a new shape

$$\sum_j^{occ} n_j(\mathbf{r}, t) p_j(\mathbf{r}, t) + c.c. = -i \sum_j^{occ} n_j(\mathbf{r}, t) \int_{-\infty}^t dt' \left(\bar{u}_{xcj}(t') - \bar{u}_{xcj}^*(t') \right), \quad (4.48)$$

with

$$p_j(\mathbf{r}, t) = -\frac{i}{\phi_j^*(\mathbf{r}, t)} \int_{-\infty}^{t_1} dt' \int d\mathbf{r}' [v_{xc}(\mathbf{r}'t') - u_{xcj}(\mathbf{r}', t')] \phi_j^*(\mathbf{r}', t') \sum_{k \neq j}^{all} \phi_k^*(\mathbf{r}, t) \phi_k(\mathbf{r}', t') \Theta(t-t'), \quad (4.49)$$

$$\bar{u}_{xcj}(t) = \int d\mathbf{r} n_j(\mathbf{r}, t) u_{xcj}(\mathbf{r}, t). \quad (4.50)$$

and

$$\int d\mathbf{r} n_j(\mathbf{r}, t) p_j(\mathbf{r}, t) = 0, \quad (4.51)$$

where $n_j(\mathbf{r}, t) = |\phi_j(\mathbf{r}, t)|^2$. From (4.48) one can then extract an expression for the xc potential, just by evaluating $\phi_j(\mathbf{r}, t) \left[-i \frac{\partial}{\partial t} + \frac{\nabla^2}{2} - v_S(\mathbf{r}, t) \right] \phi_j^*(\mathbf{r}, t) p_j(\mathbf{r}, t)$ (which only requires some straightforward algebra)

$$\begin{aligned} v_{xc}(\mathbf{r}, t) &= \frac{1}{n(\mathbf{r}, t)} \sum_j^{occ} n_j(\mathbf{r}, t) \frac{1}{2} \left(u'_{xcj}(\mathbf{r}, t) + u'^*_{xcj}(\mathbf{r}, t) \right) \\ &+ \frac{1}{n(\mathbf{r}, t)} \sum_j^{occ} n_j(\mathbf{r}, t) \left[\bar{v}_{xcj}(t) - \frac{1}{2} \left(\bar{u}_{xcj}(t) + \bar{u}_{xcj}^*(t) \right) \right] \\ &+ \frac{i}{4n(\mathbf{r}, t)} \sum_j^{occ} \nabla^2 n_j(\mathbf{r}, t) \int_{-\infty}^t dt' \left(\bar{u}_{xcj}(t') - \bar{u}_{xcj}^*(t') \right), \end{aligned} \quad (4.52)$$

where

$$u'_{xcj}(\mathbf{r}, t) = u_{xcj}(\mathbf{r}, t) + \frac{1}{n_j(\mathbf{r}, t)} \left[\frac{1}{2} \nabla \cdot (p_j(\mathbf{r}, t) \nabla n_j(\mathbf{r}, t)) + i n_j(\mathbf{r}, t) \frac{\partial}{\partial t} p_j(\mathbf{r}, t) + i \mathbf{J}_j(\mathbf{r}, t) \cdot \nabla p_j(\mathbf{r}, t) \right], \quad (4.53)$$

with the current density

$$\mathbf{J}_j(\mathbf{r}, t) = (2i)^{-1} \left(\phi_j^*(\mathbf{r}, t) \nabla \phi_j(\mathbf{r}, t) - \phi_j(\mathbf{r}, t) \nabla \phi_j^*(\mathbf{r}, t) \right) \quad (4.54)$$

and

$$\bar{v}_{xcj}(t) = \int d\mathbf{r} n_j(\mathbf{r}, t) v_{xc}(\mathbf{r}, t). \quad (4.55)$$

The advantage of (4.52) is that it is a very convenient starting point to building approximations to $v_{xc}(\mathbf{r}, t)$, as an explicit functional of $\{\phi_j(\mathbf{r}, t)\}$, through approximation of $p_j(\mathbf{r}, t)$. Among all possibilities, KLI [9] is the simplest one and is obtained by replacing p_j by its average value, which is 0 by means of (4.51):

$$\begin{aligned} v_{xc}^{KLI}(\mathbf{r}, t) &= \frac{1}{n(\mathbf{r}, t)} \sum_j^{occ} n_j(\mathbf{r}, t) \frac{1}{2} \left(u_{xcj}(\mathbf{r}, t) + u_{xcj}^*(\mathbf{r}, t) \right) \\ &+ \frac{1}{n(\mathbf{r}, t)} \sum_j^{occ} n_j(\mathbf{r}, t) \left[\bar{v}_{xcj}^{KLI}(t) - \frac{1}{2} \left(\bar{u}_{xcj}(t) + \bar{u}_{xcj}^*(t) \right) \right] \\ &+ \frac{i}{4n(\mathbf{r}, t)} \sum_j^{occ} \nabla^2 n_j(\mathbf{r}, t) \int_{-\infty}^t dt' \left(\bar{u}_{xcj}(t') - \bar{u}_{xcj}^*(t') \right). \end{aligned} \quad (4.56)$$

Ultimately, the last term of (4.56) vanishes identically for a large class of exchange-correlation actions, which includes all functionals depending on $\{\phi_j\}$ only through combinations of $\phi_j(\mathbf{r}, t)\phi_j^*(\mathbf{r}', t)$. Specifically, the term vanishes in the exchange-only limit, where

$$\begin{aligned} v_x^{KLI}(\mathbf{r}, t) &= \frac{1}{n(\mathbf{r}, t)} \sum_j^{occ} n_j(\mathbf{r}, t) \frac{1}{2} \left(u_{xj}(\mathbf{r}, t) + u_{xj}^*(\mathbf{r}, t) \right) \\ &+ \frac{1}{n(\mathbf{r}, t)} \sum_j^{occ} n_j(\mathbf{r}, t) \left[\bar{v}_{xj}^{KLI}(t) - \frac{1}{2} \left(\bar{u}_{xj}(t) + \bar{u}_{xj}^*(t) \right) \right]. \end{aligned} \quad (4.57)$$

4.2.4 TD Slater Approximation

At this point, we introduce the time-dependent Slater potential [6]

$$v_{slater}(\mathbf{r}, t) = \frac{1}{2} \sum_j^{occ} \frac{|\phi_j(\mathbf{r}, t)|^2}{n(\mathbf{r}, t)} \left[u_{xj}(\mathbf{r}, t) + c.c. \right] \quad (4.58)$$

and substitute it on (4.57), thus obtaining (after some straightforward manipulations)

$$v_x^{KLI}(\mathbf{r}, t) = v_{slater}(\mathbf{r}, t) + \frac{1}{2n(\mathbf{r}, t)} \sum_j^{occ} \phi_j^*(\mathbf{r}, t) \Delta v_j^{KLI}(t) \phi_j(\mathbf{r}, t), \quad (4.59)$$

$$\Delta v_j^{KLI}(t) = \int d\mathbf{r} \left\{ |\phi_j(\mathbf{r}, t)|^2 v_x^{KLI}(\mathbf{r}, t) - |\phi_j(\mathbf{r}, t)|^2 u_{xj}(\mathbf{r}, t) \right\} + c.c. \quad (4.60)$$

Once more, the Slater approximation consists of ignoring the second term on the right of (4.59):

$$v_x^{KLI}(\mathbf{r}, t) \approx v_{slater}(\mathbf{r}, t). \quad (4.61)$$

4.3 Electronic Response to External Fields

4.3.1 Full Solution of TD Kohn-Sham Equations

Photoabsorption spectra can be calculated either by propagating the time-dependent Kohn-Sham equations or by using linear-response theory. Here we will focus on the former.

Accordingly, let us consider that the system is perturbed by a delta potential at $t = 0$

$$v(\mathbf{r}, t) = -k_0 x_i \delta(t), \quad (4.62)$$

where $x_i = x, y, z$ are spatial coordinates, and k_0 , the amplitude, must be small in order to keep the response linear³ and dipolar. After an infinitesimal time interval, at $t = 0^+$

$$\begin{aligned} \phi_j(\mathbf{r}, t = 0^+) &= \hat{T} \exp \left\{ -i \int_0^{0^+} dt \left[\hat{H}_{KS} + v(\mathbf{r}, t) \right] \right\} \phi_j(\mathbf{r}, t = 0) \\ &= \exp(ik_0 x_i) \phi_j(\mathbf{r}, t = 0), \end{aligned} \quad (4.63)$$

where $\{\phi_j(\mathbf{r}, t = 0)\}$ are ground-state Kohn-Sham wavefunctions and \hat{T} is the time ordering propagator, whose presence in (4.63) is justified by the explicit time-dependence in the Kohn-Sham Hamiltonian. Kohn-Sham orbitals are then propagated during a finite time.

4.3.2 Dynamical Polarizability

To begin with the introduction to the concept of dynamical polarizability [25], let us consider a finite system of electrons and nuclei subject to an external electromagnetic field. At the frequencies we are interested in, usually optical frequencies, the dimensions of the atomic and molecular systems are much smaller than the wavelength of the field and we can consider the fields to be uniform in space. Consequently

$$\mathbf{E}(t) = \mathbf{E}^w \cos(\omega t), \quad (4.64)$$

where \mathbf{E}^w is a vector that defines the amplitude and the polarization direction of the field.

³In this case, linearisation is present in TDDFT as it is in linear-response theory, the difference being that TDDFT is extendable to non-linear responses, just by using larger amplitudes for the delta potential.

Usually, the response of the system is characterized by its dipole moment, which for finite systems can be Taylor expanded

$$\begin{aligned}
p_i(t) = & p_i(0) + \sum_{j=1}^3 \alpha_{ij}(w) E_j^w \cos(wt) + \frac{1}{4} \sum_{j,k=1}^3 \beta_{ijk}(0) E_j^w E_k^w + \\
& + \frac{1}{4} \sum_{j,k=1}^3 \beta_{ijk}(2w) E_j^w E_k^w \cos(2wt) + \frac{1}{8} \sum_{j,k,l=1}^3 \gamma_{ijkl}(w) E_j^w E_k^w E_l^w \cos(wt) + \\
& + \frac{1}{24} \sum_{j,k,l=1}^3 \gamma_{ijkl}(3w) E_j^w E_k^w E_l^w \cos(3wt) + \dots,
\end{aligned} \tag{4.65}$$

with α being the dynamical polarizability tensor and γ and β being hyperbolarizability tensors. If the perturbing field is small enough, non-linear terms in (4.65) can be neglected and the induced dipole moment is, in frequency domain,

$$\delta \mathbf{p}(w) = \alpha(w) \mathbf{E}(w) \tag{4.66}$$

and in the context of the full solution to TD Kohn-Sham equations, the dynamical polarizability can be obtained from

$$\alpha_i(w) = -\frac{1}{k} \int d\mathbf{r} x_i \mathcal{F} \left[n(\mathbf{r}, t) - n(\mathbf{r}, t = 0) \right], \tag{4.67}$$

where \mathcal{F} stands for Fourier transform.

4.3.3 Absorption Cross-Section

The electric field in the absence of external sources is the one that solves the curl of Maxwell's equation $\nabla \times \mathbf{E} = -\frac{1}{c} \frac{\partial \mathbf{B}}{\partial t}$:

$$\nabla \times \nabla \times \mathbf{E} = -\frac{1}{c} \frac{\partial}{\partial t} (\nabla \times \mathbf{B}). \tag{4.68}$$

Also, because $\mathbf{B} = \mu \mathbf{H}$ and $\nabla \times \mathbf{H} = \frac{1}{c} \frac{\partial \mathbf{D}}{\partial t}$,

$$\nabla(\nabla \cdot \mathbf{E}) - \nabla^2 \mathbf{E} = -\frac{1}{c} \frac{\partial}{\partial t} \left(\frac{\mu}{c} \frac{\partial \mathbf{D}}{\partial t} \right), \tag{4.69}$$

which, since $\mathbf{D} = \epsilon \mathbf{E}$ and $\nabla \cdot \mathbf{D} = 0$ (the last is valid only in the absence of external sources), is equivalent to

$$\nabla^2 \mathbf{E} = \frac{\epsilon \mu}{c^2} \frac{\partial^2 \mathbf{E}}{\partial t^2}. \tag{4.70}$$

The general solution to this equation is

$$\mathbf{E}(\mathbf{r}, t) = \mathbf{E}_0 e^{i(\mathbf{k} \cdot \mathbf{r} - wt)}, \tag{4.71}$$

with \mathbf{k} being a vector with direction equal to that of the propagating beam $\hat{\mathbf{k}}$

$$\mathbf{k} = \frac{w}{c} \sqrt{\epsilon\mu} \hat{\mathbf{k}}. \quad (4.72)$$

Furthermore, for the class of non-magnetic materials ($\mu = 1$), one can define a complex refractive index $\tilde{n} = \sqrt{\epsilon} = n + i\kappa$ and so

$$\mathbf{E}(\mathbf{r}, t) = \mathbf{E}_0 e^{i(\frac{w}{c} n \hat{\mathbf{k}} \cdot \mathbf{r} - wt)} e^{-\kappa \frac{w}{c} \hat{\mathbf{k}} \cdot \mathbf{r}}. \quad (4.73)$$

Let us now consider monochromatic radiation of frequency w and with direction $\hat{\mathbf{k}} = \hat{\mathbf{e}}_z$ passing through a medium of thickness dz with N_d molecules per unit volume. Equation (4.73) immediately simplifies to

$$E(z, t) = E(0, 0) e^{i(n \frac{w}{c} z - wt)} e^{-\kappa \frac{w}{c} z}. \quad (4.74)$$

Also, for such a system, an absorption cross-section σ can be defined which relates the number of molecules per unit area $N_d dz$ with the attenuation of the intensity of the beam:

$$\frac{dI}{dz} = -N_d \sigma(w) I. \quad (4.75)$$

The solution to this differential equation is, inside the medium,

$$I(w, z) = I(w, 0) e^{-N_d \sigma(w) z}. \quad (4.76)$$

Moreover, equations (4.74) and (4.76) are related since the intensity of the beam is proportional to the square of the electric field. Therefore, by comparing the square of the former with the latter, we obtain

$$N_d \sigma(w) = \frac{2\kappa w}{c}. \quad (4.77)$$

Additionally, $\tilde{n} = \sqrt{\epsilon} = \sqrt{1 + 4\pi\chi_e} \approx 1 + 2\pi\chi_e$, with χ_e being the magnetic susceptibility and $\tilde{n} = \sqrt{\epsilon} = n + i\kappa$, giving:

$$N_d \sigma(w) = \frac{4\pi w}{c} \text{Im}\chi_e. \quad (4.78)$$

Once that macroscopic polarization is related to the average microscopic dipole moment per molecule by

$$\mathbf{P}(w) = N_d \langle \mathbf{p}(w) \rangle = N_d \mathbf{E} \langle \alpha(w) \rangle \quad (4.79)$$

and $\mathbf{P} = \chi_e \mathbf{E}$,

$$\chi_e = N_d \langle \alpha(w) \rangle, \quad (4.80)$$

then absorption cross-section [25] is finally given by

$$\sigma(w) = \frac{4\pi w}{c} \text{Im}\langle \alpha(w) \rangle. \quad (4.81)$$

or

$$\sigma(w) = \frac{4\pi w}{c} \frac{1}{3} \text{Im} \sum_{i=1}^3 \alpha_i(w). \quad (4.82)$$

Chapter 5

Spin Density Functional Theory (SDFT)

Spin density functional theory (SDFT) stems from a Hamiltonian for interacting electrons which includes a Zeeman coupling of the spin degrees of freedom to an external magnetic field $\mathbf{B}_{ext}(\mathbf{r})$. There are three practical reasons to use SDFT: (1) When an external potential is spin-dependent; (2) Even when the potential is spin-independent, we may be interested in the physical spin magnetization (e.g., in magnetic materials); (3) Even when neither (1) nor (2) applies, our local and semi-local approximations typically work better when we use SDFT instead of DFT.

In particular, the most general description that can be considered within SDFT, the **non-collinear** one, does not require the magnetic field to have a constant direction in space and can be naturally obtained if one accepts to employ exchange-correlation functionals which explicitly depend on two-component Kohn-Sham spinors, as we will see.

Notation

Thus, in the general non-collinear formalism, for weak magnetic fields, the Hamiltonian writes ¹

$$\hat{H} = \hat{T} + \hat{V}_{ee} + \hat{S}, \quad (5.1)$$

where \hat{T} is the kinetic energy operator

$$\hat{T} = -\frac{1}{2} \sum_{\tau=\uparrow,\downarrow} \int d\mathbf{r} \hat{\psi}_{\tau}^{\dagger}(\mathbf{r}) \nabla^2 \hat{\psi}_{\tau}(\mathbf{r}), \quad (5.2)$$

\hat{V}_{ee} is the electron interaction operator and \hat{S} is the spin-potential operator

$$\hat{S} = \int d\mathbf{r} \begin{pmatrix} \hat{\psi}_{\uparrow}^{\dagger}(\mathbf{r}) & \hat{\psi}_{\downarrow}^{\dagger}(\mathbf{r}) \end{pmatrix} V_{spin}(\mathbf{r}) \begin{pmatrix} \hat{\psi}_{\uparrow}(\mathbf{r}) \\ \hat{\psi}_{\downarrow}(\mathbf{r}) \end{pmatrix}, \quad (5.3)$$

¹In order to make the Hamiltonian gauge invariant one should include the interaction of the current with the vector potential. As it stands, \hat{H} is appropriate for weak magnetic fields.

with $\hat{\psi}_\tau^\dagger(\mathbf{r})$ and $\hat{\psi}_\tau(\mathbf{r})$ being second quantization creation and annihilation fermion field operators and $V_{spin}(\mathbf{r})$ being a 2×2 matrix of the spin-potential,

$$V_{spin}(\mathbf{r}) = \begin{pmatrix} V_{\uparrow\uparrow}(\mathbf{r}) & V_{\uparrow\downarrow}(\mathbf{r}) \\ V_{\downarrow\uparrow}(\mathbf{r}) & V_{\downarrow\downarrow}(\mathbf{r}) \end{pmatrix}. \quad (5.4)$$

Another way of writing this matrix is

$$V_{spin}(\mathbf{r}) = \begin{pmatrix} V_{ext}(\mathbf{r}) + \mu_B B_{ext}^z(\mathbf{r}) & \mu_B (B_{ext}^x(\mathbf{r}) - iB_{ext}^y(\mathbf{r})) \\ \mu_B (B_{ext}^x(\mathbf{r}) + iB_{ext}^y(\mathbf{r})) & V_{ext}(\mathbf{r}) - \mu_B B_{ext}^z(\mathbf{r}) \end{pmatrix} \quad (5.5)$$

or, in a more compact form,

$$V_{spin}(\mathbf{r}) = V_{ext}(\mathbf{r}) \mathbb{1}_{2 \times 2} + \mu_B \mathbf{B}_{ext}(\mathbf{r}) \cdot \boldsymbol{\sigma}, \quad (5.6)$$

with the external potential and the magnetic field being given by

$$V_{ext}(\mathbf{r}) = \frac{V_{\uparrow\uparrow}(\mathbf{r}) + V_{\downarrow\downarrow}(\mathbf{r})}{2}, \quad (5.7)$$

$$\mu_B B_{ext}^x(\mathbf{r}) = \frac{V_{\uparrow\downarrow}(\mathbf{r}) + V_{\downarrow\uparrow}(\mathbf{r})}{2}, \quad (5.8)$$

$$\mu_B B_{ext}^y(\mathbf{r}) = \frac{V_{\uparrow\downarrow}(\mathbf{r}) - V_{\downarrow\uparrow}(\mathbf{r})}{-2i}, \quad (5.9)$$

$$\mu_B B_{ext}^z(\mathbf{r}) = \frac{V_{\uparrow\uparrow}(\mathbf{r}) - V_{\downarrow\downarrow}(\mathbf{r})}{2}, \quad (5.10)$$

and $\boldsymbol{\sigma}$ being the vector of the Pauli spin matrices.

A consequence of this separable form for the spin-potential matrix is that the operator for the spin-potential \hat{S} can also be split into a sum of operators for the potential and the magnetic field

$$\hat{S} = \hat{V}_{ext} + \hat{B}_{ext}, \quad (5.11)$$

where

$$\hat{V}_{ext} = \int d\mathbf{r} \hat{n}(\mathbf{r}) V_{ext}(\mathbf{r}), \quad (5.12)$$

$$\hat{B}_{ext} = \int d\mathbf{r} \hat{\mathbf{m}}(\mathbf{r}) \cdot \mathbf{B}_{ext}(\mathbf{r}), \quad (5.13)$$

$\hat{n}(\mathbf{r})$ being the charge density operator

$$\hat{n}(\mathbf{r}) = \sum_{\tau=\uparrow,\downarrow} \hat{\psi}_\tau^\dagger(\mathbf{r}) \hat{\psi}_\tau(\mathbf{r}), \quad (5.14)$$

and $\hat{\mathbf{m}}(\mathbf{r})$ being the magnetization density operator

$$\hat{\mathbf{m}}(\mathbf{r}) = \mu_B \begin{pmatrix} \hat{\psi}_\uparrow^\dagger(\mathbf{r}) & \hat{\psi}_\downarrow^\dagger(\mathbf{r}) \end{pmatrix} \boldsymbol{\sigma} \begin{pmatrix} \hat{\psi}_\uparrow(\mathbf{r}) \\ \hat{\psi}_\downarrow(\mathbf{r}) \end{pmatrix}. \quad (5.15)$$

Additionally, we can define the spin density \mathcal{N} as a 2×2 matrix

$$\mathcal{N}(\mathbf{r}) = \frac{1}{2} \left[n(\mathbf{r}) \mathbb{1}_{2 \times 2} + \frac{1}{\mu_B} \mathbf{m}(\mathbf{r}) \cdot \boldsymbol{\sigma} \right], \quad (5.16)$$

with

$$n(\mathbf{r}) = n_{\uparrow\uparrow}(\mathbf{r}) + n_{\downarrow\downarrow}(\mathbf{r}), \quad (5.17)$$

$$m_x(\mathbf{r}) = \mu_B [n_{\uparrow\downarrow}(\mathbf{r}) + n_{\downarrow\uparrow}(\mathbf{r})], \quad (5.18)$$

$$-im_y(\mathbf{r}) = \mu_B [n_{\uparrow\downarrow}(\mathbf{r}) - n_{\downarrow\uparrow}(\mathbf{r})], \quad (5.19)$$

$$m_z(\mathbf{r}) = \mu_B [n_{\uparrow\uparrow}(\mathbf{r}) - n_{\downarrow\downarrow}(\mathbf{r})]. \quad (5.20)$$

Kohn-Sham scheme

The presence of \mathbf{B}_{ext} in SDFT requires the usage of an additional basic density in the formulation of the energy variational principle

$$E_{v,\mathbf{B}} = \min_{n,\mathbf{m}} E_{v,\mathbf{B}}[n, \mathbf{m}], \quad (5.21)$$

with

$$E_{v,\mathbf{B}}[n, \mathbf{m}] = F[n, \mathbf{m}] + \int d\mathbf{r} v_{ext}(\mathbf{r})n(\mathbf{r}) + \int d\mathbf{r} \mathbf{m}(\mathbf{r}) \cdot \mathbf{B}_{ext}(\mathbf{r}). \quad (5.22)$$

Further, at this point a Kohn-Sham scheme for SDFT may be introduced by assuming non-interacting (v, \mathbf{B}) -representability of the interacting densities (n, \mathbf{m}) . Then $F[n, \mathbf{m}]$ may be decomposed as

$$F[n, \mathbf{m}] = T_S[n, \mathbf{m}] + J[n] + E_{xc}[n, \mathbf{m}]. \quad (5.23)$$

and the single-particle Kohn-Sham equation of SDFT reads

$$\left[-\frac{1}{2}\nabla^2 + v_S(\mathbf{r}) + \mu_B \boldsymbol{\sigma} \cdot \mathbf{B}_S(\mathbf{r}) \right] \Phi_i(\mathbf{r}) = \epsilon_i \Phi_i(\mathbf{r}), \quad (5.24)$$

where $\Phi_i(\mathbf{r})$ are two-component single-particle Pauli spinors.

What is more, as a special case of non-collinearity, there exists **collinear** SDFT, which assumes that the external magnetic field, the exchange-correlation magnetic field and the magnetization vector $(\mathbf{m}(\mathbf{r}) = (0, 0, m(\mathbf{r})))$ are all parallel along a z -direction. In practice, that corresponds to a decomposition of the Kohn-Sham spinors into spin-up ($\sigma = \uparrow$) and spin-down ($\sigma = \downarrow$) orbitals, i.e., $\Phi_i(\mathbf{r}) = (\phi_{i,\uparrow}(\mathbf{r}), 0)$ or $\Phi_i(\mathbf{r}) = (0, \phi_{i,\downarrow}(\mathbf{r}))$ [7].

5.1 Non-Uniqueness Problem

In going from DFT to SDFT one faces what at first may seem a shocking surprise: the Hohenberg-Kohn theorem as stated in DFT is not valid anymore [28]. In fact, the one-to-one correspondence between the sets of external potentials and ground state densities is missing and without a warranty that the spin-potential could be uniquely determined, the KS system would not be unique.

Of course, even in DFT the mapping can be broken in a trivial way since there is an infinite number of potentials, differing by an additive constant, that yield the same ground state density. Also, the mapping $v[\Psi]$ breaks down if finite basis sets are used to represent wavefunctions [2]. Therefore, the correspondence is not always strictly unique in DFT.

Instead, in multidensity DFT, such as SDFT, the mapping between the set of effective potentials and the set of ground state densities can break down in a non-trivial way even in the complete basis-set limit because inversion of Schrödinger's equation does not establish a unique relation between the set of densities and the set of conjugate potentials².

The problem of non-uniqueness is tackled differently in the collinear and non-collinear cases, as we should see in what follows.

5.1.1 Collinear SDFT

Since the mapping $\Psi[n]$ remains intact (in collinear SDFT), and internal-energy functionals can be defined exclusively in terms of wavefunctions,

$$F[n] = \langle \Psi[n] | \hat{T} + \hat{U} | \Psi[n] \rangle, \quad (5.25)$$

then the functionals $E_v[n] = F[n] + V[n]$, $T_S[n] = \langle \Phi[n] | \hat{T} | \Phi[n] \rangle$ and $E_{xc}[n] = F[n] - E_H[n] - T_S[n]$ still exist³, where Φ stands for a Slater determinant, and Ψ for a general many-body wavefunction⁴.

5.1.2 Non-collinear SDFT

Before introducing the problem of invertibility arising within non-collinearity, let us distinguish between pure- and impure-spin states:

²Reference [2] explores solutions to the breaking of $\Psi[n]$ alone and to the breaking of both mappings.

³However, we stress out that we are only proving the existence of functionals, not their differentiability. In fact, in open systems all these functionals are expected to display derivative discontinuities.

⁴Nevertheless, within the aim of collinear SDFT, Capelle and Vignale discovered two cases of freedom in determining the spin-potential. First, for a system of electrons that are all spin-polarized in one direction, say, $n_\uparrow(\mathbf{r}) > 0$, $n_\downarrow(\mathbf{r}) = 0$, the spin component of the potential in the other direction, $V_\downarrow(\mathbf{r})$, is completely arbitrary (as long as the system remains fully polarized). Even so, this kind of indeterminacy cannot have any practical consequence as there are no electrons to experience the arbitrariness. Second, together with the freedom of a constant shift in the potential, there is an additional freedom of a constant shift in the magnetic field, B_0 , appearing because the magnetization operator commutes with \hat{H} . Together, and according to Capelle and Vignale, these two examples represent an **accidental** nonuniqueness (i.e. arising from special features of the ground state) and a **systematic** nonuniqueness (i.e. arising from a conserved quantity), respectively.

- **Pure-spin states** are states which through a local rotation of the spin coordinates may be transformed to have a definite number of spin-up and -down electrons;
- **Impure-spin states** are states which cannot be transformed to have a definite number of spin-up and -down electrons under any local spin rotation.

In this context, impure-spin states are of special importance because it can be proven that they do not lead to any kind of nonuniqueness [5]. On that account, the question about the invertibility of the mapping between spin-potentials and ground states for non-collinear spin Hamiltonians boils down to the existence or not of a local transformation that spin diagonalizes \hat{H} .

Theorem The Hamiltonian \hat{H} cannot be transformed to spin-diagonal form, unless the magnetic field is collinear.

Proof We begin the proof by introducing the general unitary transformation that rotates locally, at every point in real space, the spin degrees of freedom,

$$U(\mathbf{r}) = \begin{pmatrix} e^{i\theta(\mathbf{r})} \cos w(\mathbf{r}) & -e^{i\zeta(\mathbf{r})} \sin w(\mathbf{r}) \\ e^{-i\zeta(\mathbf{r})} \sin w(\mathbf{r}) & e^{-i\theta(\mathbf{r})} \cos w(\mathbf{r}) \end{pmatrix}, \quad (5.26)$$

with $\theta(\mathbf{r})$, $\zeta(\mathbf{r})$ and $w(\mathbf{r})$ real functions. The result of applying the transformation is

$$\begin{pmatrix} \hat{\Psi}_\uparrow^\dagger(\mathbf{r}) & \hat{\Psi}_\downarrow^\dagger(\mathbf{r}) \end{pmatrix} = \begin{pmatrix} \hat{\psi}_\uparrow^\dagger(\mathbf{r}) & \hat{\psi}_\downarrow^\dagger(\mathbf{r}) \end{pmatrix} U^\dagger(\mathbf{r}), \quad (5.27)$$

for the second quantized fermion field operator;

$$\hat{T} = \frac{1}{2} \int d\mathbf{r} \begin{pmatrix} \hat{\Psi}_\uparrow^\dagger(\mathbf{r}) & \hat{\Psi}_\downarrow^\dagger(\mathbf{r}) \end{pmatrix} [-i\nabla + \mathbf{A}]^2 \begin{pmatrix} \hat{\Psi}_\uparrow(\mathbf{r}) \\ \hat{\Psi}_\downarrow(\mathbf{r}) \end{pmatrix}, \quad (5.28)$$

for the kinetic-energy operator \hat{T} , where $\mathbf{A}(\mathbf{r}) = -iU(\mathbf{r})\nabla U^\dagger(\mathbf{r})$ is a gauge vector potential in spin space;

$$\hat{N}_{U\tau} = \int d\mathbf{r} \hat{\Psi}_\tau^\dagger(\mathbf{r}) \hat{\Psi}_\tau(\mathbf{r}), \quad \tau = \uparrow, \downarrow, \quad (5.29)$$

for the spin-up and -down number operators;

$$\hat{b}_U = \hat{N}_{U\downarrow} - \hat{N}_{U\uparrow}, \quad (5.30)$$

for the magnetization operator. In fact, a rotation in spin space may transform locally \hat{b}_U to diagonal form, even though \hat{V}_{ext} and \hat{V}_{ee} do not change form since they are independent of spin. Moreover, rotating back to the original spin space, we see that \hat{b}_U is the operator of a magnetic field $\mathbf{b}_U(\mathbf{r})/\mu_B$:

$$\hat{b}_U = \int d\mathbf{r} \hat{\mathbf{m}}(\mathbf{r}) \cdot \frac{\mathbf{b}_U(\mathbf{r})}{\mu_B}, \quad (5.31)$$

where $\mathbf{b}_U(\mathbf{r})$ is in general non-collinear.

In practice, the question is whether an operator \hat{b}_U exists that commutes with \hat{H} , because in that case \hat{H} could be brought to spin-diagonal form. To answer the question, we need the commutator $[\hat{H}, \hat{b}_U]$. Therefore, we have $[\hat{V}_{ee}, \hat{b}_U] = [\hat{V}_{ext}, \hat{b}_U] = 0$ and

$$[\hat{T}, \hat{b}_U] = i \sum_{\alpha=x,y,z} \int d\mathbf{r} \hat{\mathbf{j}}_{\alpha}(\mathbf{r}) \cdot \nabla b_{U\alpha}(\mathbf{r}), \quad (5.32)$$

$$[\hat{B}_{ext}, \hat{b}_U] = 4i \int d\mathbf{r} \hat{\mathbf{m}}(\mathbf{r}) \cdot \frac{\mathbf{B}_{ext}(\mathbf{r}) \times \mathbf{b}_U(\mathbf{r})}{\mu_B}, \quad (5.33)$$

where

$$\hat{\mathbf{j}}_{\alpha}(\mathbf{r}) = \frac{i}{2} \left\{ [\nabla(\hat{\psi}_{\uparrow}^{\dagger}(\mathbf{r}))\hat{\psi}_{\downarrow}^{\dagger}(\mathbf{r})]\sigma_{\alpha} \begin{pmatrix} \hat{\psi}_{\uparrow}(\mathbf{r}) \\ \hat{\psi}_{\downarrow}(\mathbf{r}) \end{pmatrix} - (\hat{\psi}_{\uparrow}^{\dagger}(\mathbf{r})\hat{\psi}_{\downarrow}^{\dagger}(\mathbf{r}))\sigma_{\alpha} \left[\nabla \begin{pmatrix} \hat{\psi}_{\uparrow}(\mathbf{r}) \\ \hat{\psi}_{\downarrow}(\mathbf{r}) \end{pmatrix} \right] \right\}, \quad \alpha = x, y, z. \quad (5.34)$$

These two commutators correspond to different physical quantities: $i[\hat{T}, \hat{b}_U]$ describes the interaction of currents with vector potentials and $i[\hat{B}_{ext}, \hat{b}_U]$ the energy of a magnetic moment in a magnetic field, and hence they cannot cancel each other. As so, in order to have $[\hat{H}, \hat{b}_U] = 0$, each commutator must vanish separately. From (5.32), we have $\nabla b_{U\alpha}(\mathbf{r}) = 0$, i.e., \mathbf{b}_U is independent of \mathbf{r} . From (5.33) we have $\mathbf{B}_{ext}(\mathbf{r}) \times \mathbf{b}_U = 0$ and so $\mathbf{B}_{ext}(\mathbf{r})$ must be collinear, as it has to be parallel to \mathbf{b}_U , which does not depend on \mathbf{r} . \square

Hence, in the non-collinear case the Hamiltonian cannot be spin diagonalized by a rotation in spin space, and for many-electron systems the mapping between spin-potentials and ground states is invertible.

5.2 The Exchange-Correlation Functional

5.2.1 Non-collinear LSDA and GGA

The problem of obtaining the equivalent of the local spin-density approximation (LSDA) and generalized gradient approximation (GGA) for the exchange and correlation energy functional E_{xc} in the non-collinear case was tackled by employing collinear functionals to simulate non-collinearity. This way, the process begins with a rotation of the magnetization density to locally spin-diagonal form,

$$\mathbf{m}(\mathbf{r}) \cdot \boldsymbol{\sigma} \rightarrow U(\mathbf{r})\mathbf{m}(\mathbf{r}) \cdot \boldsymbol{\sigma}U^{\dagger}(\mathbf{r}) = M_z(\mathbf{r})\sigma_z. \quad (5.35)$$

Then, the locally diagonal spin magnetization $M_z(\mathbf{r})$ is viewed momentarily as if it was the magnetization density of a collinear system and the corresponding exchange and correlation collinear magnetic field $B_{xc}^z(\mathbf{r})$ is found by taking the functional derivative of the collinear exchange and correlation functional E_{xc}^0 :

$$B_{xc}^z(\mathbf{r}) = \frac{\delta E_{xc}^0[n, M_z]}{\delta M_z(\mathbf{r})}. \quad (5.36)$$

Finally, $B_{xc}^z(\mathbf{r})$ is rotated back,

$$B_{xc}^z(\mathbf{r})\sigma_z \rightarrow U^\dagger(\mathbf{r})B_{xc}^z(\mathbf{r})\sigma_z U(\mathbf{r}) = \mathbf{B}_{xc}(\mathbf{r}) \cdot \boldsymbol{\sigma}, \quad (5.37)$$

to obtain the non-collinear magnetic field $\mathbf{B}_{xc}(\mathbf{r})$.

5.2.2 Optimized Potential Method (OPM)

When dealing with the magnetic properties of many-electron systems, LDA- and GGA-type approximations (within SDFT) are awkward to use in practical calculations [30]:

- **Landau Levels** When a uniform electron gas is exposed to an external magnetic field, Landau levels form and, for given magnetic field, the xc energy density exhibits derivative discontinuities as a function of the density whenever a new Landau level is filled;
- **Time-dependent extension** As stated before, LDA's and GGA's non-collinear spin extension is obtained through the assumption of local collinearity. Such approximations that lead to local collinear magnetization and xc magnetic field cause $\mathbf{m}(\mathbf{r}) \times \mathbf{B}_{xc}(\mathbf{r})$ to vanish everywhere in space and this fact renders the adiabatic time-dependent extension of these functionals improper for the study of spin dynamics.

Alternatively, to solve those problems, it is attractive to use explicitly orbital-dependent approximations to E_{xc} because a natural non-collinear description is immediately obtained if one accepts to employ exchange-correlation functionals which explicitly depend on two-component Kohn-Sham spinors without further restricting their form.

In order to derive the Optimized Effective Potential (OEP) equations in the general non-collinear case, we start with the KS equation for two-component spinors Φ_i , which has the form of a Pauli equation:

$$\left(-\frac{1}{2}\nabla^2 + v_S(\mathbf{r}) + \mu_B \boldsymbol{\sigma} \cdot \mathbf{B}_S(\mathbf{r}) \right) \Phi_i(\mathbf{r}) = \epsilon_i \Phi_i(\mathbf{r}). \quad (5.38)$$

For a given external potential v_{ext} and magnetic field B_{ext} , the total energy reads

$$\begin{aligned} E[n, \mathbf{m}] &= T_S[n, \mathbf{m}] + \int n(\mathbf{r})v_{ext}(\mathbf{r})d\mathbf{r} + \int \mathbf{m}(\mathbf{r}) \cdot \mathbf{B}_{ext}(\mathbf{r})d\mathbf{r} + J[n] + E_{xc}[n, \mathbf{m}] \\ &= \sum_i^{occ} \epsilon_i - \int n(\mathbf{r})v_{xc}(\mathbf{r})d\mathbf{r} - \int \mathbf{m}(\mathbf{r}) \cdot \mathbf{B}_{xc}(\mathbf{r})d\mathbf{r} - J[n] + E_{xc}[n, \mathbf{m}]. \end{aligned} \quad (5.39)$$

The xc potential and xc magnetic field are given by

$$v_{xc}(\mathbf{r}) = \frac{\delta E_{xc}[n, \mathbf{m}]}{\delta n(\mathbf{r})} \quad \text{and} \quad \mathbf{B}_{xc}(\mathbf{r}) = \frac{\delta E_{xc}[n, \mathbf{m}]}{\delta \mathbf{m}(\mathbf{r})}, \quad (5.40)$$

respectively.

Assuming that the densities (n, \mathbf{m}) are non-interacting (v, \mathbf{B}) -representable, one may minimize the total-energy functional over the effective scalar potential and magnetic field:

$$\left. \frac{\delta E[n, \mathbf{m}]}{\delta v_S(\mathbf{r})} \right|_{\mathbf{B}_S} = 0 \quad \text{and} \quad \left. \frac{\delta E[n, \mathbf{m}]}{\delta \mathbf{B}_S(\mathbf{r})} \right|_{v_S} = 0. \quad (5.41)$$

That being the case, for the energy functional (5.39), using the EXX approximation to E_{xc} , one obtains the following coupled integral equations for the exchange potential and magnetic field:

$$\begin{aligned} \frac{\delta E_x}{\delta v_S(\mathbf{r})} &= \int d\mathbf{r}' \left[\frac{\delta E_x}{\delta n(\mathbf{r}')} \frac{\delta n(\mathbf{r}')}{\delta v_S(\mathbf{r})} + \frac{\delta E_x}{\delta \mathbf{m}(\mathbf{r}')} \cdot \frac{\delta \mathbf{m}(\mathbf{r}')}{\delta v_S(\mathbf{r})} \right] = \\ &= \int d\mathbf{r}' \sum_k^{occ} \left[\frac{\delta \Phi_k^\dagger(\mathbf{r}')}{\delta v_S(\mathbf{r})} \frac{\delta E_x}{\delta \Phi_k^\dagger(\mathbf{r}')} + c.c. \right], \end{aligned} \quad (5.42)$$

$$\begin{aligned} \frac{\delta E_x}{\delta \mathbf{B}_S^{(i)}(\mathbf{r})} &= \int d\mathbf{r}' \left[\frac{\delta E_x}{\delta n(\mathbf{r}')} \frac{\delta n(\mathbf{r}')}{\delta \mathbf{B}_S^{(i)}(\mathbf{r})} + \sum_{j=1}^3 \frac{\delta E_x}{\delta \mathbf{m}^{(j)}(\mathbf{r}')} \frac{\delta \mathbf{m}^{(j)}(\mathbf{r}')}{\delta \mathbf{B}_S^{(i)}(\mathbf{r})} \right] = \\ &= \int d\mathbf{r}' \sum_k^{occ} \left[\frac{\delta \Phi_k^\dagger(\mathbf{r}')}{\delta \mathbf{B}_S^{(i)}(\mathbf{r})} \frac{\delta E_x}{\delta \Phi_k^\dagger(\mathbf{r}')} + c.c. \right]. \end{aligned} \quad (5.43)$$

Following a procedure analogous to that applied to spin-unpolarized OPM:

$$\frac{\delta \Phi_k(\mathbf{r}')}{\delta v_S(\mathbf{r})} = \sum_{j \neq k}^{all} \frac{\Phi_j(\mathbf{r}') \Phi_j^\dagger(\mathbf{r})}{\epsilon_k - \epsilon_j} \Phi_k(\mathbf{r}) = -G_k(\mathbf{r}', \mathbf{r}) \Phi_k(\mathbf{r}), \quad (5.44)$$

$$\frac{\delta \Phi_k(\mathbf{r}')}{\delta \mathbf{B}_S(\mathbf{r})} = \sum_{j \neq k}^{all} \frac{\Phi_j(\mathbf{r}') \Phi_j^\dagger(\mathbf{r})}{\epsilon_k - \epsilon_j} \boldsymbol{\sigma} \Phi_k(\mathbf{r}) = -\mu_B G_k(\mathbf{r}', \mathbf{r}) \boldsymbol{\sigma} \Phi_k(\mathbf{r}). \quad (5.45)$$

Moreover, through the use of perturbation theory, one can derive the sixteen components of the linear response tensor

$$\chi_{nn}(\mathbf{r}', \mathbf{r}) = \frac{\delta n(\mathbf{r}')}{\delta v_S(\mathbf{r})} = - \sum_k^{occ} \Theta_k \left[\Phi_k^\dagger(\mathbf{r}') G_k(\mathbf{r}', \mathbf{r}) \Phi_k(\mathbf{r}) + c.c. \right], \quad (5.46)$$

$$\chi_{nm}(\mathbf{r}', \mathbf{r}) = \frac{\delta n(\mathbf{r}')}{\delta \mathbf{B}_S(\mathbf{r})} = -\mu_B \sum_k^{occ} \Theta_k \left[\Phi_k^\dagger(\mathbf{r}') \boldsymbol{\sigma} G_k(\mathbf{r}, \mathbf{r}') \Phi_k(\mathbf{r}') + c.c. \right], \quad (5.47)$$

$$\chi_{mm}(\mathbf{r}', \mathbf{r}) = \frac{\delta \mathbf{m}(\mathbf{r}')}{\delta v_S(\mathbf{r})} = \mu_B \sum_k^{occ} \Theta_k \left[\Phi_k^\dagger(\mathbf{r}') G_k(\mathbf{r}, \mathbf{r}') \boldsymbol{\sigma} \Phi_k(\mathbf{r}') + c.c. \right], \quad (5.48)$$

$$\chi_{mm}^{(i,j)}(\mathbf{r}', \mathbf{r}) = \frac{\delta \mathbf{m}^{(i)}(\mathbf{r}')}{\delta \mathbf{B}_S^{(j)}(\mathbf{r})} = \mu_B^2 \sum_k^{occ} \Theta_k \left[\Phi_k^\dagger(\mathbf{r}) \sigma_j G_k(\mathbf{r}, \mathbf{r}') \sigma_i \Phi_k(\mathbf{r}') + c.c. \right], \quad (5.49)$$

and by using equations (5.40) and (5.44)-(5.49) in (5.42) and (5.43), one finally arrives to the OEP equations:

$$\begin{aligned} & \int d\mathbf{r}' \{ v_x(\mathbf{r}') \chi_{nn}(\mathbf{r}', \mathbf{r}) + \mathbf{B}_x(\mathbf{r}') \cdot \chi_{mn}(\mathbf{r}', \mathbf{r}) \} = \\ & = - \int d\mathbf{r}' \sum_k^{occ} \left\{ \Phi_k^\dagger(\mathbf{r}) G_k(\mathbf{r}, \mathbf{r}') \frac{\delta E_x}{\delta \Phi_k^\dagger(\mathbf{r}')} + c.c. \right\}, \end{aligned} \quad (5.50)$$

$$\begin{aligned} & \int d\mathbf{r}' \left\{ v_x(\mathbf{r}') \chi_{nm}^{(i)}(\mathbf{r}', \mathbf{r}) + \sum_{j=1}^3 \mathbf{B}_x^{(j)}(\mathbf{r}') \chi_{mm}^{(j,i)}(\mathbf{r}', \mathbf{r}) \right\} = \\ & = -\mu_B \int d\mathbf{r}' \sum_k^{occ} \left\{ \Phi_k^\dagger(\mathbf{r}) \sigma_i G_k(\mathbf{r}, \mathbf{r}') \frac{\delta E_x}{\delta \Phi_k^\dagger(\mathbf{r}')} + c.c. \right\}. \end{aligned} \quad (5.51)$$

5.2.3 Krieger-Li-Iafrate (KLI) Approximation

Once more, a full solution of (5.50) and (5.51) requires evaluation and storage of all occupied and unoccupied KS states. Such a problem is solved by approximating the denominator in $G_k(\mathbf{r}, \mathbf{r}')$ (equation (5.44)) to an average value $\Delta \bar{\epsilon}$:

$$G_k(\mathbf{r}, \mathbf{r}') \approx \sum_{l \neq k}^{all} \frac{\Phi_l(\mathbf{r}) \Phi_l^\dagger(\mathbf{r}')}{\Delta \bar{\epsilon}} = \frac{\delta^{(3)}(\mathbf{r} - \mathbf{r}') - \Phi_k(\mathbf{r}) \Phi_k^\dagger(\mathbf{r}')}{\Delta \bar{\epsilon}}. \quad (5.52)$$

Therefore, one reaches the KLI equations ⁵, with $\mathbf{m}(\mathbf{r}) = \mu_B \sum_k^{occ} \Phi_k^\dagger(\mathbf{r}) \boldsymbol{\sigma} \Phi_k(\mathbf{r})$:

$$n(\mathbf{r}) v_x(\mathbf{r}) - \mathbf{m}(\mathbf{r}) \cdot \mathbf{B}_x(\mathbf{r}) = \frac{1}{2} \sum_k^{occ} \left\{ \left[\Phi_k^\dagger(\mathbf{r}) \frac{\delta E_x}{\delta \Phi_k^\dagger(\mathbf{r})} + c.c. \right] + \Phi_k^\dagger(\mathbf{r}) \Phi_k(\mathbf{r}) \Delta v_k^{KLI} \right\}, \quad (5.53)$$

$$\frac{\mathbf{m}(\mathbf{r})}{\mu_B} v_x(\mathbf{r}) - n(\mathbf{r}) \mu_B \mathbf{B}_x(\mathbf{r}) = \frac{1}{2} \sum_k^{occ} \left\{ \left[\Phi_k^\dagger(\mathbf{r}) \boldsymbol{\sigma} \frac{\delta E_x}{\delta \Phi_k^\dagger(\mathbf{r})} + c.c. \right] + \Phi_k^\dagger(\mathbf{r}) \boldsymbol{\sigma} \Phi_k(\mathbf{r}) \Delta v_k^{KLI} \right\}, \quad (5.54)$$

$$\Delta v_k^{KLI} = \int d\mathbf{r}' \left\{ \Phi_k^\dagger(\mathbf{r}') \left[v_x(\mathbf{r}') - \mu_B \boldsymbol{\sigma} \cdot \mathbf{B}_x(\mathbf{r}') - u_{x,k}^\dagger(\mathbf{r}') \right] \Phi_k(\mathbf{r}') + c.c. \right\}, \quad (5.55)$$

⁵The coefficient $\Delta \bar{\epsilon}$ is ignored as it is irrelevant in the exact exchange level.

$$u_{x,k}^\dagger(\mathbf{r}') = \frac{1}{\Phi_k(\mathbf{r}') \delta\Phi_k^\dagger(\mathbf{r}')}. \quad (5.56)$$

Since one has to deal with relations between two groups of four objects, it is convenient to use Einstein's summation convention and the usual notation from Special Relativity, even though this is not a relativistic theory. Accordingly, due to the use of atomic units, one defines the metric matrix as $\nu^{\mu,\nu} = \text{diag}(1, 1, 1, 1) = \mathbb{1}_{4 \times 4}$. Also, we define the vector exchange potential and the four-density as

$$v_x^\mu(\mathbf{r}) = (v_x(\mathbf{r}), -\mu_B \mathbf{B}_x(\mathbf{r})) \quad n^\mu(\mathbf{r}) = \left(n(\mathbf{r}), \frac{\mathbf{m}(\mathbf{r})}{\mu_B} \right), \quad (5.57)$$

and by establishing the following four-vector

$$\sigma^\mu = (\mathbb{1}_{2 \times 2}, \boldsymbol{\sigma}) \quad (5.58)$$

one can rewrite the four KLI equations in the compact form

$$M^{\mu\nu}(\mathbf{r}) v_{x,\nu}^{KLI}(\mathbf{r}) = \Lambda_x^\mu(\mathbf{r}), \quad (5.59)$$

with

$$M^{\mu\nu} = \begin{pmatrix} n(\mathbf{r}) & \frac{m_x(\mathbf{r})}{\mu_B} & \frac{m_y(\mathbf{r})}{\mu_B} & \frac{m_z(\mathbf{r})}{\mu_B} \\ \frac{m_x(\mathbf{r})}{\mu_B} & n(\mathbf{r}) & 0 & 0 \\ \frac{m_y(\mathbf{r})}{\mu_B} & 0 & n(\mathbf{r}) & 0 \\ \frac{m_z(\mathbf{r})}{\mu_B} & 0 & 0 & n(\mathbf{r}) \end{pmatrix} \quad (5.60)$$

and

$$\Lambda_x^\mu(\mathbf{r}) = \frac{1}{2} \sum_k^{occ} \left\{ \left[\Phi_k^\dagger(\mathbf{r}) \sigma^\mu \frac{\delta E_x}{\delta \Phi_k^\dagger(\mathbf{r})} + c.c. \right] + \Phi_k^\dagger(\mathbf{r}) \sigma^\mu \Phi_k(\mathbf{r}) \Delta v_k^{KLI} \right\}, \quad (5.61)$$

$$\Delta v_k^{KLI} = \int d\mathbf{r}' \left\{ \Phi_k^\dagger(\mathbf{r}') \left[\sigma_\mu v_x^{KLI} \mu(\mathbf{r}') - u_{x,k}^\dagger(\mathbf{r}') \right] \Phi_k(\mathbf{r}') + c.c. \right\}, \quad (5.62)$$

$$v_x^{KLI} \mu(\mathbf{r}) = (v_x^{KLI}(\mathbf{r}), -\mu_B \mathbf{B}_x^{KLI}(\mathbf{r})). \quad (5.63)$$

Besides, this system of equations can be inverted⁶ in order to obtain a set of coupled integral equations which can then be solved iteratively or linearised. Firstly, inverting the matrix $M^{\mu\nu}$ in (5.59) yields

$$v_x^{KLI} \mu(\mathbf{r}) = \Gamma(\mathbf{r}) N^{\mu\nu}(\mathbf{r}) \Lambda_{x,\nu}(\mathbf{r}), \quad (5.64)$$

⁶There is the question of whether $[\Gamma(\mathbf{r})]^{-1}$ is 0 because when multiplied by the density it constitutes the determinant of $M^{\mu\nu}(\mathbf{r})$. Reference [21] contains a few calculations on the conditions for Γ to be different from zero.

with

$$[\Gamma(\mathbf{r})]^{-1} = n(\mathbf{r}) \left[n^2(\mathbf{r}) - \frac{\mathbf{m}(\mathbf{r}) \cdot \mathbf{m}(\mathbf{r})}{\mu_B^2} \right] \quad (5.65)$$

and

$$N^{00}(\mathbf{r}) = n^2(\mathbf{r}), \quad (5.66)$$

$$N^{0i}(\mathbf{r}) = -n(\mathbf{r}) \frac{m_i(\mathbf{r})}{\mu_B} = N^{i0}(\mathbf{r}), \quad (5.67)$$

$$N^{ii}(\mathbf{r}) = n^2(\mathbf{r}) + \sum_{j=1}^3 (\delta_{ij} - 1) \frac{m_j^2(\mathbf{r})}{\mu_B^2}, \quad (5.68)$$

$$N_{i \neq j}^{ij}(\mathbf{r}) = \frac{m_i(\mathbf{r})m_j(\mathbf{r})}{\mu_B^2}. \quad (5.69)$$

Secondly, in order to linearise (5.64), one calculates the scalar product $\sigma_\mu v_x^{KLI\mu}$:

$$\sigma_\mu v_x^{KLI\mu} = \Gamma \sigma_\mu N^{\mu\nu} \Lambda_{x,v} = \Gamma \begin{pmatrix} N^{0v} \Lambda_{x,v} + N^{3v} \Lambda_{x,v} & N^{1v} \Lambda_{x,v} - iN^{2v} \Lambda_{x,v} \\ N^{1v} \Lambda_{x,v} + iN^{2v} \Lambda_{x,v} & N^{0v} \Lambda_{x,v} - N^{3v} \Lambda_{x,v} \end{pmatrix} \quad (5.70)$$

and it can be easily obtained that

$$N^{0v}(\mathbf{r}) \Lambda_{x,v}(\mathbf{r}) = n(\mathbf{r}) \sum_k^{occ} \left\{ \Phi_k^\dagger(\mathbf{r}) \left[\frac{n(\mathbf{r})}{2} - \boldsymbol{\sigma} \cdot \frac{\mathbf{m}(\mathbf{r})}{2\mu_B} \right] \left[u_{x,k}^\dagger(\mathbf{r}) + \frac{\Delta v_k^{KLI}}{2} \right] \Phi_k(\mathbf{r}) + c.c. \right\}, \quad (5.71)$$

$$\begin{aligned} N^{iv}(\mathbf{r}) \Lambda_{x,v}(\mathbf{r}) &= -\frac{m_i(\mathbf{r})}{\mu_B} \sum_k^{occ} \left\{ \Phi_k^\dagger(\mathbf{r}) \left[\frac{n(\mathbf{r})}{2} - \boldsymbol{\sigma} \cdot \frac{\mathbf{m}(\mathbf{r})}{2\mu_B} \right] \left[u_{x,k}^\dagger(\mathbf{r}) + \frac{\Delta v_k^{KLI}}{2} \right] \Phi_k(\mathbf{r}) + c.c. \right\} \\ &+ \frac{1}{2\Gamma(\mathbf{r})n(\mathbf{r})} \sum_k^{occ} \left\{ \Phi_k^\dagger(\mathbf{r}) \sigma_i \left[u_{x,k}^\dagger(\mathbf{r}) + \frac{\Delta v_k^{KLI}}{2} \right] \Phi_k(\mathbf{r}) + c.c. \right\}. \end{aligned} \quad (5.72)$$

Combining (5.70)-(5.72), it comes that the resulting expression for $\sigma_\mu v_x^{KLI\mu}(\mathbf{r})$ is

$$\begin{aligned} \sigma_\mu v_x^\mu(\mathbf{r}) &= 2\Gamma(\mathbf{r}) \left[\frac{n(\mathbf{r})}{2} - \boldsymbol{\sigma} \cdot \frac{\mathbf{m}(\mathbf{r})}{2\mu_B} \right] \sum_k^{occ} \left\{ \Phi_k^\dagger(\mathbf{r}) \left[\frac{n(\mathbf{r})}{2} - \boldsymbol{\sigma} \cdot \frac{\mathbf{m}(\mathbf{r})}{2\mu_B} \right] \left[u_{x,k}^\dagger(\mathbf{r}) + \frac{\Delta v_k^{KLI}}{2} \right] \Phi_k(\mathbf{r}) + c.c. \right\} + \\ &+ \frac{1}{2n(\mathbf{r})} \sum_k^{occ} \left\{ \Sigma_{x,k}(\mathbf{r}) + \Sigma_{x,k}^\dagger(\mathbf{r}) + \Delta_k(\mathbf{r}) \Delta v_k^{KLI} \right\}, \end{aligned} \quad (5.73)$$

with ⁷

$$\Sigma_{x,k}(\mathbf{r}) = \begin{pmatrix} \Phi_k^\dagger(\mathbf{r})\sigma_3 u_{x,k}^\dagger(\mathbf{r})\Phi_k(\mathbf{r}) & \Phi_k^\dagger(\mathbf{r})(\sigma_1 - i\sigma_2)u_{x,k}^\dagger(\mathbf{r})\Phi_k(\mathbf{r}) \\ \Phi_k^\dagger(\mathbf{r})(\sigma_1 + i\sigma_2)u_{x,k}^\dagger(\mathbf{r})\Phi_k(\mathbf{r}) & -\Phi_k^\dagger(\mathbf{r})\sigma_3 u_{x,k}^\dagger(\mathbf{r})\Phi_k(\mathbf{r}) \end{pmatrix}, \quad (5.74)$$

$$\Delta_k(\mathbf{r}) = \begin{pmatrix} \Phi_k^\dagger(\mathbf{r})\sigma_3\Phi_k(\mathbf{r}) & \Phi_k^\dagger(\mathbf{r})(\sigma_1 - i\sigma_2)\Phi_k(\mathbf{r}) \\ \Phi_k^\dagger(\mathbf{r})(\sigma_1 + i\sigma_2)\Phi_k(\mathbf{r}) & -\Phi_k^\dagger(\mathbf{r})\sigma_3\Phi_k(\mathbf{r}) \end{pmatrix}. \quad (5.75)$$

The great advantage of left multiplying by the Pauli matrices is the possibility of changing the representation of the main objects of SDFT from four-vectors to two by two hermitian matrices. As so, let the following matrix be the exchange potential

$$V_x^{KLI}(\mathbf{r}) = \sigma_\mu v_x^{KLI\mu} \quad (5.76)$$

and $\mathcal{N}(\mathbf{r})$ be the density in its matrix form

$$\mathcal{N}(\mathbf{r}) = \frac{n(\mathbf{r})}{2} \mathbb{1}_{2 \times 2} + \boldsymbol{\sigma} \cdot \frac{\mathbf{m}(\mathbf{r})}{2\mu_B}. \quad (5.77)$$

The inverse of the density matrix is represented by $\rho(\mathbf{r})$, apart from a factor which is its determinant:

$$\rho(\mathbf{r}) = \frac{n(\mathbf{r})}{2} \mathbb{1}_{2 \times 2} - \boldsymbol{\sigma} \cdot \frac{\mathbf{m}(\mathbf{r})}{2\mu_B}. \quad (5.78)$$

Thus, (5.73) can be rewritten as

$$\begin{aligned} V_x^{KLI}(\mathbf{r}) &= 2\Gamma(\mathbf{r})\rho(\mathbf{r}) \sum_k^{occ} \left\{ \Phi_k^\dagger(\mathbf{r})\rho(\mathbf{r}) \left[u_{x,k}^\dagger(\mathbf{r}) + \frac{\Delta v_k^{KLI}}{2} \right] \Phi_k(\mathbf{r}) + c.c. \right\} \\ &+ \frac{1}{2n(\mathbf{r})} \sum_k^{occ} \left\{ \Sigma_{x,k}(\mathbf{r}) + \Sigma_{x,k}^\dagger(\mathbf{r}) + \Delta_k(\mathbf{r})\Delta v_k^{KLI} \right\}. \end{aligned} \quad (5.79)$$

5.2.4 Slater Potential

Again, the exchange potential can be separated into two main components: one independent of Δv_k^{KLI} , the Slater potential V_{slater} ,

$$V_{slater}(\mathbf{r}) = \sum_k^{occ} \left\{ 2\Gamma(\mathbf{r})\rho(\mathbf{r}) \left[\Phi_k^\dagger(\mathbf{r})\rho(\mathbf{r})u_{x,k}^\dagger(\mathbf{r})\Phi_k(\mathbf{r}) + c.c. \right] + \frac{1}{2n(\mathbf{r})} \left[\Sigma_{x,k}(\mathbf{r}) + \Sigma_{x,k}^\dagger(\mathbf{r}) \right] \right\}, \quad (5.80)$$

and another component that depends on Δv_k^{KLI} , such that:

⁷There is no factor 1/2 before Δv_k^{KLI} as one should note that $\Delta_k(\mathbf{r}) = \Delta_k^\dagger(\mathbf{r})$.

$$V_x^{KLI}(\mathbf{r}) = V_{slater}(\mathbf{r}) + \sum_k^{occ} \left\{ 2\Gamma(\mathbf{r})\rho(\mathbf{r})\Phi_k^\dagger(\mathbf{r})\rho(\mathbf{r})\Phi_k(\mathbf{r}) + \frac{1}{2n(\mathbf{r})}\Delta_k(\mathbf{r}) \right\} \Delta v_k^{KLI}. \quad (5.81)$$

In the Slater approximation, the exchange potential is approximated to the Slater part:

$$V_x^{KLI}(\mathbf{r}) \approx V_{slater}(\mathbf{r}). \quad (5.82)$$

Chapter 6

Results and Discussion

6.1 Technical Details

6.1.1 Pseudopotential

The first step consisted of generating a pseudopotential for Xe, using a relativistic extension of the Troullier-Martins method, as implemented in the code APE.

For this purpose, the Dirac version of the Kohn-Sham equation was solved for a closed-shell (spin-unpolarized) atom with LDA exchange (relativistically corrected) and modified Perdew-Wang LDA correlation. Moreover, the chosen cutoff radii were 1.35 a.u. for the $5s$ component, 1.50 a.u. for $5p_{1/2}$, 1.55 a.u. for $5p_{3/2}$ and 2.10 a.u. for $5d$.

6.1.2 Geometry Optimization

Equilibrium geometries were calculated for Xe_3^+ (+1 charge) using the code OCTOPUS and the following exchange-correlation functionals: LDA with modified Perdew-Wang version for correlation, LDA+ADSIC (the same Perdew-Wang version for LDA correlation), OEP exchange (SLATER, KLI, FULL). The states were represented by Pauli spinors, except for LDA+ADSIC which is incompatible with a spin-noncollinear formalism. In that case one is forced to restrict the calculation to a spin-polarized level which disables the inclusion of spin-orbit correction.

Additionally, geometry optimization was performed using the FIRE algorithm, which combines molecular dynamics applied to the calculation of new geometries and velocities, with a conjugated gradients algorithm for the optimization *per se*. The process was controlled by a convergence criterion of 1.9447×10^{-5} a.u. in the forces on every atom.

Finally, the grid was a set of minimal simulation boxes, i.e. spheres centered on each nuclei with a radius of 4.0 Å and a spacing of 0.16 Å each.

6.1.3 TDDFT/Absorption Spectrum

Time-dependent Kohn-Sham equations were solved by time propagation. The system was initially perturbed by a delta-like field with $0.01/\text{Å}$, corresponding to an excitation

in all frequencies. The specific values used for TD variables are identified on Table 6.1, for each particular case. All other input options were the same as the ones used previously in the geometry optimization procedure, except the parallelization options, which had to be modified in OEP-KLI calculations (forced the code to parallelize in domains), since otherwise the process would terminate with an error.

XC Functional	Time-step/eV ⁻¹	N ^o steps	TD Exp. Method
LDA	0.001	20000	Taylor
LDA+ADSIC no SO	0.001	20000	Taylor
LDA+ADSIC no SO (LDA geom.)	0.001	20000	Taylor
OEP-SLATER	0.001	20000	Lanczos
OEP-SLATER (LDA geom.)	0.0001	159762	Lanczos
OEP-KLI	0.001	15082	Taylor
OEP-KLI (LDA geom.)	0.001	12300	Taylor
OEP-FULL (KLI geom.)	0.001	20000	Taylor
OEP-FULL (LDA geom.)	0.001	15585	Taylor

Table 6.1: Time-propagation step-length, number of steps and exponential method chosen for each exchange-correlation functional.

6.2 Results and Discussion

6.2.1 Geometry Optimization

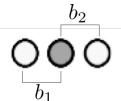
Cluster	Method	$b_1/\text{Å}$	$b_2/\text{Å}$	E/eV
	DIM+IDID+SO	3.273	3.273	
	LDA	3.337	3.337	-1266.1425431761
	LDA+ADSIC no SO	2.799912	2.799912	-1263.1645581338
	OEP-SLATER	3.177113	3.177113	-1249.4156106451
	OEP-KLI	3.384512	3.384512	-1249.5996588188

Table 6.2: Xe₃⁺ ground state geometry (linear) and total energy, as predicted by the different exchange-correlation functionals. The quantities b_1 and b_2 are the bond lengths (from the left to the right). DIM values were taken from reference [26].

The following observations result from the analysis of Table 6.2:

- LDA geometry is the closest to DIM geometry;
- LDA+ADSIC result is far from being a good prediction for the geometry, so in principle spin-orbit coupling must play a fundamental role in the prediction of equilibrium geometries;

- OEP-SLATER and OEP-KLI approach the DIM result with approximately the same difference, but from opposite directions.

It was not possible to reach an equilibrium geometry using OEP-FULL. Unexpectedly big forces guided the two external ions to extremely distant positions.

6.2.2 TDDFT/Absorption Spectrum

LDA

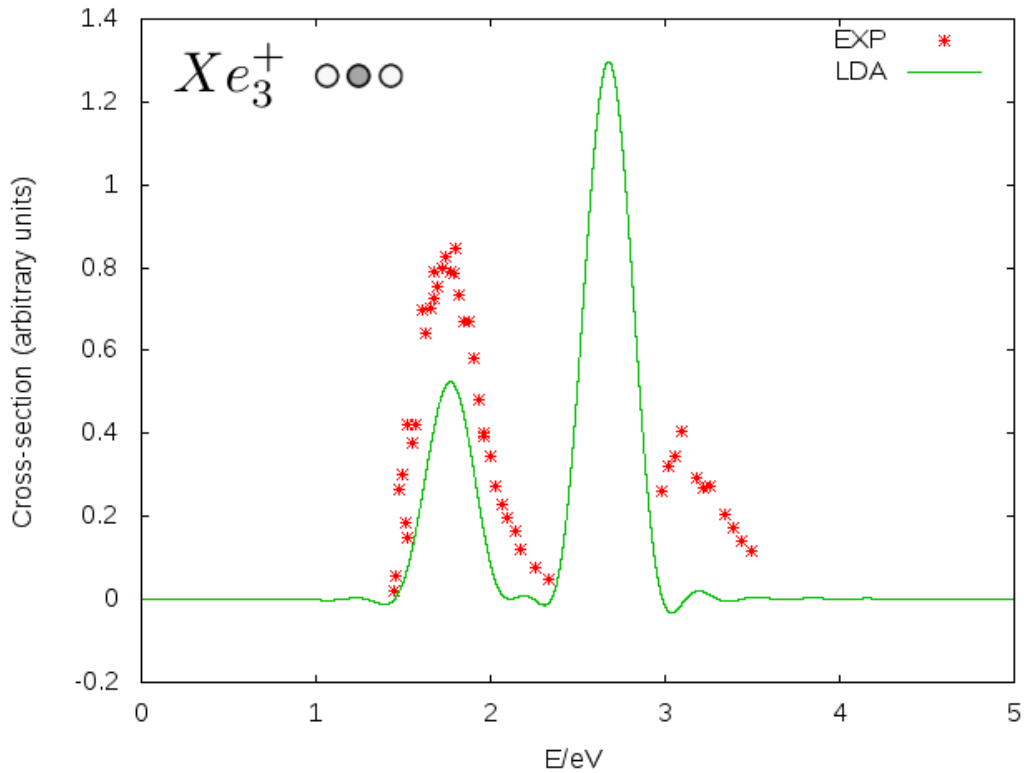


Figure 6.1: Absorption cross-section of linear Xe_3^+ calculated using the LDA functional for both geometry optimization and time propagation. Comparison to the experimental results, from reference [11].

In Figure 6.1, peak positioning seems to be in good agreement with the experimental data, but oscillator strengths are switched.

LDA+ADSIC no SO

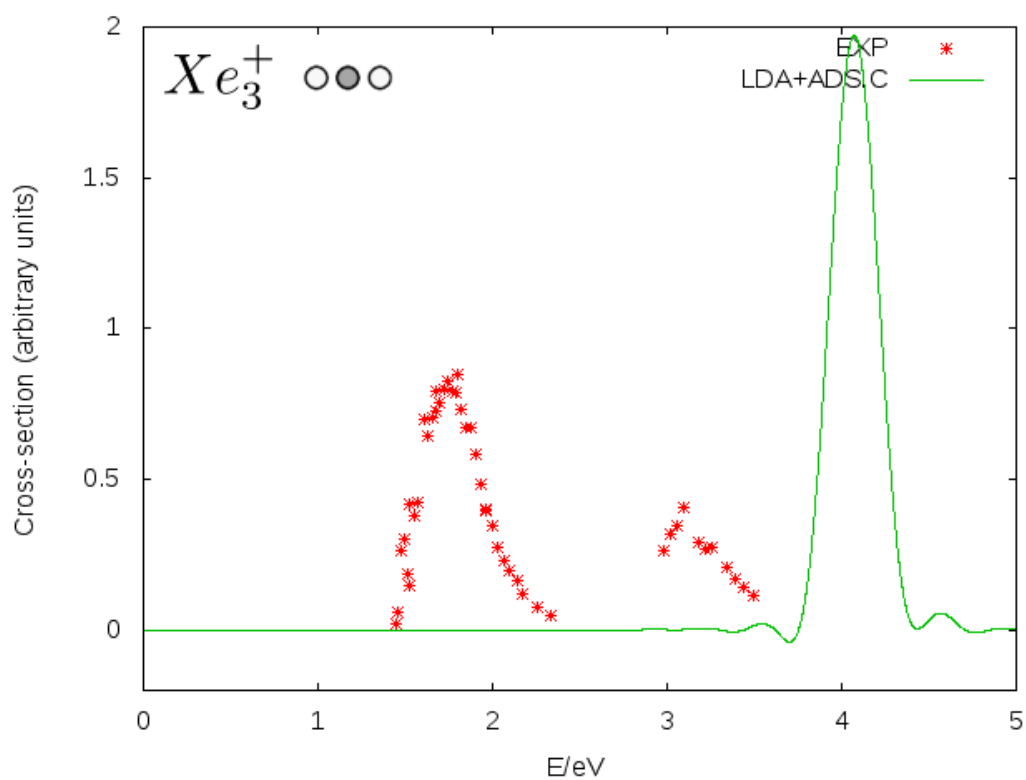


Figure 6.2: Absorption cross-section of linear Xe_3^+ calculated using the LDA+ADSIC functional for both geometry optimization and time propagation. Comparison to the experimental results, from reference [11].

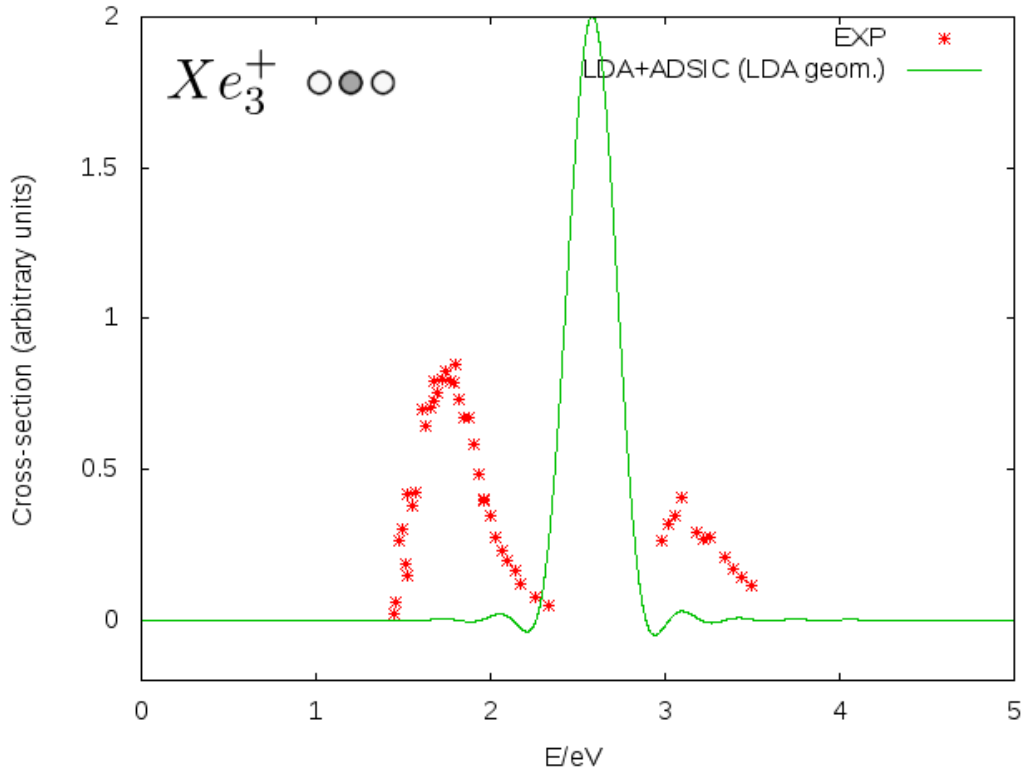


Figure 6.3: Absorption cross-section of linear Xe_3^+ calculated using the LDA functional for geometry optimization and LDA+ADSIC for time propagation. Comparison to the experimental results, from reference [11].

As can be seen in the previous two graphics, only one peak can be observed when spin-orbit coupling is not included as a correction to the Hamiltonian. Also, obtaining a correct geometry is essential for a good agreement with the experimental positioning of the peak: when the propagation is done over LDA's geometry the peak is centered between the two experimental peaks, but when the geometry is as predicted by LDA+ADSIC, the peak moves to higher energies.

OEP-SLATER

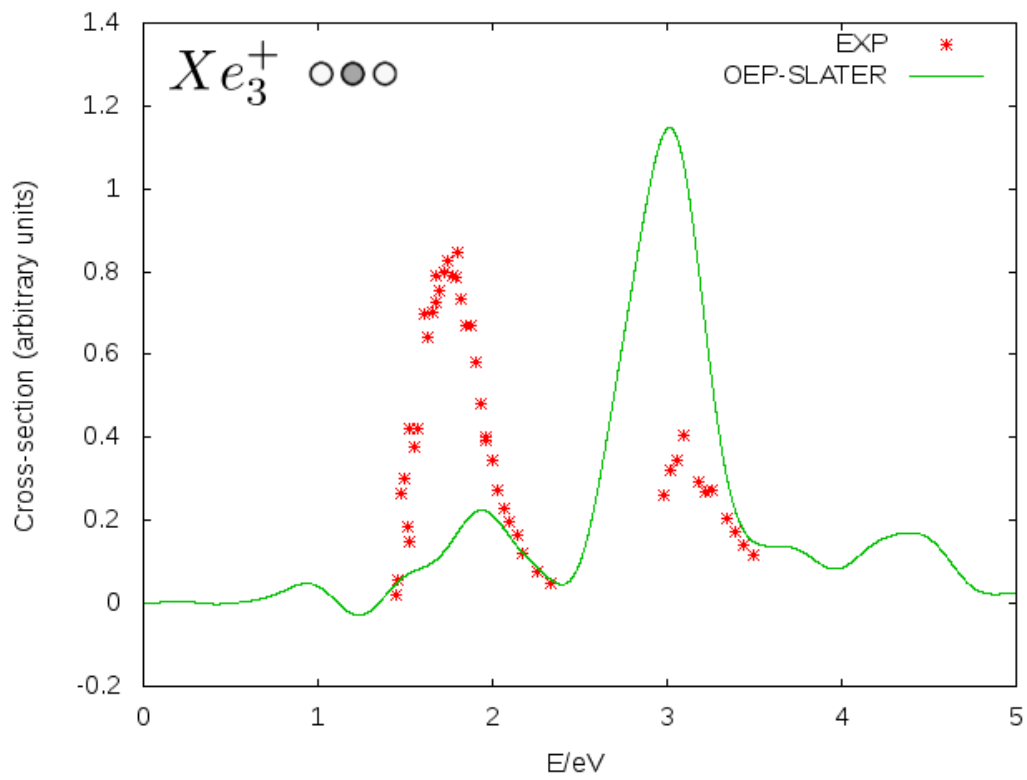


Figure 6.4: Absorption cross-section of linear Xe_3^+ calculated using OEP-SLATER for both geometry optimization and time propagation. Comparison to the experimental results, from reference [11].

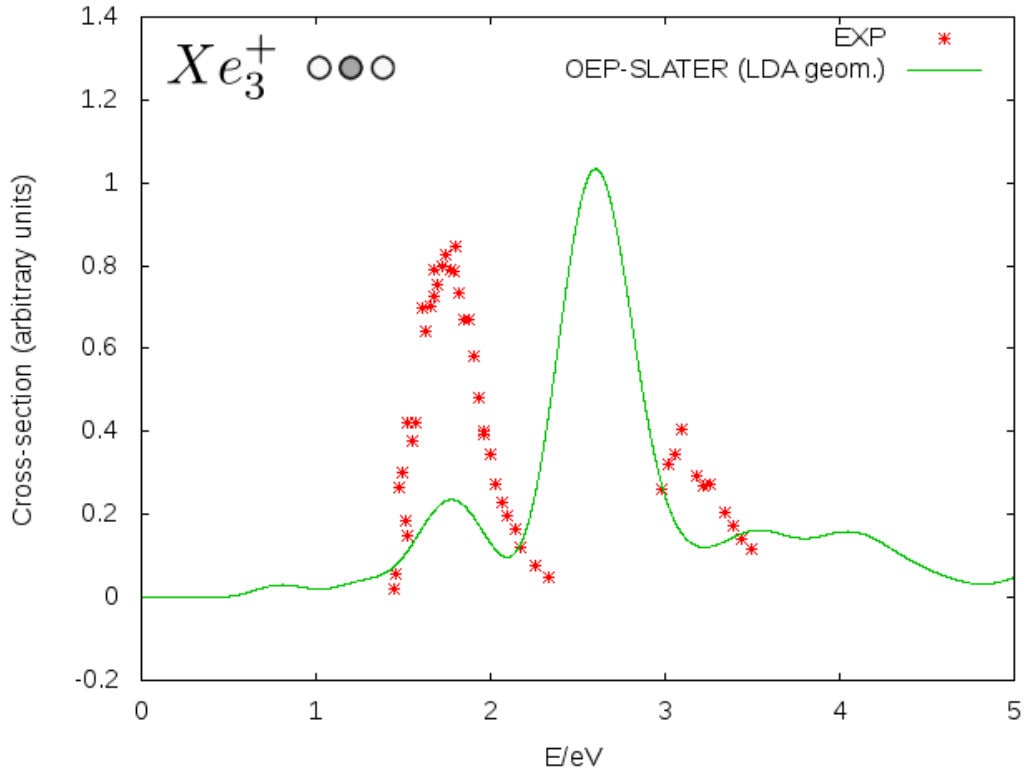


Figure 6.5: Absorption cross-section of linear Xe_3^+ calculated using LDA for geometry optimization and OEP-SLATER for time propagation. Comparison to the experimental results, from reference [11].

OEP-SLATER exchange provides an excellent prediction for the position of the peaks when time-propagation is also done over SLATER's geometry. When performed over LDA's, the result is also good. However, no peak inversion was observed so far. It may be that at the SLATER level the amount of exchange is not enough to invert the peaks.

OEP-KLI

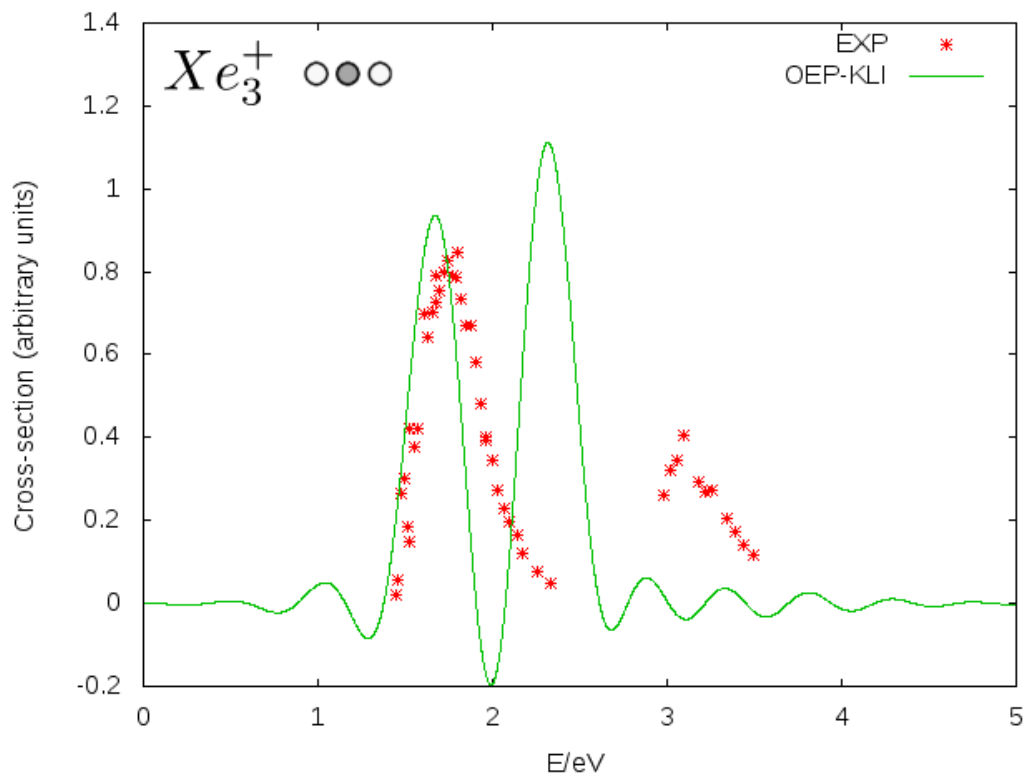


Figure 6.6: Absorption cross-section of linear Xe_3^+ calculated using OEP-KLI for both geometry optimization and time propagation. Comparison to the experimental results, from reference [11].

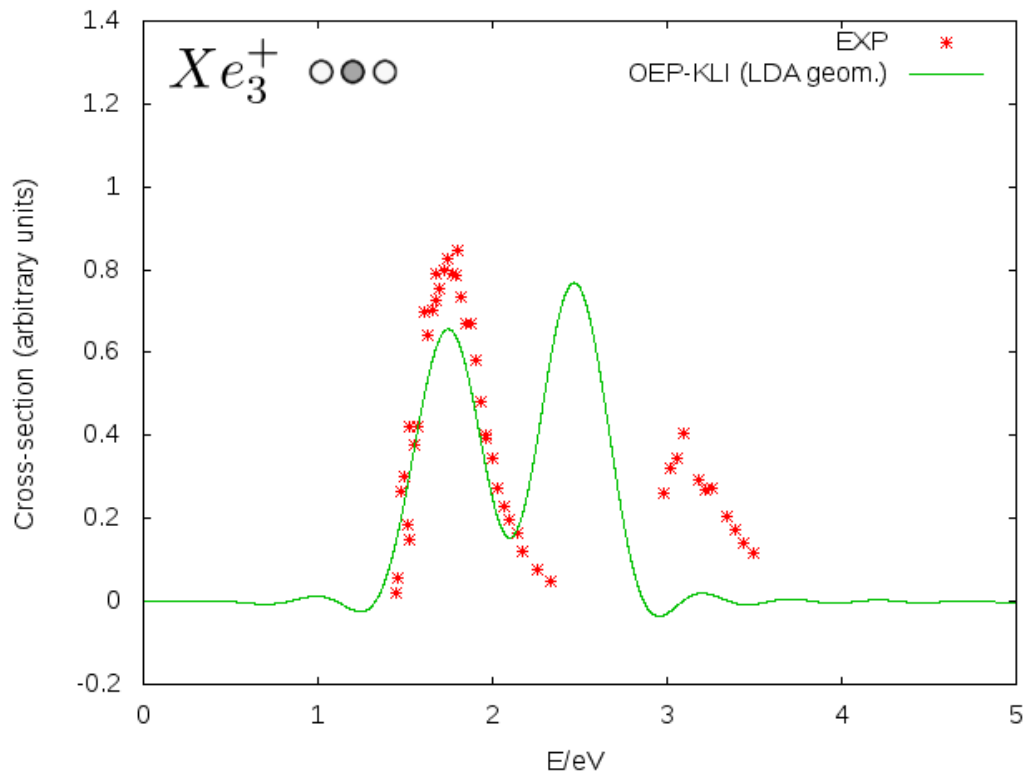


Figure 6.7: Absorption cross-section of linear Xe_3^+ calculated using LDA for geometry optimization and OEP-KLI for time propagation. Comparison to the experimental results, from reference [11].

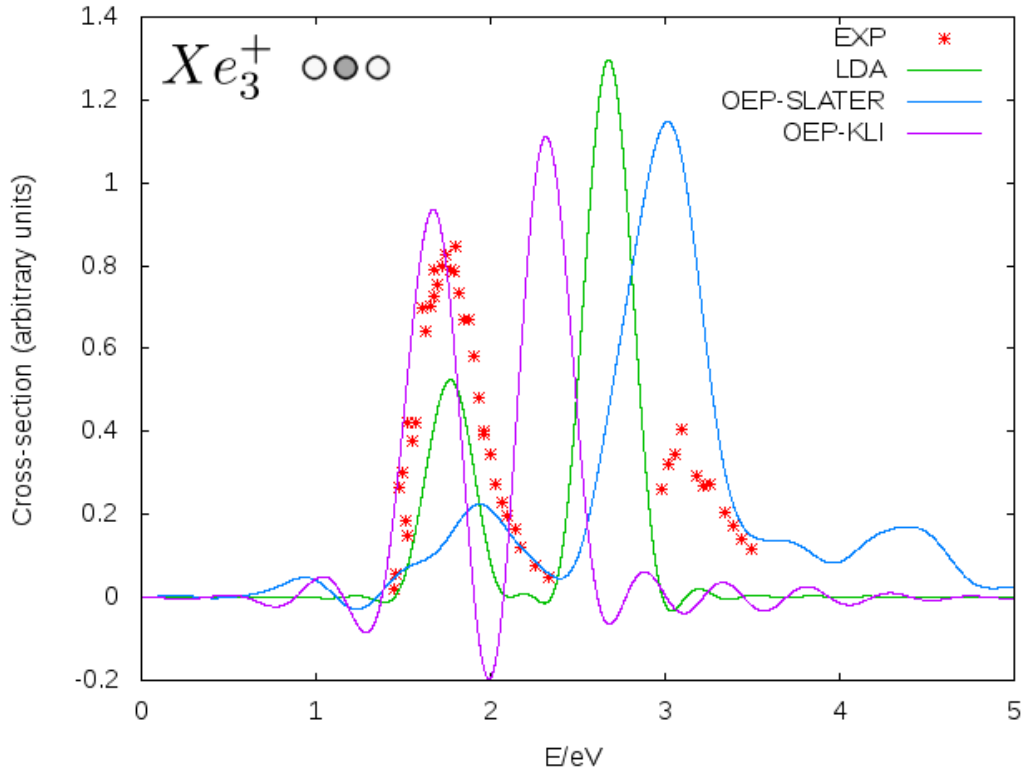


Figure 6.8: Comparison between the experimental absorption spectrum of linear Xe_3^+ and theoretical spectra calculated using LDA, OEP-SLATER and OEP-KLI (with the corresponding ground state geometries).

In Figure 6.6 there is a small negative valley between the two peaks, but its strength is small when compared to the height of the positive peaks and, moreover, peak positioning is not as good as the one previously got with SLATER. However, and even though the relative strength of the peaks haven't changed its sign yet, it is getting smaller (see Figure 6.8). Perhaps the shift would be observed with the addition of more exchange. Propagation with OEP-FULL could, in principle, confirm such an hypothesis.

Additionally, comparing the two graphics generated on the KLI level, we notice that there are no major differences between them, except perhaps those resulting from different propagation intervals (12300 iterations for the first graphic and 15083 iterations for the second).

OEP-FULL

It was not possible to find the correct OEP-FULL geometry. Nevertheless, by knowing that the KLI potential is an excellent approximation to the full OEP, the OEP-FULL spectrum was propagated over the KLI ground state geometry.

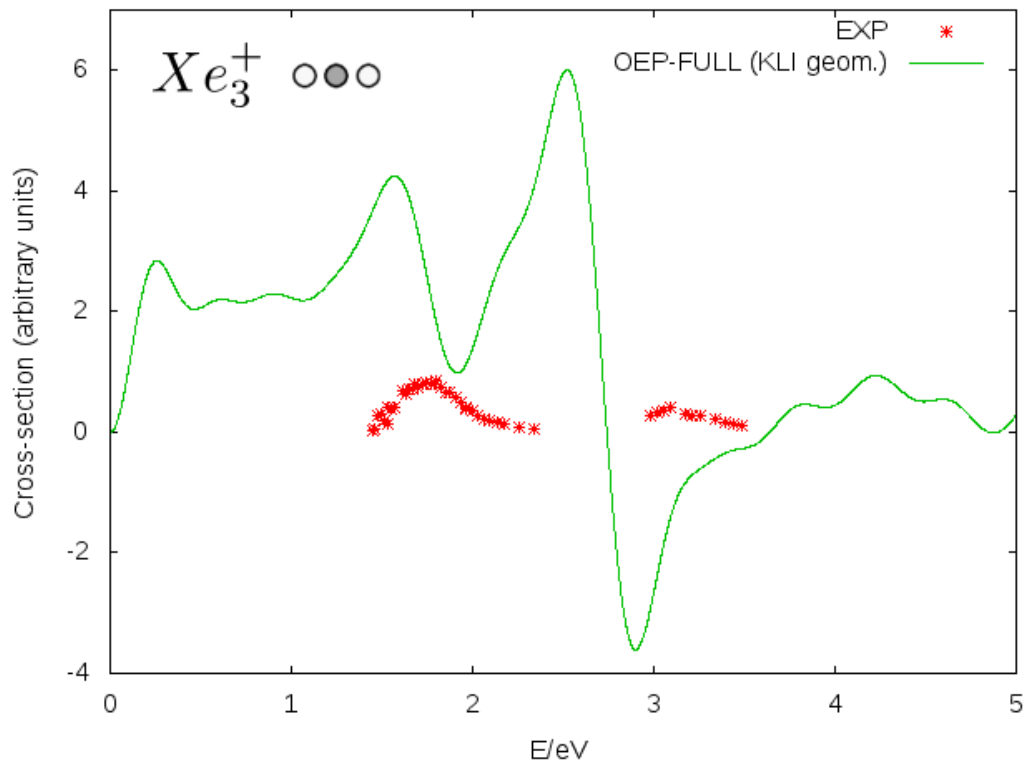


Figure 6.9: Absorption cross-section of linear Xe_3^+ calculated using OEP-KLI for geometry optimization and OEP-FULL for time propagation. Comparison to the experimental results, from reference [11].

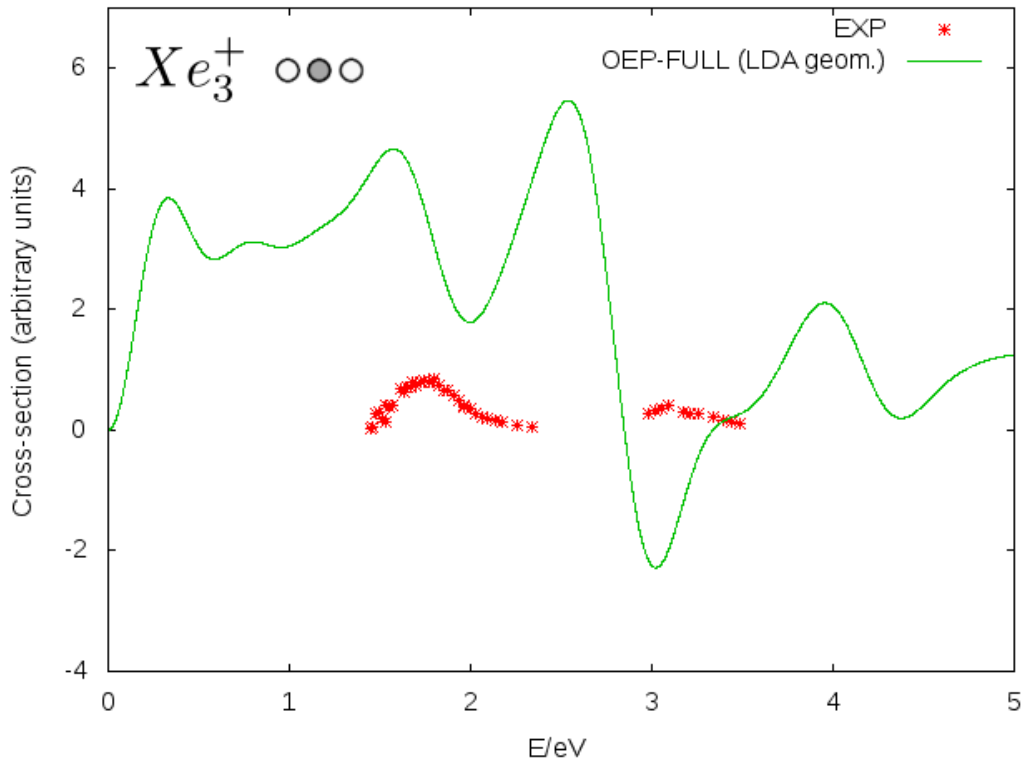


Figure 6.10: Absorption cross-section of linear Xe_3^+ calculated using LDA for geometry optimization and OEP-FULL for time propagation. Comparison to the experimental results, from reference [11].

This is not a good result: peaks are unrecognizable and there is a strong negative peak. This can be a consequence of a wrong ground state geometry. Changing it to the LDA one did not improve the spectrum. In fact, there are no major differences between the last two plots: the few ones being related to the fact that the first case is the result of a time propagation of 20000 iterations while the second propagation only lasted for 15585 iterations.

Chapter 7

Conclusions and Future Work

The general conclusion of this work is that the correct treatment of exchange is mandatory if we want to obtain reliable oscillator strengths in the absorption spectrum of Xe_3^+ clusters. In fact, peak inversion was observed on the Hartree-Fock level. On a DFT level, LDA+ADSIC promise to be capable of solving exchange-related problems, while being considerably fast. However, in OCTOPUS it is not yet possible to combine LDA+ADSIC with spin-orbit correction. Much more time consuming are the tested OEP alternatives. Within them, it was verified that the bigger the amount of exchange added, the closer the peaks are of inverting intensities. Nevertheless, OEP-FULL probably is the level of theory required to reach inversion. Here we were unable to test OEP-FULL, possibly due to the lack of a proper ground state geometry.

Concerning ground state geometries, spectra generated with the same functional for the geometry and the propagation were better than their counterparts generated with LDA geometries, except in the LDA+ADSIC case. Moreover, peak positioning is better in the LDA level and worsens in OEP-SLATER and even more in OEP-KLI.

In the future, it would be interesting to find a way of converging the ground state geometry using OEP-FULL. Also, it would be very useful to try to implement LDA+ADSIC in OCTOPUS for non-collinear spin systems.

Appendix A

Definition of Density Matrices

Let us consider a system of N identical fermions with coordinates $\mathbf{x}_1, \mathbf{x}_2, \dots, \mathbf{x}_N$ - being $\mathbf{x}_i = (\mathbf{r}_i, \boldsymbol{\sigma}_i)$, with \mathbf{r}_i and σ_i the space and spin coordinates, respectively - moving under the influence of a fixed potential framework and their mutual interaction. The physical situation is described by an assumably normalized wave function which fulfills the antisymmetry condition

$$P\Psi(\mathbf{x}_1, \mathbf{x}_2, \dots, \mathbf{x}_N) = (-1)^p\Psi(\mathbf{x}_1, \mathbf{x}_2, \dots, \mathbf{x}_N), \quad (\text{A.1})$$

where P is a permutation operator working on the indices of the N coordinates and p is the parity of such a permutation.

A physical quantity Ω associated to the system is represented in the configuration space by an Hermitian operator $\hat{\Omega}$ which is symmetrical in the particle indices. That operator may be expanded in a series of zero-, one-, two-, ..., or many-particle operators

$$\hat{\Omega} = \hat{\Omega}_{(0)} + \sum_i \hat{\Omega}_i + \frac{1}{2!} \sum'_{ij} \hat{\Omega}_{ij} + \frac{1}{3!} \sum'_{ijk} \hat{\Omega}_{ijk} + \dots, \quad (\text{A.2})$$

where the prime on the summation signs indicates omission of all terms having two or more equal indices. For the expectation value of the second order term, one has ^{1 2}

$$\begin{aligned} \int \Psi^\dagger \left(\frac{1}{2} \sum'_{ij} \hat{\Omega}_{ij} \right) \Psi(dx) &= \binom{N}{2} \int \{ \Psi^\dagger(1'2'3\dots N) \hat{\Omega}_{12} \Psi(123\dots N) \}_{x'_1=x_1, x'_2=x_2} dx_1 dx_2 (dx_{12})' \\ &= \int \{ \hat{\Omega}_{12} \Gamma(\mathbf{x}'_1 \mathbf{x}'_2 | \mathbf{x}_1 \mathbf{x}_2) \}_{x'_1=x_1, x'_2=x_2} dx_1 dx_2, \end{aligned} \quad (\text{A.3})$$

with

¹In the previous expressions we adopted the convention according to which operators $\hat{\Omega}_{ij}$ only act on unprimed coordinates and that only after operations are carried out we set the equalities $\mathbf{x}'_i = \mathbf{x}_i$, etc.

²Here, (dx) indicate integration-summation over all coordinates and (dx'_{ij}) the same over all coordinates except \mathbf{x}_i and \mathbf{x}_j , etc.

$$\Gamma(\mathbf{x}'_1 \mathbf{x}'_2 | \mathbf{x}_1 \mathbf{x}_2) = \binom{N}{2} \int \Psi^\dagger(1'2'3\dots N) \Psi(123\dots N)(dx'_{12}), \quad (\text{A.4})$$

being the second-order density matrix. Inspired by ((A.3)), we arrive at the following expression for the expectation value of operator ((A.2)):

$$\begin{aligned} \langle \hat{\Omega} \rangle &= \hat{\Omega}_{(0)} + \int \hat{\Omega}_1 \gamma(\mathbf{x}'_1 | \mathbf{x}_1) dx_1 \\ &+ \int \hat{\Omega}_{12} \Gamma(\mathbf{x}'_1 \mathbf{x}'_2 | \mathbf{x}_1 \mathbf{x}_2) dx_1 dx_2 \\ &+ \int \hat{\Omega}_{123} \Gamma(\mathbf{x}'_1 \mathbf{x}'_2 \mathbf{x}'_3 | \mathbf{x}_1 \mathbf{x}_2 \mathbf{x}_3) dx_1 dx_2 dx_3 \\ &+ \dots \end{aligned} \quad (\text{A.5})$$

Therefore we will now introduce a series of density matrices of various orders:

$$\gamma(\mathbf{x}'_1 | \mathbf{x}_1) = N \int \Psi^\dagger(1'23\dots N) \Psi(123\dots N)(dx'_1), \quad (\text{A.6})$$

$$\Gamma(\mathbf{x}'_1 \mathbf{x}'_2 | \mathbf{x}_1 \mathbf{x}_2) = \binom{N}{2} \int \Psi^\dagger(1'2'3\dots N) \Psi(123\dots N)(dx'_{12}), \quad (\text{A.7})$$

...

$$\Gamma^{(p)}(\mathbf{x}'_1 \mathbf{x}'_2 \dots \mathbf{x}'_p | \mathbf{x}_1 \mathbf{x}_2 \dots \mathbf{x}_p) = \binom{N}{p} \int \Psi^\dagger(1'2'3' \dots p' \dots N) \Psi(123 \dots p \dots N)(dx'_{12 \dots p}), \quad (\text{A.8})$$

...

$$\Gamma^{(N)}(\mathbf{x}'_1 \mathbf{x}'_2 \dots \mathbf{x}'_N | \mathbf{x}_1 \mathbf{x}_2 \dots \mathbf{x}_N) = \Psi^\dagger(1'2'3' \dots N') \Psi(123 \dots N), \quad (\text{A.9})$$

where (dx'_i) indicate integration over all coordinates except \mathbf{x}_i and (dx'_{ij}) the same over all coordinates except \mathbf{x}_i and \mathbf{x}_j .

Among the many properties of these matrices, the following recurrence relation between density matrices of successive orders proves to be useful in various contexts:

$$\Gamma^{(p-1)}(\mathbf{x}'_1 \mathbf{x}'_2 \dots \mathbf{x}'_{p-1} | \mathbf{x}_1 \mathbf{x}_2 \dots \mathbf{x}_{p-1}) = \frac{p}{N+1-p} \int \Gamma^{(p)}(\mathbf{x}'_1 \mathbf{x}'_2 \dots \mathbf{x}'_{p-1} \mathbf{x}'_p | \mathbf{x}_1 \mathbf{x}_2 \dots \mathbf{x}_{p-1} \mathbf{x}_p) dx_p. \quad (\text{A.10})$$

Moreover, diagonal elements are of special importance

$$\gamma(\mathbf{x}_1) = \gamma(\mathbf{x}_1 | \mathbf{x}_1), \quad (\text{A.11})$$

$$\Gamma(\mathbf{x}_1, \mathbf{x}_2) = \Gamma(\mathbf{x}_1 \mathbf{x}_2 | \mathbf{x}_1 \mathbf{x}_2), \quad (\text{A.12})$$

...

and have the following physical interpretation:

- $\gamma(\mathbf{x}_1)dv_1 =$ number of particles \times probability of finding a particle within volume dv_1 around \mathbf{r}_1 having spin $\boldsymbol{\sigma}_1$ when all the other particles have arbitrary space and spin coordinates;
- $\Gamma(\mathbf{x}_1, \mathbf{x}_2)dv_1dv_2 =$ number of pairs \times probability of finding one particle within the volume dv_1 around the point \mathbf{r}_1 with spin $\boldsymbol{\sigma}_1$ and another within the volume dv_2 around the point \mathbf{r}_2 with the spin $\boldsymbol{\sigma}_2$, all others having arbitrary space and spin coordinates.

Appendix B

Linearisation of the KLI equations

This appendix contains an overview of the linearisation scheme applied to three versions of the KLI equation: KLI applied to spin-unpolarized and time-independent systems (Simple KLI); time-dependent (spin-unpolarized) KLI; KLI applied to non-collinear spin systems (Non-collinear KLI).

B.1 Simple KLI

By taking the diagonal matrix elements of the KLI potential

$$v_x^{KLI}(\mathbf{r}) = v_{slater}(\mathbf{r}) + \frac{1}{2n(\mathbf{r})} \sum_k^{occ} \phi_k^*(\mathbf{r}) \Delta v_k^{KLI} \phi_k(\mathbf{r}), \quad (\text{B.1})$$

$$\Delta v_k^{KLI} = \int d\mathbf{r}' \left\{ |\phi_k(\mathbf{r}')|^2 v_x^{KLI}(\mathbf{r}') - |\phi_k|^2 u_{xk}(\mathbf{r}') \right\} + c.c., \quad (\text{B.2})$$

$$u_{xk}(\mathbf{r}') = \frac{1}{\phi_k^*(\mathbf{r}')} \frac{\delta E_x[\phi_k]}{\delta \phi_k(\mathbf{r}')}, \quad (\text{B.3})$$

one obtains

$$\langle i | v_x^{KLI}(\mathbf{r}) | i \rangle = \langle i | v_{slater}(\mathbf{r}) | i \rangle + \sum_k^{occ} \frac{1}{2} M_{i,k} \Delta v_k^{KLI}, \quad M_{i,k} = \int d\mathbf{r} \frac{|\phi_i(\mathbf{r})|^2 |\phi_k(\mathbf{r})|^2}{n(\mathbf{r})}. \quad (\text{B.4})$$

Definition of the exchange potential $u_{x,k}(\mathbf{r})$

$$\frac{\delta E_x}{\delta \phi_k^*(\mathbf{r})} = u_{x,k}^*(\mathbf{r}) \phi_k(\mathbf{r}), \quad (\text{B.5})$$

allows rewriting Δv_k^{KLI} with a different notation:

$$\Delta v_k^{KLI} = \left[\langle k | \Theta_k v_x^{KLI}(\mathbf{r}) | k \rangle - \langle k | u_{x,k}(\mathbf{r}) | k \rangle \right] + c.c. \quad (\text{B.6})$$

Now, by adding and subtracting $\langle i | u_{x,i}(\mathbf{r}) | i \rangle$ to (B.4), one gets

$$\langle i | v_x^{KLI}(\mathbf{r}) - u_{x,i}(\mathbf{r}) | i \rangle - \sum_k^{\text{occ}} \frac{1}{2} M_{i,k} \Delta v_k^{KLI} = \langle i | v_{Slater}(\mathbf{r}) | i \rangle - \langle i | u_{x,i}(\mathbf{r}) | i \rangle \quad (\text{B.7})$$

and the complex conjugate

$$\langle i | v_x^{KLI*}(\mathbf{r}) - u_{x,i}^*(\mathbf{r}) | i \rangle - \sum_k^{\text{occ}} \frac{1}{2} M_{i,k} \Delta v_k^{KLI} = \langle i | v_{Slater}^*(\mathbf{r}) | i \rangle - \langle i | u_{x,i}^*(\mathbf{r}) | i \rangle. \quad (\text{B.8})$$

Finally, by adding these two equations, one arrives at (Θ_k becomes redundant because now the sum is performed only over occupied states)

$$\begin{aligned} \Delta v_i^{KLI} - \sum_k^{\text{occ}} M_{i,k} \Delta v_k^{KLI} &= \langle i | v_{slater} - u_{x,i} | i \rangle + c.c. \Leftrightarrow \\ \sum_k^{\text{occ}} [\delta_{i,k} - M_{i,k}] \Delta v_k^{KLI} &= \langle i | v_{slater} - u_{x,i} | i \rangle + c.c.. \end{aligned} \quad (\text{B.9})$$

B.2 Time-dependent KLI

Given the final form of the TDKLI equation

$$v_x^{KLI}(\mathbf{r}, t) = v_{slater}(\mathbf{r}, t) + \frac{1}{2n(\mathbf{r}, t)} \sum_j^{\text{occ}} \phi_j^*(\mathbf{r}, t) \Delta v_j^{KLI}(t) \phi_j(\mathbf{r}, t), \quad (\text{B.10})$$

$$\Delta v_j^{KLI}(t) = \int d\mathbf{r} \left\{ |\phi_j(\mathbf{r}, t)|^2 v_x^{KLI}(\mathbf{r}, t) - |\phi_j(\mathbf{r}, t)|^2 u_{x,j}(\mathbf{r}, t) \right\} + c.c. \quad (\text{B.11})$$

and its clear similarities with (B.1), (B.2), the process of linearisation is a repetition of what was developed in the previous section for the time-independent case and will therefore be omitted.

B.3 Non-collinear KLI

In order to obtain an equation for Δv_k^{KLI} like (B.9), one should write

$$\langle i | V_x^{KLI} | i \rangle - \langle i | u_{x,i}^\dagger | i \rangle = \langle i | V_{slater} | i \rangle - \langle i | u_{x,i}^\dagger | i \rangle + \sum_k^{\text{occ}} M_{i,k} \Delta v_k^{KLI}, \quad (\text{B.12})$$

$$\langle i | V_x^{KLI\dagger} | i \rangle - \langle i | u_{x,i} | i \rangle = \langle i | V_{slater}^\dagger | i \rangle - \langle i | u_{x,i} | i \rangle + \sum_k^{occ} M_{i,k} \Delta v_k^{KLI}, \quad (\text{B.13})$$

with

$$M_{i,k} = \int d\mathbf{r} \left\{ 2\Gamma(\mathbf{r}) \Phi_i^\dagger(\mathbf{r}) \rho(\mathbf{r}) \Phi_i(\mathbf{r}) \Phi_k^\dagger(\mathbf{r}) \rho(\mathbf{r}) \Phi_k(\mathbf{r}) + \frac{1}{2n(\mathbf{r})} \Phi_i^\dagger(\mathbf{r}) \Delta_k(\mathbf{r}) \Phi_i(\mathbf{r}) \right\}, \quad (\text{B.14})$$

$$u_{x,i}^\dagger(\mathbf{r}) = \frac{1}{\Phi_i(\mathbf{r})} \frac{\delta E_x}{\delta \Phi_i^\dagger(\mathbf{r})}. \quad (\text{B.15})$$

Given that

$$\Delta v_i^{KLI} = \langle i | V_x^{KLI} | i \rangle - \langle i | u_{x,i}^\dagger | i \rangle + c.c., \quad (\text{B.16})$$

one can add the two previous equations, thus obtaining

$$\Delta v_i^{KLI} - \sum_k^{occ} 2M_{i,k} \Delta v_k^{KLI} = \langle i | V_{slater} - u_{x,i}^\dagger | i \rangle + c.c. \Leftrightarrow \quad (\text{B.17})$$

$$\sum_k^{occ} [\delta_{i,k} - 2M_{i,k}] \Delta v_k^{KLI} = \langle i | V_{slater} - u_{x,i}^\dagger | i \rangle + c.c.. \quad (\text{B.18})$$

Appendix C

Van der Waals Forces

Van der Waals bonding ¹ is very typical of inert atoms whose electrons do not participate in covalent bonds or ionic bonds and also between inert molecules. As a matter of fact, even though those atoms or molecules may be very far from each other, there possibly remains a van der Waals attraction between them.

In order to understand the origin of the corresponding van der Waals force, let us begin by considering a two-level quantum mechanical system, as a simplified model for an atom/molecule:

$$|\Psi\rangle = c_1 |\phi_1\rangle + c_2 |\phi_2\rangle. \quad (\text{C.1})$$

In the previous equation, $|\phi_1\rangle$ and $|\phi_2\rangle$ are proper states of the Hamiltonian operator \hat{H} .

Even though the atom/molecule may have a zero dipole moment on average, the net dipole moment of each of its levels is finite. Due to the energy-time quantum mechanical relation ²,

$$\Delta E \Delta t \sim 1, \quad (\text{C.2})$$

the system is allowed to fluctuate momentarily between the two energy levels, and so between the two dipole moments, with a frequency

$$w \sim 2\pi|E_2 - E_1|. \quad (\text{C.3})$$

Consequently, if the first atom/molecule obtains a momentary polarization \mathbf{P}_A , it will create an electric field \mathbf{E} , which will correspondingly induce a polarization \mathbf{P}_B in the second atom/molecule

$$\mathbf{P}_B = \chi_e \mathbf{E}, \quad (\text{C.4})$$

with χ_e being the magnetic susceptibility.

Consequently, the result is an attractive force between the two bodies [31].

¹Sometimes known as fluctuating dipole forces or molecular bonding.

²In atomic units.

Bibliography

- [1] Carsten A. Ullrich. *Time-dependent density-functional theory. Concepts and applications*. Jan. 2012, pp. 259–262.
- [2] K. Capelle, C. A. Ullrich, and G. Vignale. “Degenerate ground states and nonunique potentials: Breakdown and restoration of density functionals”. In: *Physical Review A* 76.1 (July 2007). DOI: 10.1103/physreva.76.012508.
- [3] Eberhard Engel and Reiner M. Dreizler. *Density Functional Theory*. Springer Berlin Heidelberg, 2011. DOI: 10.1007/978-3-642-14090-7. URL: <https://doi.org/10.1007/978-3-642-14090-7>.
- [4] E. Engel et al. “Relativistic optimized-potential method: Exact transverse exchange and Møller-Plesset-based correlation potential”. In: *Physical Review A* 58.2 (Aug. 1998), pp. 964–992. DOI: 10.1103/physreva.58.964.
- [5] H. Eschrig and W.E. Pickett. “Density functional theory of magnetic systems revisited”. In: *Solid State Communications* 118.3 (Apr. 2001), pp. 123–127. DOI: 10.1016/S0038-1098(01)00053-9. URL: [https://doi.org/10.1016/S0038-1098\(01\)00053-9](https://doi.org/10.1016/S0038-1098(01)00053-9).
- [6] Carlos Fiolhais, Fernando Nogueira, and Miguel A. L. Marques, eds. *A Primer in Density Functional Theory*. Springer Berlin Heidelberg, 2003. DOI: 10.1007/3-540-37072-2.
- [7] Nikitas I. Gidopoulos. “Potential in spin-density-functional theory of noncollinear magnetism determined by the many-electron ground state”. In: *Physical Review B* 75.13 (Apr. 2007). DOI: 10.1103/physrevb.75.134408.
- [8] T Grabo et al. “Orbital Functionals in Density Functional Theory: The Optimized Effective Potential Method”. In: *Strong Coulomb Correlations in Electronic Structure Calculations: Beyond the Local Density Approximation* (Jan. 2000), pp. 203–311.
- [9] E. K. U. Gross, C. A. Ullrich, and U. J. Gossmann. *Density Functional Theory of Time-Dependent Systems*. Ed. by Eberhard K. U. Gross and Reiner M. Dreizler. Boston, MA: Springer US, 1995.
- [10] E.K.U. Gross et al. *Density Functional Theory*. B]: [NATO ASI series. Springer, 1995. ISBN: 9780306449055.

- [11] Hellmut Haberland et al. “Electronic and geometric structure of Ar and Xe clusters: The solvation of rare-gas ions by their parent atoms”. In: *Physical Review Letters* 67.23 (Dec. 1991), pp. 3290–3293. DOI: 10.1103/physrevlett.67.3290. URL: <https://doi.org/10.1103/physrevlett.67.3290>.
- [12] Bernd A. Heß et al. “A mean-field spin-orbit method applicable to correlated wavefunctions”. In: *Chemical Physics Letters* 251.5-6 (Mar. 1996), pp. 365–371. DOI: 10.1016/0009-2614(96)00119-4. URL: [https://doi.org/10.1016/0009-2614\(96\)00119-4](https://doi.org/10.1016/0009-2614(96)00119-4).
- [13] P. Hohenberg and W. Kohn. “Inhomogeneous Electron Gas”. In: *Physical Review* 136.3B (Nov. 1964), B864–B871.
- [14] W. Kohn and L. J. Sham. “Self-Consistent Equations Including Exchange and Correlation Effects”. In: *Physical Review* 140.4A (Nov. 1965), A1133–A1138. DOI: 10.1103/physrev.140.a1133.
- [15] Robert van Leeuwen. “Causality and Symmetry in Time-Dependent Density-Functional Theory”. In: *Physical Review Letters* 80.6 (Feb. 1998), pp. 1280–1283. DOI: 10.1103/physrevlett.80.1280.
- [16] C Legrand, E Suraud, and P-G Reinhard. “Comparison of self-interaction-corrections for metal clusters”. In: *Journal of Physics B: Atomic, Molecular and Optical Physics* 35.4 (Feb. 2002), pp. 1115–1128. DOI: 10.1088/0953-4075/35/4/333. URL: <https://doi.org/10.1088/0953-4075/35/4/333>.
- [17] Mel Levy. “Electron densities in search of Hamiltonians”. In: *Physical Review A* 26.3 (Sept. 1982), pp. 1200–1208.
- [18] Elliott H. Lieb. “Density functionals for coulomb systems”. In: *International Journal of Quantum Chemistry* 24.3 (Sept. 1983), pp. 243–277.
- [19] Miguel A.L. Marques, Micael J.T. Oliveira, and Tobias Burnus. “Libxc: A library of exchange and correlation functionals for density functional theory”. In: *Computer Physics Communications* 183.10 (Oct. 2012), pp. 2272–2281. DOI: 10.1016/j.cpc.2012.05.007.
- [20] R.D. Mattuck. *A Guide to Feynman Diagrams in the Many-body Problem*. Dover Books on Physics Series. Dover Publications, 1992. ISBN: 9780486670478.
- [21] P. Melo. *Orbital dependent functionals in non-collinear spin systems*. 2012.
- [22] Frank Neese. “Software update: the ORCA program system, version 4.0”. In: *Wiley Interdisciplinary Reviews: Computational Molecular Science* 8.1 (July 2017), e1327. DOI: 10.1002/wcms.1327. URL: <https://doi.org/10.1002/wcms.1327>.
- [23] Frank Neese. “The ORCA program system”. In: *Wiley Interdisciplinary Reviews: Computational Molecular Science* 2.1 (June 2011), pp. 73–78. DOI: 10.1002/wcms.81. URL: <https://doi.org/10.1002/wcms.81>.

- [24] Micael J.T. Oliveira and Fernando Nogueira. “Generating relativistic pseudo-potentials with explicit incorporation of semi-core states using APE, the Atomic Pseudo-potentials Engine”. In: *Computer Physics Communications* 178.7 (Apr. 2008), pp. 524–534.
- [25] M.J.T. Oliveira. “Relativistic effects in the optical response of low-dimensional structures: new developments and applications within a time-dependent density functional theory framework”. PhD thesis. University of Coimbra, 2008.
- [26] Petr Paška, Daniel Hrivňák, and René Kalus. “Diatomics-in-molecules study of the geometric and electronic structure of Xen clusters”. In: *Chemical Physics* 286.2-3 (Jan. 2003), pp. 237–248. DOI: 10.1016/s0301-0104(02)00934-5. URL: [https://doi.org/10.1016/s0301-0104\(02\)00934-5](https://doi.org/10.1016/s0301-0104(02)00934-5).
- [27] J. Perdew and K. Schmidt. “Jacob’s ladder of density functional approximations for the exchange-correlation energy”. In: 2001.
- [28] Stefano Pittalis. “Spinor-orbital functionals and the optimized effective potential method”. PhD thesis. Freie Universität Berlin, 2008.
- [29] Erich Runge and E. K. U. Gross. “Density-Functional Theory for Time-Dependent Systems”. In: *Physical Review Letters* 52.12 (Mar. 1984), pp. 997–1000. DOI: 10.1103/physrevlett.52.997.
- [30] S. Sharma et al. “First-Principles Approach to Noncollinear Magnetism: Towards Spin Dynamics”. In: *Physical Review Letters* 98.19 (May 2007). DOI: 10.1103/physrevlett.98.196405.
- [31] S.H. Simon. *The Oxford Solid State Basics*. OUP Oxford, 2013. ISBN: 9780191502101.
- [32] J. C. Slater. “A Simplification of the Hartree-Fock Method”. In: *Physical Review* 81.3 (Feb. 1951), pp. 385–390. DOI: 10.1103/physrev.81.385.
- [33] C. A. Ullrich, U. J. Gossmann, and E. K. U. Gross. “Time-Dependent Optimized Effective Potential”. In: *Physical Review Letters* 74.6 (Feb. 1995), pp. 872–875. DOI: 10.1103/physrevlett.74.872.

